Aalborg University
Department of Health Science and Technology

Synopsis:

The goal of brain-computer interface (BCI) research is to develop technologies that will benefit patients suffering from severe neurological impairments. BCI utilizes brain signals to control computers and external devices.
To achieve a more reliable and robust BCI system the use of error-related potentials (ErrP) has been suggested. ErrPs have previously been detected during subjects' erroneous response to a task and during errors made by the interface. In this study the presence of ErrPs after incorrectly classification of imaginary task was investigated. Six subjects participated in the study. EEG recordings were bandpass filtered and EOG were removed using independent component analysis. Three subjects showed a larger negative deflection around 500 ms after feedback in error trials compared to correct trials, which is in accordance with other reported findings.
Different methods for feature extraction including wavelet based features, statistical features and principal component analysis were tried. Also four different classification methods were investigated. These were template matching, linear discriminant analysis, multilayer perceptron and support vector machine (SVM).
The best classification accuracy was obtained using signal samples as input vector to the SVM. The averaged accuracy was 62.6% and 66.7% for error and correct trials respectively. Two of the subjects however showed accuracies around 80%. The results obtained in this study imply that an ErrP can be detected after erroneous feedback to an imaginary task.

Title:
Detection of error-related potentials to improve brain-computer interfaces

Theme:
Biomedical Engineering and Informatics

Project group:
Group 1088a

Group members:
Esben Wermuth Ingstrup
Christian Kannegård Nikolajsen

Supervisors:
Omar Feix do Nascimento
Dario Farina

Number of copies: 5

Pages: 84

Aalborg University∗ Fredrik Bajers Vej 7 ∗ DK-9220 Aalborg
Tlf: +45 96 35 80 80 ∗ Fax: +45 98 15 97 57

Preface

This report is written by group 1088a during 9th and 10th semester of the Biomedical Engineering and Informatics education at Aalborg University, in the period from September 1st 2007 to June 2nd 2008. This report is the product of an experimental study done during the 9th semester in the Department of Computing and Electronic Systems, University of Essex. The authors would like to thank Dr. Francisco Sepulveda, Coordinator - Brain-Computer Interfaces, for help and supervision during the project. An additional study was made during the 10th semester which builds on many of the methods and ideas proposed in this report. The second study is documented with a paper and some supplementary worksheets enclosed in this report. In addition a CD, containing experimental data, MATLAB and LabView code, is attached.

Readers guide:
The report is divided into 3 parts: Part one is the introduction which leads to the hypothesis. It contains a literature study of some of the work done with error-related potentials. The introduction is followed by a description of the experimental study. Part two describes the signal processing used to analyze the data obtained from the experimental study. It includes preprocessing of the signal, feature extraction and classification. Furthermore it includes evaluation of different classification methods. The third part contains the discussion of the results obtained in this project and a conclusion.

Esben Wermuth Ingstrup

Christian Kannegård Nikolajsen

Contents

Part I

Introduction

Chapter 1

Preanalysis

In this chapter the research area of the Brain-Computer Interface (BCI) will be introduced. The problems with BCI will be described and a possible solution to these problems will be proposed. The proposed solution will lead to a hypothesis there will be sought to be confirmed or rejected within the work presented in this report.

1.1 Brain-computer interfaces

The BCI utilizes neurological signals from the human brain and converts them into command signals which can control computers and external devices. The goal of BCI research is to develop technologies that will benefit severely disabled people by improving their independence and ability to perform daily activities and potentially restore lost function.[Kübler et al., 2006] Important applications of BCI systems are to give new non-muscular communication or movement possibilities to people suffering from severe neurological impairments which affect the neural pathways that control muscles or affect the muscles themselves.[Sanei & Chambers, 2007]

Wolpaw et al. [2006] have categorized the potential users of BCI into three groups. The first group includes people who are totally locked-in due to end-stage amyotrophic lateral sclerosis (ALS) or severe cerebral palsy. These people have no muscular function, not even eye movement. With this group it is not certain if the cognitive functions and vision remain intact and therefore unclear whether this group will be able to use BCI systems. However people who start using BCI in earlier stages of ALS may still be able to use BCI in the end-stage.

In the second group of potential BCI users people have very limited muscular control. This group is much larger than the first group and includes people with late-stage ALS, brain stem stroke and severe cerebral palsy. These diseases affect nearly two million people in the United States alone, and far more around the world [Wolpaw et al., 2002]. The incidence of amyotrophic lateral sclerosis is about 1.5-2:100,000 and seems to be growing [Kübler et al., 2001]. Modern life-support technology allows these people to live long lives, so that the personal, social, and economic burdens of their disabilities are prolonged and severe. Studies have shown that with adequate physical and social support they can lead lives that they and their families and friends consider worthwhile and enjoyable and giving them the opportunity to communicate their life quality will be highly increased.[Wolpaw et al., 2002, 2006]

The third group which is the largest includes people who are expected to retain enough muscular control to speak and use their hands. These will be able to continue to operate communication devices and therefore will not have much benefit of current BCI systems.[Wolpaw et al., 2006] The second group and people progressing to the first group is therefore the most likely to benefit from BCI systems.

Other applications for BCI have also been suggested including stroke rehabilitation, neurofeedback therapies.[Graimann et al., 2007] People suffering from stroke of a spinal cord injury may have difficulties in initiating movements. Their intention may only lead to a small twitch of the muscle early in the recovery process. This action may gain strength and precision if the patients are able to practice. Neurofeedback from a BCI system could help improve the recruitment or order of recruitment of motor pools to enhance the control of the motor task.[Dobkin, 2007] Also in games for both educational and entertainment purposes BCI systems have application possibilities.[Werkhoven & van Erp, 2007]

A BCI system consist of different parts normally including signal acquisition, preprocessing, feature extraction, classification (detection), and application interface as seen in figure 1.1. The input to the system, the brain signal, has to be acquired using recording electrodes, amplifier and an analog to digital converter. Further information on signal acquisition can be found in appendix B. The recorded and digitized signal then has to be processed. Preprocessing in terms of filtering the brain signal is necessary to improve the signal to noise ratio by reducing the surrounding noise. From the command signal features has to be extracted to classify and thereby decode the users intent. Possible features include time and frequency domain parameters like amplitude measurements and the spectral content of the signal. The task of the classifier component is to use the signal features provided by the feature extractor to assign the recorded samples of the signal to a category of brain patterns. The classification step can consist of simple threshold methods or more sophisticated linear or nonlinear classifiers. Finally an application interface uses the output of the classifier to control a spelling device on a computer, neuroprosthesis or a wheelchair etc.[Pfurtscheller et al., 2005; Wolpaw et al., 2002]

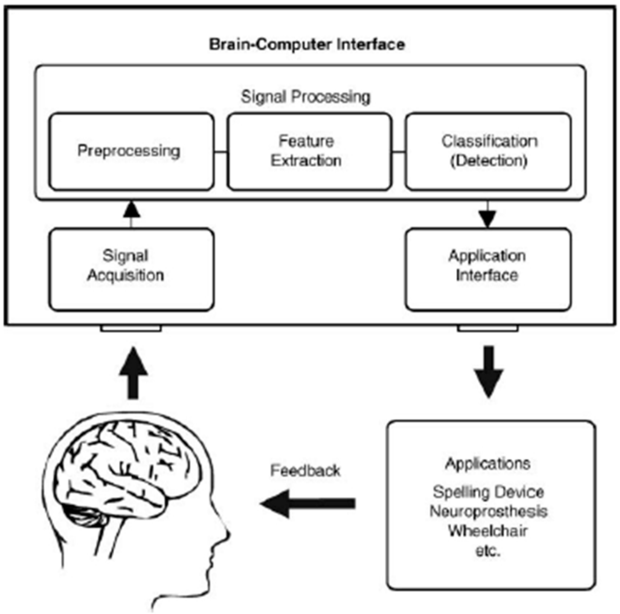

Figure 1.1: *The different parts of a BCI system. [Pfurtscheller et al., 2005]*

1.2 Event-related potentials

There are different approaches in the use of electroencephalography (EEG) for BCI. The most used brain signals in BCI are event related potentials (ERPs). ERPs are an electrical response of the cortex to a sensory, affective, or cognitive event. The ERP is generated by a lot of actions potentials in one area firing at the same time, typical in response to a peripheral or external stimulation. For an introduction to brain anatomy and EEG generation read appendix A and C. ERPs are small (1-30 μM) relative to the background EEG activity and a signal averaging procedure is often necessary to visually reveal their waveform. The ERP waveforms can be quantitatively characterized across three main dimensions: amplitude, latency, and scalp distribution. The ERP may also be characterized by relative latencies between its subcomponents. [Sanei & Chambers, 2007] The ERPs used in BCI can be divided into 5 categories:

- Beta and mu rhythms. These signals are associated with activity in the motor cortex and can be detected during physical or imaginary movements.[Sanei & Chambers, 2007][Wolpaw et al., 2002]
- P300 evoked potential. This is the most studied and widely used ERP. The P300 is a positive potential normally appearing between 300 ms and 400 ms after an auditory, visual or somatosensory stimulus although latencies can range from 250 ms to 900 ms [Patel & Azzam, 2005], see example in figure 1.2. The P300 is elicited by a rare or significant stimuli and its amplitude is strongly related to the unpredictability of the stimulus. The more unpredictable stimuli, the higher the amplitude, which usually have the range of 5 μV to 20 μV though amplitudes as high as 40 μV have been reported [Patel & Azzam, 2005]. The P300 can be divided into two subcomponents, P300a having a more frontal distribution and P300b having a more parietal distribution. The P300a reflects an automatic orientation of attention to novel or salient stimuli. The P300a is characterized by a more rapid habituation

to frequent stimuli than the P300b. After repetition of the stimulus the P300a will quickly decrease whereas the P300b seems to be less affected by the repetition, which suggests that the P300b reflects a categorization process of the stimulus.[Sanei & Chambers, 2007; Friedmann et al., 2001] The P300 is often investigated using an oddball paradigm, in which subjects are exposed to continuous succession of two types of stimuli, one frequent stimuli and one infrequent stimuli.[Sanei & Chambers, 2007; Wolpaw et al., 2002]

- N200. This component is typically evoked 180 to 325 ms following a visual or auditory stimulus and is a negativity resulting from a deviation in form or context of prevailing stimulus [Patel & Azzam, 2005], see example in figure 1.2. Also visual N100 and P200 have been reported. These potentials appears after rapid visual stimulation.[Sanei & Chambers, 2007; Wolpaw et al., 2002]
- Steady-state visual evoked potentials (SSVEP). These potentials are responses to visual stimulations at specific frequencies. The brain generates activity at the same frequency as the visual stimulus.[Sanei & Chambers, 2007; Wolpaw et al., 2002]
- Movement-related cortical potentials (MRCPs). The MRCPs can be seen as slow negative shifts in the EEG about 1500 ms to 1000 ms prior to the actual movement depending of the body segment doing the movement, see example in figure 1.3 on the next page. The amplitudes are also depending on which body segment is used, for example foot movements generates higher MRCP amplitudes than finger movement.[Brunia & van den Bosch, 1984] The MRCPs can also be seen before imaginary movements, but with lower amplitude than real movements. In addition it has been shown possible that the rate of force development can be used to discriminate MRCPs.[do Nascimento et al., 2006; Farina et al., 2007]

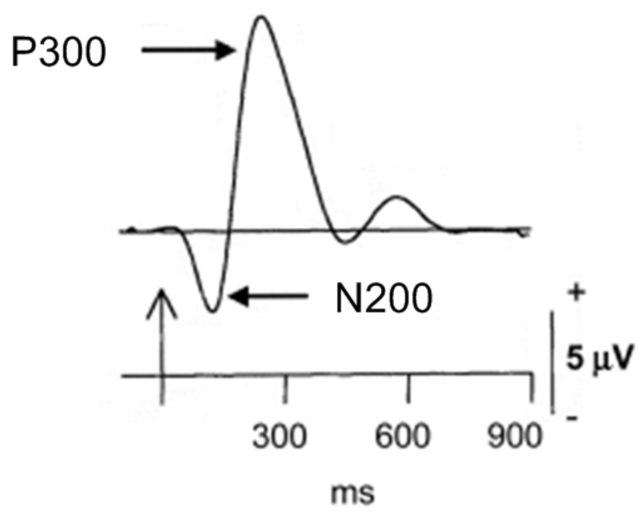

Figure 1.2: *An example of an averaged response to a deviant stimulus where a clear N200 and P300 is present.[Friedmann et al., 2001]*

1.2.1 Problems with BCI

For a reliable BCI system a suitable control signal from the EEG has to be determined. Due to the nature of the EEG it can be difficult to find a control signal which can be precisely charac-

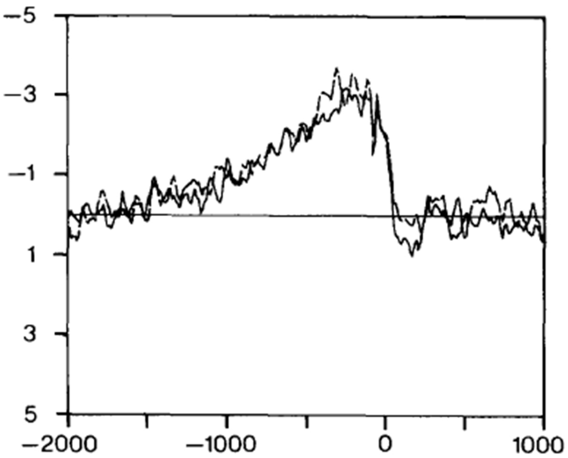

Figure 1.3: *An example of an averaged MRCP before foot movement.[Brunia & van den Bosch, 1984]*

terized, readily modulated and be detected and tracked consistently and reliably.

One problem in BCI is separating the control signals from the background EEG. Another problem with the use of EEG signal is artifacts which are interfering with the signal. In order to have an artifact free EEG to extract the control signals, the EEG have to be restored from the artifacts, such as eye-blinking, muscle activity, electrocardiograms, and any other internal or external disturbing effects.[Sanei & Chambers, 2007]
A third issue concerning the stability of a BCI system is the intra- and inter-user variations in the EEG signals. Signal features are likely to differ greatly between different users an there will possibly be even more variation in users with disabilities. The EEG will in addition naturally change over time, both between different sessions and within a single session. Studies have shown pronounced intra-individual variations in the BCI performance occurring within minutes. These changes can be due to individual factors like level of alertness, reaction speed, working memory capacity and the ability to perform parallel tasks.[Wolpaw et al., 2002; Parra et al., 2003; Buttfield et al., 2006]

The signal variations obviously generate great challenges for the development of BCI systems. To deal with these variations the classifier of the BCI system needs to adapt throughout its use and keep it tuned to drift in the signals it is receiving.[Parra et al., 2003; Buttfield et al., 2006]

1.3 Error-related potentials

To achieve a more reliable and robust BCI system the classifier needs a feedback on its performance. First of all it could be useful to detect if the classifier makes a wrong decision based on the recorded EEG and stop the BCI from executing incorrect commands. During ongoing use it might be possible to improve the performance of the classifier as well, by constantly adjusting it. One option could be to use error-related potentials (ErrP) as feedback of the classifiers performance. [Buttfield et al., 2006]

An ErrP is an event-related response from the brain as a response to an error. ErrPs provide important evaluative information, since they indicate that a behavior was inadequate given the current context and that, in future, a different response needs to be selected [Holroyd & Coles, 2002]. ErrPs can be elicited by negative feedback and by error commission itself and the generation of the ErrP is equally sensitive to errors committed by different motor modalities. Investigations suggest that the ErrP is generated in anterior cingulate cortex and it is elicited by a high-level error processing system. The anterior cingulate cortex has a great diversity of inputs from cortical and subcortical areas and is believed to be a neural center where motor intentions are mapped into action. It is believed to provide a critical pathway for emotional and motivational factors influencing motor activity and that anterior cingulate motor areas are involved in learning the mapping from intention to action by reward-related information carried to the anterior cingulate cortex by the mesencephalic dopamine system. An illustration of the error processing system can be seen in figure 1.4.[Holroyd & Coles, 2002]

A simple example of a real BCI application where ErrPs would improve the performance could be

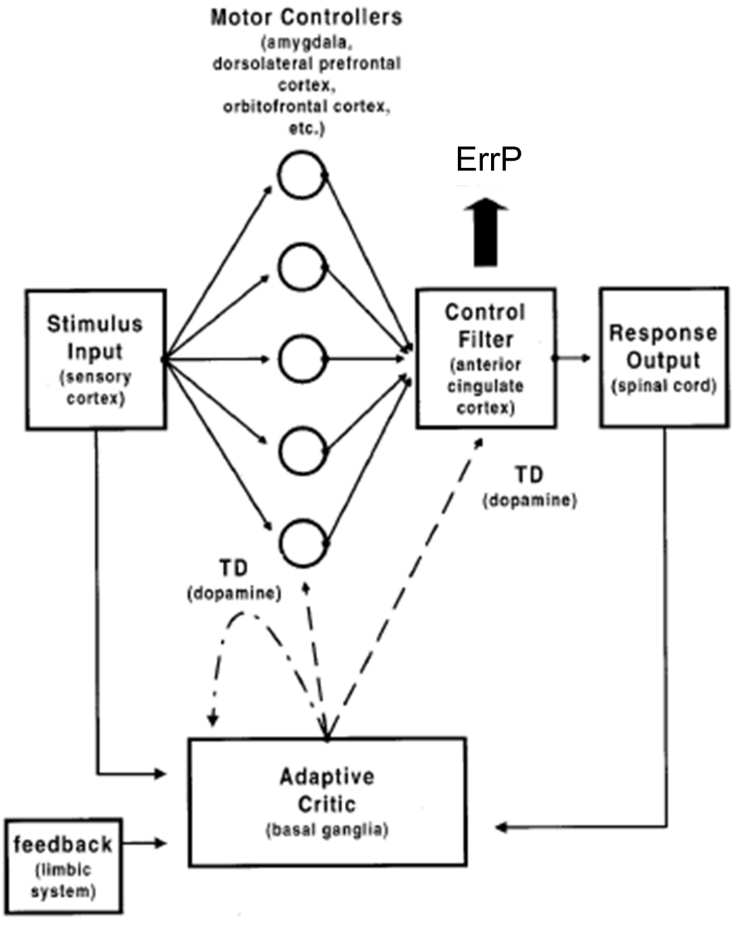

Figure 1.4: *A model of the error processing system in the brain modified from Holroyd & Coles [2002].*

to make some kind of navigation to the left and to the right based on two imaginary movements. This application could be useful if the BCI user in the long run would be able to control for example an electrical wheelchair. The classification of either left or right could maybe be improved by correcting or supporting the decision with an ErrP. The ErrP would appear from the user when a wrong decision is made based on the classification of the two imaginary movements. Detection of ErrP could either correct the decision by choosing the opposite choice or prevent executing the decision. In addition the ErrP could be used to adapt the classifier so that the users intent will be classified correctly next time.

1.3.1 Former investigations of error-related potentials

ErrPs have been investigated by different psychophysiology research groups [Falkenstein et al., 2000; Holroyd & Coles, 2002; Krigolson & Holroyd, 2006, 2007] and in recent years also in the context of BCI research [Schalk et al., 2000; Parra et al., 2003; Blankertz et al., 2003; Ferrez & del R. Millán, 2005; Buttfield et al., 2006; Ferrez & del R. Millán, 2007].

The studies can be distinguished by how the ErrP is triggered. One way is to use reaction tasks, where time pressure makes the subjects perform the task incorrectly. The ErrP can be triggered by recognition of an incorrect response by the subject itself or by feedback. Ferrez & del R. Millán [2007] uses respectively the terms 'response ErrP' and 'feedback ErrP'.

Response ErrP

In context of BCI the 'response ErrP' has been investigated in Schalk et al. [2000], where subjects were told to choose either 'YES' or 'NO' on a computer screen using a cursor controlled by the subject brain signals. The 'YES' and 'NO' appeared alternating in the top or bottom of the screen. For every selection of a word, either correct or wrong, the selected word was blinking three times, whether or not it was the correct selection. In figure 1.5 the ErrP reported by Schalk et al. [2000] is shown. The average EEG is computed for all correct hits and for all incorrect hits and subtracted. Here the dominant components are a positive peak 180 ms and a negative peak approximately 500 ms after incorrect response.

Blankertz et al. [2003] used a modified 'd2-test' where the subject should press one key when a target appeared on the screen and another key if a non-target appeared. Targets in the d2-test were compound symbols consisting of the letter 'd' and exactly two horizontal bars that may occur in four possible positions each. Non-targets either show the letter 'b' and an arbitrary number of bars (0-4) or the letter 'd' and a number of bars that differ from two. In figure 1.6 the ErrP reported by Blankertz et al. [2003] is shown. Here the components are negative peak at 30 ms and positive at 250 ms after incorrect response.

Falkenstein et al. [2000] used several Go/NoGo reaction tasks and the main components of the ErrPs reported are a negative potential showing up 80 ms after the incorrect response followed by a larger positive peak showing up approximately 300 ms after the incorrect response see figure 1.7.

Feedback ErrP

'Feedback ErrP' have been investigated by Holroyd & Coles [2002]. In their study the subject was given two different visual stimuli presented on a computer screen. The stimuli were mapped to either the left or right button. The feedback was delivered randomly as either a money-bonus reward or penalty independent on how the subject responded to the stimuli. In this study the incorrect response was characterized by a negative component peaking 250 ms after feedback, see figure 1.8.

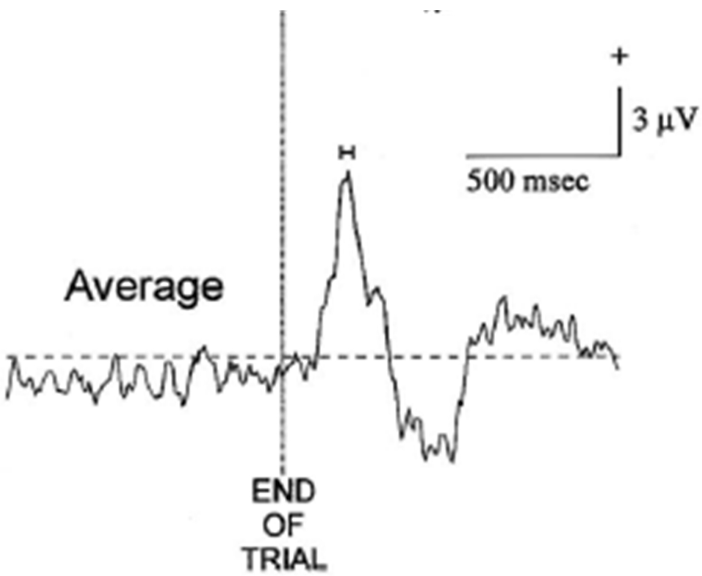

Figure 1.5: *The ErrP detected in the study by Schalk et al. [2000]. The signal shown is a grand average of difference in wave shapes (error minus correct). The signal is measured at electrode location Cz.*

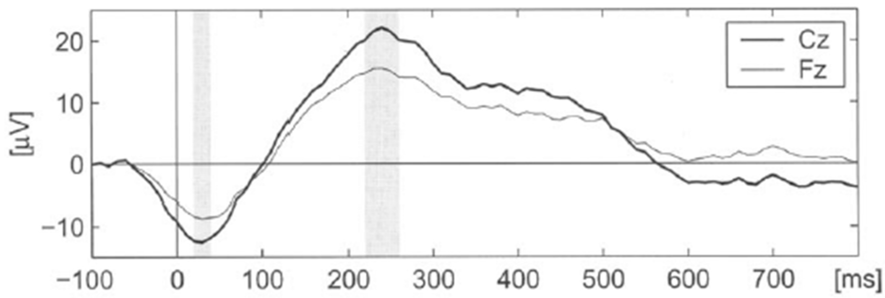

Figure 1.6: *The ErrP detected in the study by Blankertz et al. [2003]. The signals shown are grand averages of the difference in wave shapes (error minus correct). The signals are measured at electrode location Cz and Fz.*

Interaction ErrP

Recently, ErrPs triggered by the errors made by the interface and not by the subject itself has been investigated, referred to as 'interaction ErrP' [Ferrez & del R. Millán, 2005; Buttfield et al., 2006; Krigolson & Holroyd, 2007; Ferrez & del R. Millán, 2007]. In these studies, ErrP has successfully been identified in response to errors made by the BCI system. To make sure the errors is caused by interface mistakes and not the user, the task has to be quite simple. In Ferrez & del R. Millán [2007] the experiment of detecting the existence of the ErrP was accomplished by a test subject giving repetitive commands simulating the task of bringing a robot to the left or right side of a room by pressing either right or left key. The test subject receives feedback by a cursor moving to either the left or the right side of a computer screen. The interface makes a mistake during 20% of the task executions and provides the wrong feedback.

The 'interaction ErrP' seems to be quite similar to event potentials which are a response to an event the brain has been exposed to. Ferrez & del R. Millán [2005] describes the ErrP as

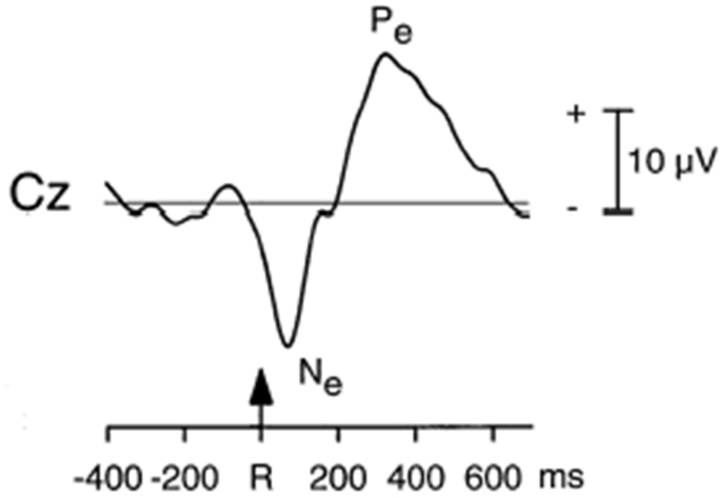

Figure 1.7: *The ErrP detected in the study by Falkenstein et al. [2000]. The signal shown is a grand average of the difference in wave shapes (error minus correct). The signal is measured at electrode location Cz.*

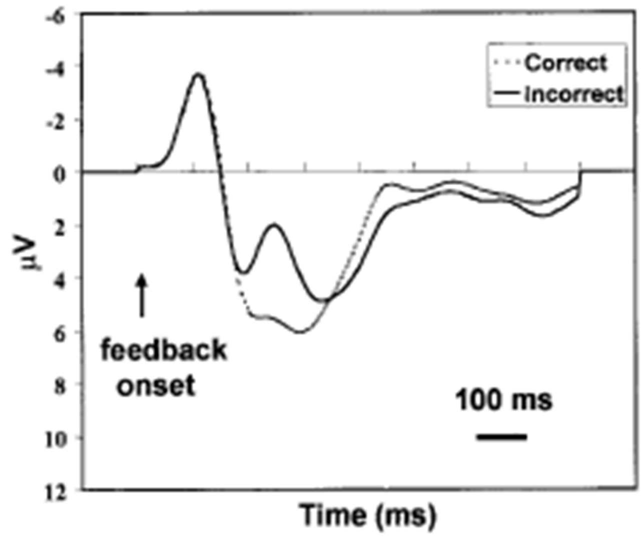

Figure 1.8: *The ErrP detected in the study by Holroyd & Coles [2002]. Mind that this is not the difference signal (error minus correct), but the response from correct and incorrect feedback. The signal is measured at electrode location Cz.*

three wave forms. First a sharp negative peak (Ne) appearing 270 ms after the test subject receives the feedback. A later positive peak (Pe) appears between 350 and 450 ms after the feedback. These two waves are the same appearing as a response to an event. But the ErrP separates from the event potentials with an additional negative peak appearing 550 ms after the feedback. In the latter study by Ferrez & del R. Millán [2007] the main components are reported to be, at first a relatively small positive peak 200 ms after the feedback, a negative peak and a positive peak 250 ms and 320 ms after the feedback, respectively and finally, a second broader negative peak about 450 ms after the feedback, see figure 1.9.

In all studies the ErrPs have been recorded within the medial-frontal cortex and it is expected that the cortical areas involved in error processing are the presupplementary motor area and anterior cingulate cortex. [Holroyd & Coles, 2002; Ferrez & del R. Millán, 2007]

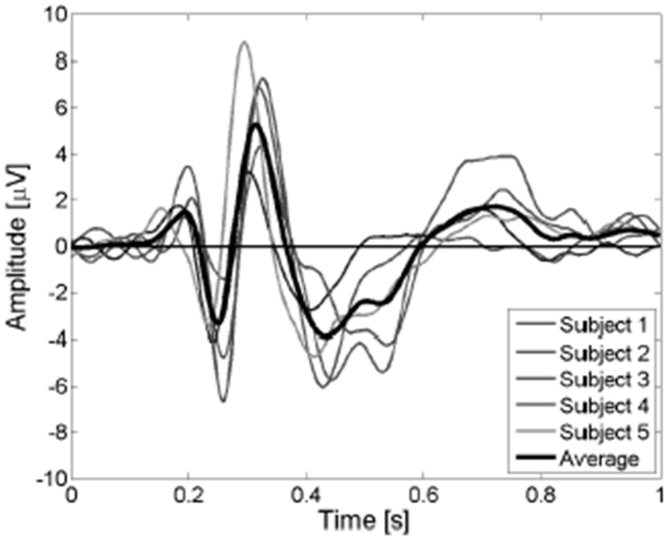

Figure 1.9: *The ErrP detected in the study by Ferrez & del R. Millán [2007].*

1.3.2 ErrP investigation in this project

To summarize last section several studies have been conducted to investigate the presence of ErrPs. Different findings due to the different approaches have been reported. Error potentials induced by the interface are still not as well documented as ErrPs induced by the users own mistakes. The two studies by Ferrez & del R. Millán [2005] and Ferrez & del R. Millán [2007] have investigated the ErrP when the interface response incorrectly to a manual task (key press) performed by the subject. Obviously this task is not representing a realistic BCI situation, which only uses the subject brain signals for task execution. Therefore it will be interesting to investigate the presence of ErrPs induced by the interfaces incorrectly response to the subjects intent only, as when no task is performed by the user manually.
The hypothesis for this study is:

'ErrPs induced by incorrectly classification of imaginary movements can be detected and classified successfully.'

The detection of ErrPs should be used to improve the accuracy of a BCI system described in Farina et al. [2007]. The system classifies MRCPs generated by variation in force related parameters during foot movement. The ErrPs should therefore follow an incorrectly classification of imaginary foot movements. It have not been possible to find any investigations of ErrPs, in relation to MRCPs during imaginary motor tasks, reported in the literature. In the following chapters of this report the work done to confirm or reject the hypothesis is presented. The work includes data collection through an experiment with a number of subjects, signal preprocessing, signal analysis, feature extraction and classification.

Chapter 2

Protocol

In this chapter the experiment which was conducted to investigate error-related potentials (ErrPs) is explained. First follows the design considerations and second the description of the setup and experiment execution.

2.1 Experimental design

The purpose of the experiment is to make a setup which will generate ErrPs which are easy to isolate and classify in a group of test subjects. To simulate a realistic BCI situation the test subject should perform an imaginary task followed by feedback on the performance of this task. That is, if the BCI system could classify the intended imaginary task correctly or not. As the detection of ErrPs should be used to improve the BCI system, described in Farina et al. [2007], the imaginary tasks chosen for the experiment are two plantar flexions with different force rates. Although no online BCI system currently is available for this type of input it was chosen to convince the subjects that an actual online classification of the recorded EEG was made. Thus the feedback to the subjects was given without any correspondence to the subjects actual performance. The outcome of this experiment is therefore dependent on how well the test subjects are convinced that their movements are classified in accordance to their intent. Furthermore is the ratio between the number of correct and error feedbacks crucial if the subject is to stay motivated during the entire session.

2.2 Experimental activity

The experiment included six subjects (three males and three females) without any right foot or ankle pathologic history. The volunteers did not suffer from any brain neurological pathology. The subject was initially convinced that he/she was in an experiment in which a BCI system was being tested and that the imaginary movements of the foot were measured and classified online.

Preparation

For preparation of the experiment the subjects were asked to perform two different tasks involving real plantar flexion of the right foot. This preparation period was made to prime the subject for the imaginary movements. The task consisted of real voluntary plantar flexion using two different rates, high rate (ballistic) and low rate (moderate). In both ballistic and moderate movement the aim was 70% of maximum voluntary contraction (MVC). Where ballistic was reaching 70% of MVC as fast as possible and the moderate was a steady increase of force

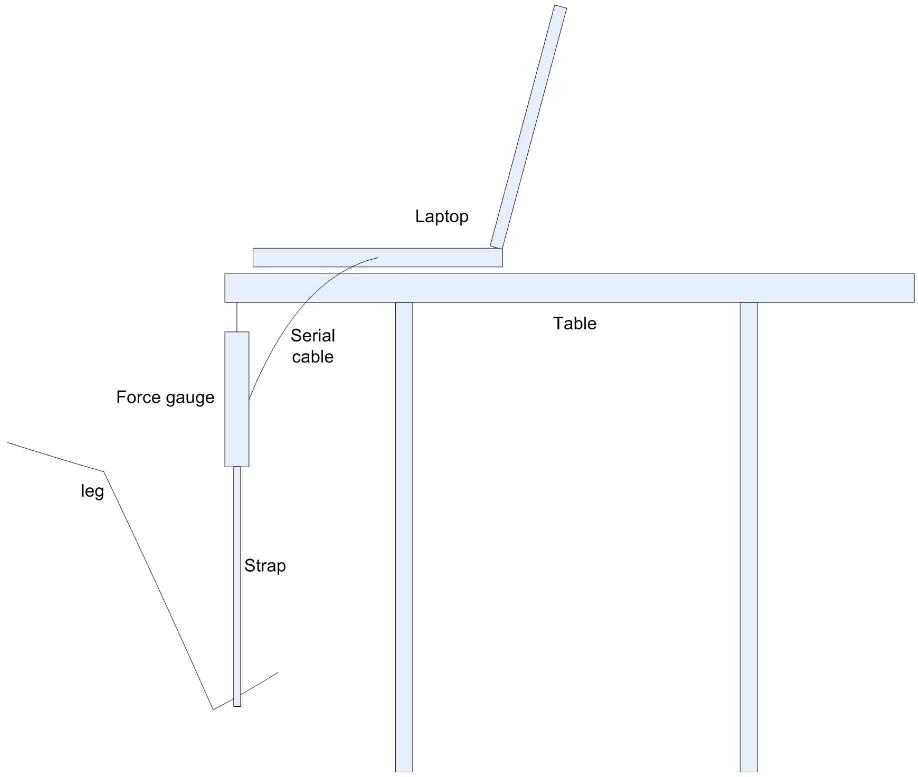

Figure 2.1: *In the figure the experimental setup for the preparation period is shown. The force applied on the strap during ankle flexion was visualized on a computer.*

with 20% of MVC per second. The test subject was instructed to place the right foot in a strap attached to a force transducer, which returned a visual feedback of the force produced by the subject through the graphical user interface. The subjects were asked to repeat each of the tasks 20 times. The setup can be seen in figure 2.1.

Actual experiment

Because the experiment was based on imaginary movements the subject was told not to move the ankle, but only imagine the movement during the experiment. They were instructed to follow the same parameters for the imaginary movement as they did during the preparation. From a computer screen the subjects were instructed to perform either an imaginary moderate plantar flexion or imaginary ballistic plantar flexion. The graphical user interface was made in LabView, view figure 2.2. The subject had to do 40 of each task chosen in randomly order to prevent the type of task affecting the outcome. A progress bar showed on the screen determined the duration of the imaginary task. After each task the subject received a feedback in terms of either "correct" or "wrong", appearing in a pop-up window on the screen, view figure 2.3. The feedback was chosen randomly (75% correct and 25% error). The subject was going through the same three sessions, run at three different days. One session contained 80 trials which were divided in groups of ten trials. One trial consisted of a preparation period before the task and a performance period where the subject had to imagine the task as instructed from the graphical user interface. In between the ten trials there was a waiting period of ten seconds. In this waiting period a pop-up window with no relevant information (the letter X) randomly appeared ten times

Figure 2.2: *The graphical user interface which instructed the test subject to do either a moderate or a ballistic movement. In the bottom of the screen the progress bar timed the task execution.*

Figure 2.3: *The pop-up window which provided feedback about the subjects performance.*

during a session, view figure 2.4. The reason for this feedback was to investigate the difference

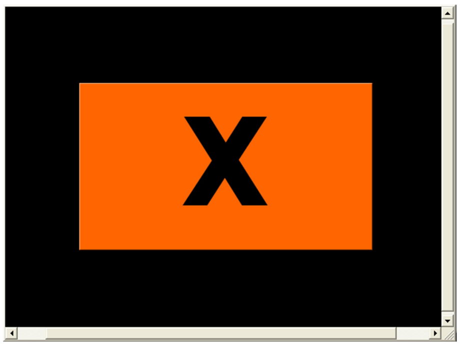

Figure 2.4: *The event pop-up window which purpose was to make a P300 response from the test subject.*

between ErrP and P300 signals. After every group of ten trials there was a short break of approximately two minutes. During the experiment the subject was settled down in a comfortable chair.

2.3 Signal acquisition and analysis

The EEG was recorded by 64 + 7 electrodes with a BioSemi digital DC amplifier using the ActiView acquisition software. The 64 electrodes scalp electrodes was mounted on an electrode cap, see electrode locations in figure 2.5. One ear lobe electrode was used as reference. The BioSemi used 2 feedback electrodes for the amplifier. The sample frequency was 512 Hz. Eye movements and blinking was recorded by 4 electrodes to make a more efficient removal of EOG from the EEG. Two electrodes were positioned above and beneath the right eye and two electrodes were positioned on the outer and inner canthi on the right eye. All recordings from all channels were preprocessed for signal enhancement. From the preprocessed recordings the signal epochs of one second before, to one second after onset of imaginary movement, were extracted for analysis of MRCPs. One second following feedback were extracted for analysis of ErrPs. Trigger signals sent from the computer showing the graphical user interface to the amplifier simplified this extraction. The analysis was focused on the channels Fz, Cz and Pz.

In figure 2.6 the signal processing of the experimental data of this study is shown.

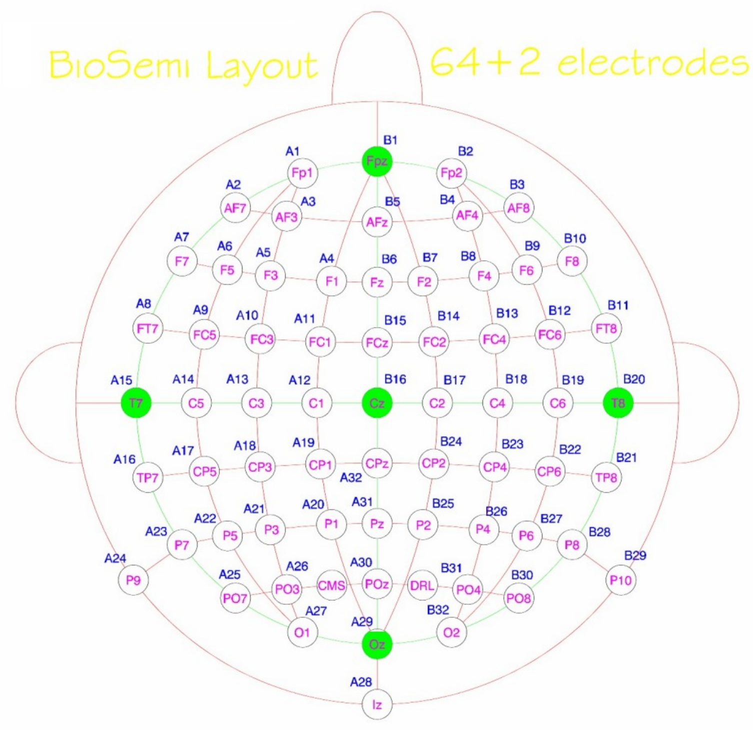

Figure 2.5: *Electrode locations for the EEG recording.[BioSemi, 2008]*

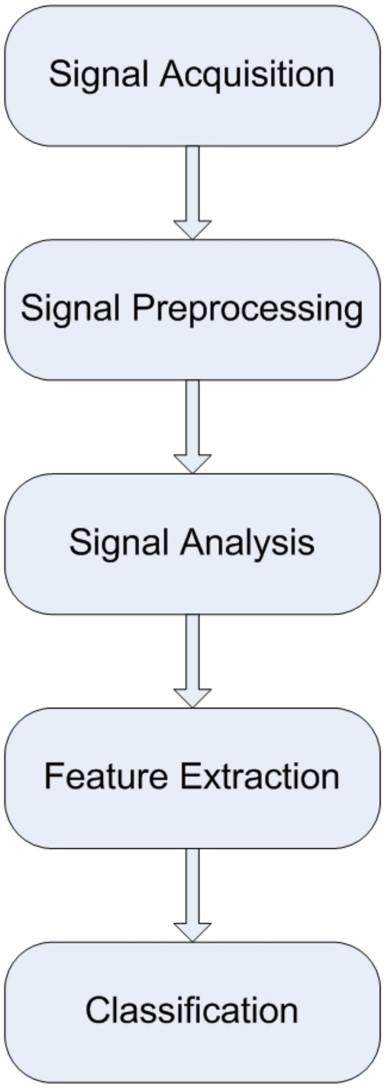

Figure 2.6: *The figure illustrates the working process of this study.*

Part II

Signal processing

Chapter 3

Preprocessing

Before the signals were useful for feature extraction and classification, the signal to noise ratio had to be improved and artifacts removed. The signal was filtered with linear filters and electrooculography (EOG) which was causing large peaks in the EEG signal was removed by independent component analysis (ICA).

3.1 Filtering

The first step of preprocessing is filtering. This part is very important for improving the signal to noise ratio. Before any filtering it is necessary to know the requirements of the filter. The easiest filter to use, but still very efficient, is a linear filter. The linear filter attenuates the signal components which are outside the stop band. The linear filter can be used as a finite impulse response (FIR) filter or an infinite impulse response (IIR) filter. The FIR has the advantage of always being stable and having linear phase shifts however they are more computationally demanding than IIR filters. The primary advantage of IIR filters over FIR filters is that they can meet a specific cutoff sharpness or slope, with a much lower filter order. The disadvantage of IIR filters is that they have nonlinear phase characteristics. However if the filtering is used on a data sequence where the entire signal is available, such as offline analysis, a noncausal technique can be used to produce zero phase filters.[Semmlow, 2004] The analysis in this project was done offline. As a result an IIR filter was chosen because it is possible to make backwards-forwards filtering which prevent time shift of the signal.

The analysis of error-related potentials (ErrPs) required a bandpass filter suited for filtering event-related potentials (ERPs). To remove low frequency baseline drift and high frequency noise from the EEG a bandpass filter is normally used. The ErrP is reported to be a low frequency signal in the range 1-10 Hz [Buttfield et al., 2006]. The response signals were bandpass filtered using a 4th order highpass Butterworth filter with cutoff frequency at 1 Hz and a 5th order lowpass Butterworth filter with cutoff frequency at 10 Hz.

The movement-related cortical potentials (MRCPs) are relatively slow cortical potentials which require a highpass filter with low cutoff frequency to prevent removing some of the low frequencies components in the signal.[do Nascimento et al., 2006] A 1st order highpass Butterworth filter with cutoff frequency at 0.1 Hz was chosen. To make sure none of the interesting components of the signal were removed and no 50 Hz powerline noise was present in the signal a 10th order lowpass Butterworth filter with cutoff frequency at 45 Hz was chosen.

The filters were implemented using forward-backward filtering giving a zero phase response. The signals were then referenced to the right ear. An alternative reference is the average signal of all EEG channels which is used by [Ferrez & del R. Millán, 2007] before detection of ErrPs. This reference method was also tried in this project but it was not preferable compared to the ear reference method. The reason for this is that the ErrP will possibly be recorded in the entire mediofrontal cortex and by using the average reference method some of the important information may be removed. Finally to remove offset every channel had its mean set to zero.

3.2 EOG removal

Before the signal can be used for feature extraction and classification, interference from EOG has to be removed. EOG causes very big distortion in the EEG signal. If an eye blink is present it can completely distort the signal and make it impossible to determine whether it is a correct or an error response. The easiest way to prevent eye blinks is to make an experimental design where the test subject has plenty of time to blink elsewhere during the trial, and instruct the subject to avoid eye blinks during the part of interest. However for some test subjects it is still not enough to prevent eye blinks in the interesting parts so it has to be removed from the signal after the experiment.

In Fatorechi et al. [2007] they investigate the methods for EOG removal used by different research groups. Most groups do not deal with EOG or they reject the trials which are distorted manually. The methods which are used to remove EOG are linear filtering, linear combination and regression, blind source separation and some non-linear adaptive methods.

- The linear filtering has already been used to remove baseline and higher frequencies, but they do not deal with any of the frequencies between the two filters. [Fatorechi et al., 2007]
- Linear combination and regression is based on subtraction some small area from an EOG channel from the desired channel, however subtracting the EOG signal may remove parts of the EEG signal, which can ruin the classification as well. [Fatorechi et al., 2007]
- Blind source separation (BSS), is an approach to estimate and recover the independent source signals using only the raw mixed EEG signal (figure 3.1). A used method for making BSS is independent components analysis (ICA). The concept of ICA is to decompose the EEG signal into their independent components and because the EOG is an independent component it should be easy to remove. However a disadvantage of this method is that it is very slow to calculate which makes it almost impossible to use online. In addition the EOG components have to be identified before removal. [Fatorechi et al., 2007]
- Non-linear adaptive methods has according to Fatorechi et al. [2007] not shown to be an efficient way of removing EOG.

Based on the conclusion in Fatorechi et al. [2007]; Li et al. [2006]; Jung et al. [2000]; Krishnaveni et al. [2006] it was assumed that the most suited method for removing EOG in this project was by blind source separation. There was no need of online removal of EOG because the data analysis was done offline. The other issue about blind source separation is to choose which of the components to remove and which to keep. This problem was approached by implementing an automatic method which removed the components that were most alike the EOG signals recorded with the eye electrodes.

3.2.1 Independent component analysis

The EEG signal is a mix of the electrical activity of all the neurons in the brain and different kind of interfering artifacts from the body itself and the measuring equipment. In the use of BCI it is typically specific signal components which are of interest. The concept of ICA is to decompose the EEG signal into their independent components (ICs). Using the simplest assumptions about the mixing medium of the EEG signal; the source signals arrive at the sensors at the same time, the BSS model can be formulated as:

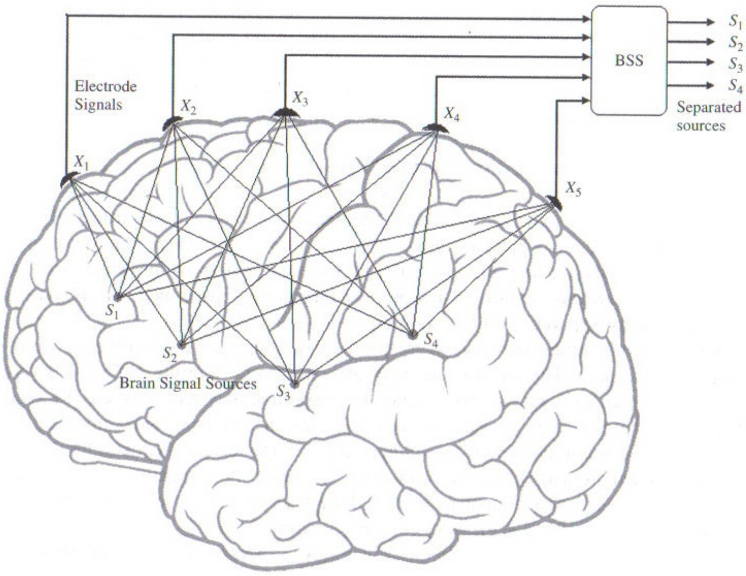

Figure 3.1: *The figure illustrates the concept of blind source separation applied to EEG recordings.[Sanei & Chambers, 2007]*

$$\bar{x}(n) = \bar{H}\bar{s}(n) + \bar{v}(n) \tag{3.1}$$

Where $\bar{s}(n)$ has the dimensions of $(m \times 1)$, and $\bar{x}(n)$ $(n_e \times 1)$ and $\bar{v}(n)$ $(n_e \times 1)$ denote respectively the vectors for source signal, observed signal, and noise at discrete time n. The n_e denotes the number of electrodes used to record the EEG signal and m the unknown number of independent sources in the brain. $\bar{H}$ is a mixing matrix of size $n_e \times m$. To reconstruct the original EEG signal is performed by:

$$\bar{y}(n) = \bar{W}\bar{x}(n) \tag{3.2}$$

Where $\bar{W}$ is a separating matrix of size $m \times n_e$, which uses only the information about $\bar{x}(n)$. If this assumption is left out of account different delays and attenuation from the different sources has to be considered. The mixing process may be given as:

$$x_i(n) = \sum_{j=1}^{M} h_{ij}s_j(n - \delta_{ij}) + v_i(n), \quad for\ i = 1, \ldots, N \tag{3.3}$$

Where the attenuation, h_{ij}, and delay, δ_{ij}, of source j to sensor i is determined by the distance between the source and sensor. With this mixing process the reconstruction process will be expanded as well:

$$y_j(m) = \sum_{i=1}^{N} w_{ji} x_i(m - \delta_{ji}), \qquad for\ j = 1, \ldots, M \tag{3.4}$$

Where w_{ji} is the elements of W. This model is difficult to apply on EEG signal because the number of sources is unknown which makes the separation matrix impossible to construct. This problem has been solved by different kind of statistics. One method is the fast ICA. The main part of using this method is nongaussianity. This is a result of probability theory telling that the distribution of a sum of two independent random variables usually has a distribution that is closer to Gaussian than any of the two original random variables. By using statistic tools as kurtosis the sources can be extracted one-by-one. [Sanei & Chambers, 2007]

The method used for ICA in this project is the one included in the EEGLAB toolbox which is based on the infomax algorithm developed by Bell & Sejnowski [1995] [CNL/The Salk Institute, 2008]. The ICA algorithm is based on minimizes the mutual information among the data projections or maximizes their joint entropy. The method seeks to find component time courses that are mutually independent, meaning that component cross-correlations as well as all the higher order moments of the signals are zero.[Delorme & Makeig, 2004]

3.2.2 Implementation considerations of ICA

The main use of ICA in the project was to remove EOG from the recorded EEG which could improve the detection of the ErrP. In figure 3.2 the original recorded EEG with eye blink is illustrated, the high spike in the middle of the signal across the channels is a eye blink which clearly will give problems for detection of the ErrPs. Instead of using manually selection of the EOG components from the EEG, which can be done by investigation the time course and the corresponding spatial scalp topography of each IC, an automatically detection of the EOG components are used. In figure 3.3 some of the independent components are showed. The EOG components from the ICA are selected by comparing the ICs with EOG recorded from electrodes placed around the eye. To use the eye recorded EOG to remove the right IC a similarity or distance between each decomposed independent components and the EOG has to be calculated. Li et al. [2006] proposed to calculate the angle between each scalp topography of the IC and a template topography made from manually detected eye blinks in the EEG. In this project it was proposed to use the angle to calculate the similarity between the recorded EOG and the decomposed IC. The angle between the eye recorded EOG channels and the ICs was calculated by following equation:

$$\alpha_{j,i} = cos^{-1}\left[\frac{ICeeg_j \cdot EOG_i}{\|ICeeg_j\|\,\|EOG_i\|}\right] \tag{3.5}$$

The eye recorded EOG is termed EOG and calculated for each of the four EOG channels, the scalp recorded independent components being $ICeeg_j,\ j = 1, ..., N$, where N is the number of independent components and $i = 1, .., K$ where K is the number of recorded EOG channels. If α_j was less or higher than two predefined thresholds the j'th IC was assumed to be an eye blink component and removed. The high and low thresholds were set to 1.8 and 1.4 radians, where 1.6 corresponds to completely independence between the IC and EOG. The corrected EEG can be seen in figure 3.4 after removing ICs which was classified as EOG.

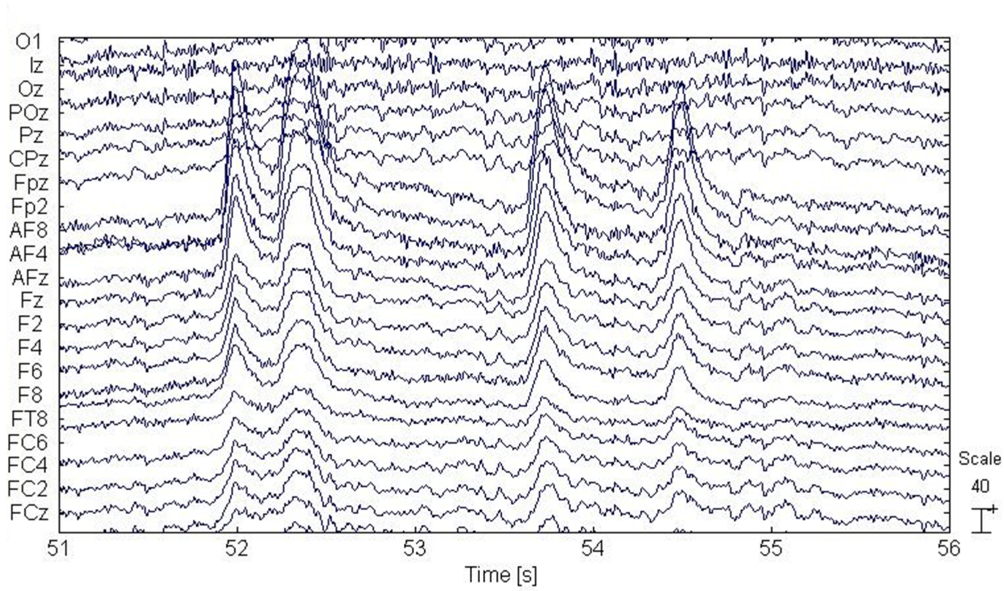

Figure 3.2: *The spikes in the middle of the figure are eye blinks from which have the highest amplitude in the frontal part of the head.*

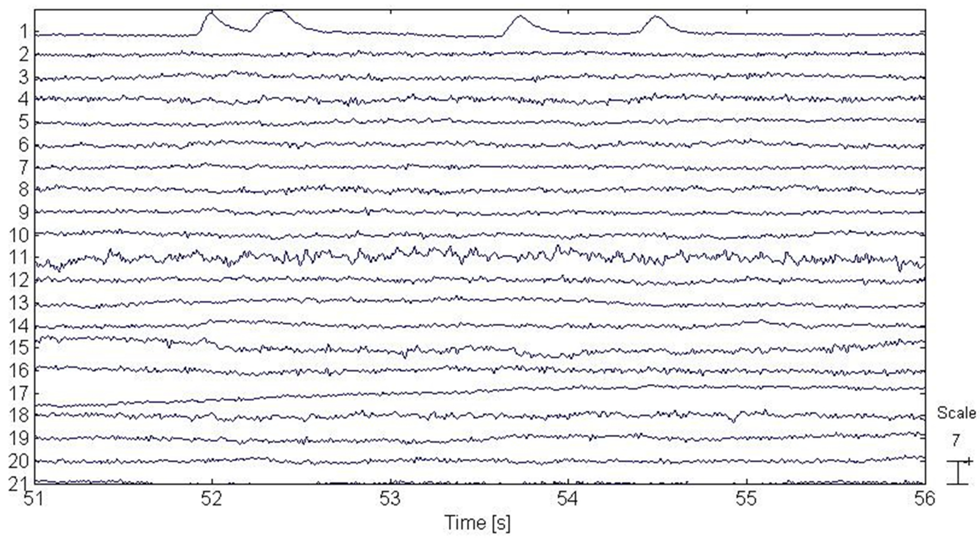

Figure 3.3: *The independent components from the signal are showed. It is clear that the first IC is related to EOG.*

3.2.3 Evaluation of EOG correction

It is clearly very important for further analysis and classification of the EEG signals that the ICA method efficiently removes EOG components from the EEG without any distortion of the

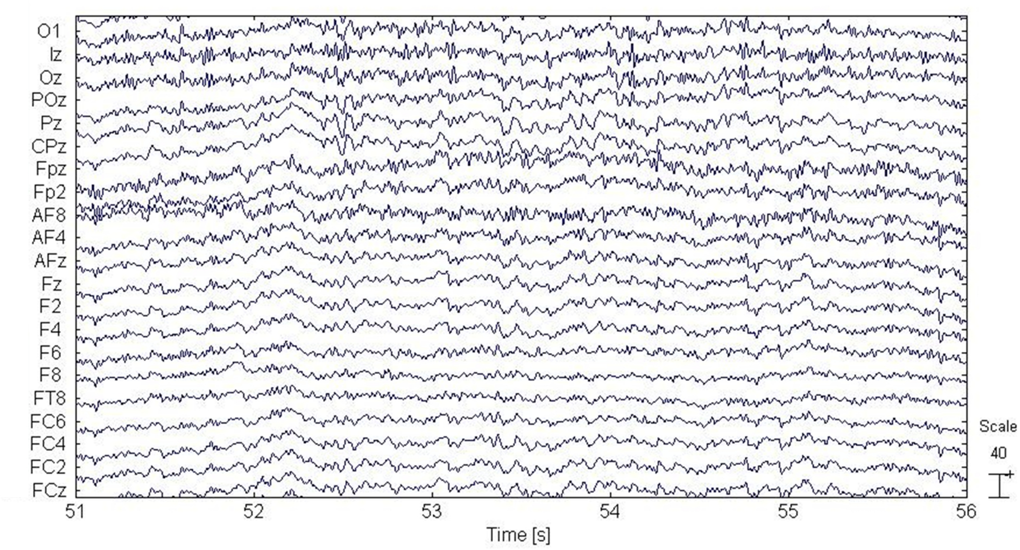

Figure 3.4: *The corrected EEG.*

signal. Figure 3.4 shows that the method removed most EOG leaving only a minimal corruption. To evaluate if the method distort the EEG in any other way is more complicated. The easiest approach is to manually take out all trials not corrupted by EOG and calculate the average of these signals (manually-corrected average). By comparing that manually-corrected average to the average of all trials with EOG correction (ICA-corrected average) one can visually evaluate if the two waveforms have a similar shape or if the EOG correction have caused a distortion. In figure 3.5 (A) and 3.6 (A) the outcome of this approach can be seen for subject 1 and subject 4 respectively. Subject 1 and 4 were chosen because they were the only two where it was possible to extract trials without any interference from EOG, to make the manually-corrected average. Only correct trials were used for this evaluation. It can be seen that the wave shapes of the ICA-corrected average and manually-corrected average have very similar characteristics and time course. It has to be taken into account that the ICA-corrected waveforms were made by average of 180 trials whereas the others were made of only 20 and 34 trials for subject 1 and 4 respectively. In (B) the average of all correct trials without any EOG correction is shown. Especially for subject 1 the shape of the waveform differs from the ones shown in (A) as a large negative deflection caused by eye blinking is present around 600 ms after feedback.

In figure 3.7 all steps of the signal preprocessing are illustrated. After these steps the signal to noise ratio of the EEG signals should be increased to improve the following feature extraction and classification.

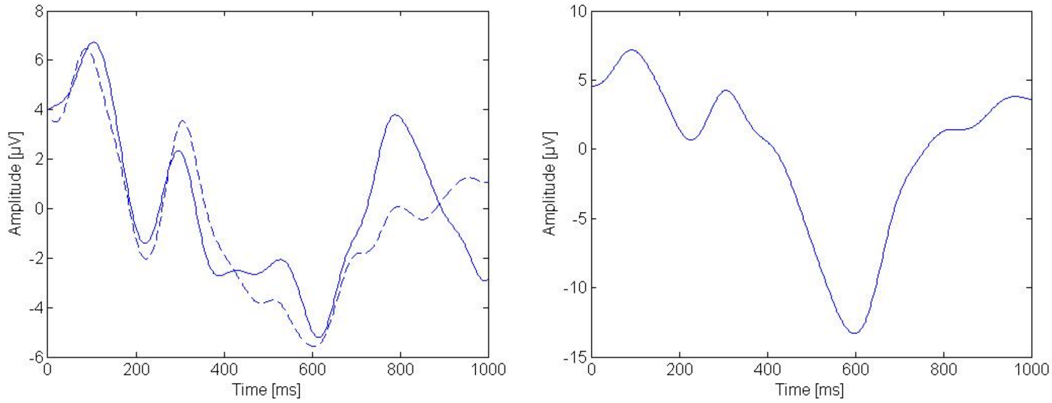

(A) ***(B)***

Figure 3.5: *In (A) is the ICA-correcte average (dashed) of the all correct trials (n=180) shown for subject 1. The manually-corrected average (solid, n=20). In (B) the average of all correct trials without any EOG correction is shown.*

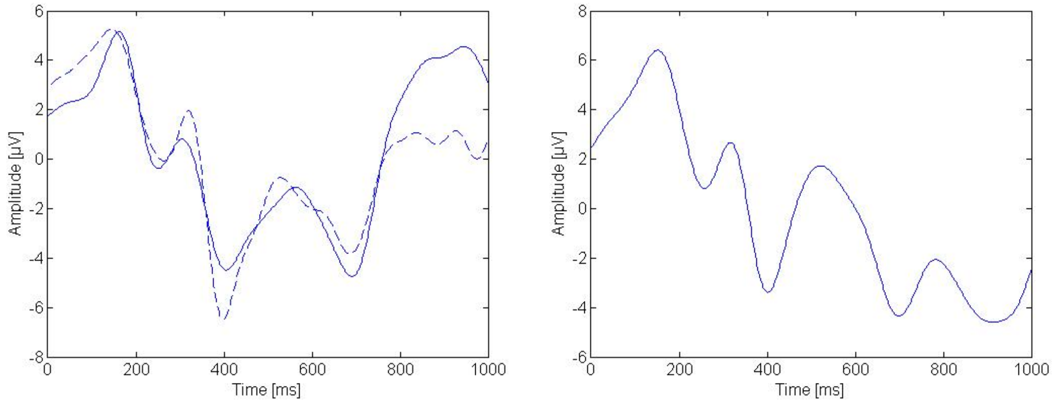

(A) ***(B)***

Figure 3.6: *In (A) is the ICA-correcte average (dashed) of the all correct trials (n=180) shown for subject 4. The manually-corrected average (solid, n=34). In (B) the average of all correct trials without any EOG correction is shown.*

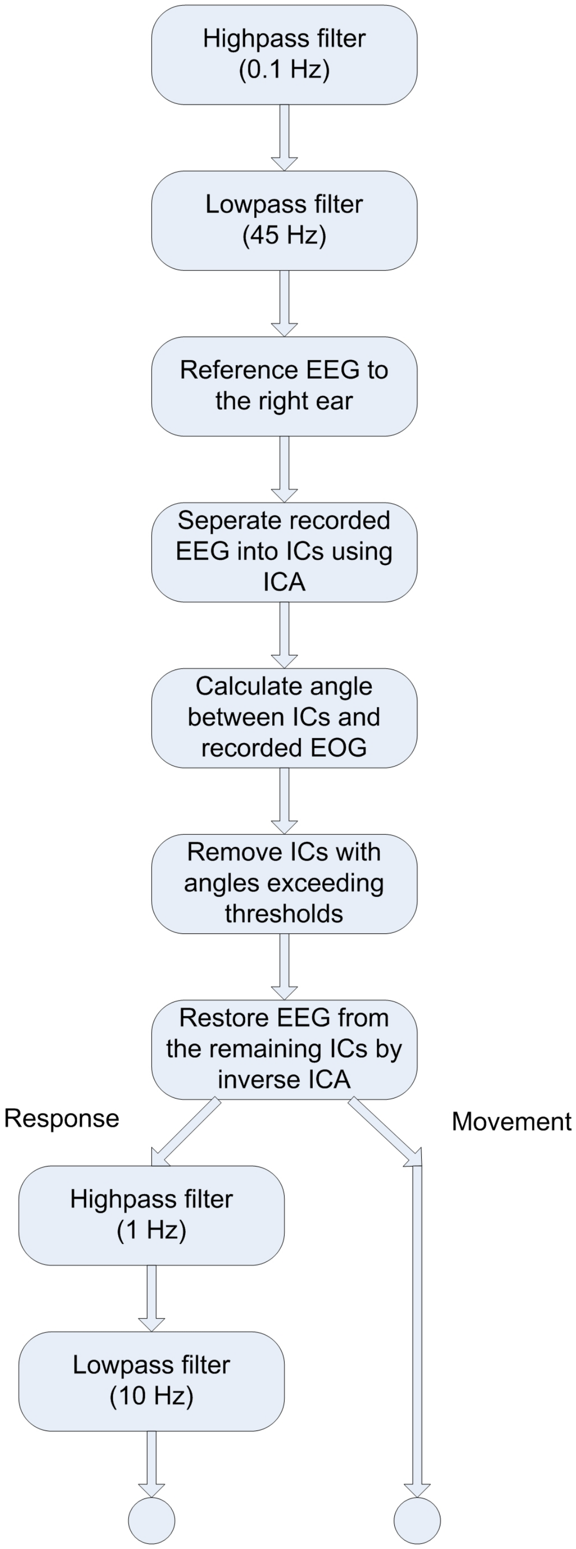

Figure 3.7: *Illustration of the preprocessing steps.*

Chapter 4

Signal analysis

In this chapter the preprocessed EEG recordings will be analysed to see if signal averages reveal the presence of the error related potential (ErrP). This chapter should give an insight to the signal quality and characteristics of the subjects included in the experiment.

As explained in the pre-analysis the appearance of the signals vary quite a lot from study to study, which was the case in this study as well. There were also large variations from subject to subject. Former investigations suggest that the ErrPs are generated in the anterior cingulate cortex and presupplementary motor cortex.[Ferrez & del R. Millán, 2007; Holroyd & Coles, 2002] To validate if this information holds for this study as well, a grand average of the six subjects scalp topographies is made, see figure 4.1 and 4.2. The topographies are made of the recorded response at time instances from 0 to 950 ms after feedback with a interval of 50 ms. Especially the topographies at the time instances 200 ms, 300 ms and 500 ms are of interest as this approximately are the latencies for the ErrP described by Ferrez & del R. Millán [2007]. From the topographies it seems that most cortical activity is generated along the central line of the brain. During one second after feedback there is activity in both frontal, central and parietal areas of the brain and it is therefore interesting to analyze the response recorded from electrode location Fz, Cz and Pz. The topographies give no information about difference in the brain areas activated after error and correct feedback.

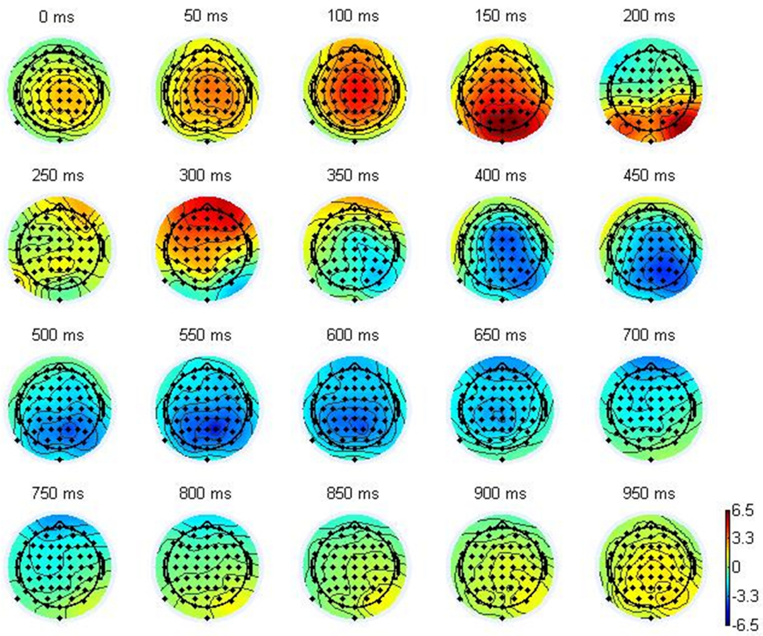

Figure 4.1: *The grand average scalp topographies for all subjects from 0 to 950 ms after correct feedback. The channels P2, P8 P10 and O2 are removed due to large noise interference.*

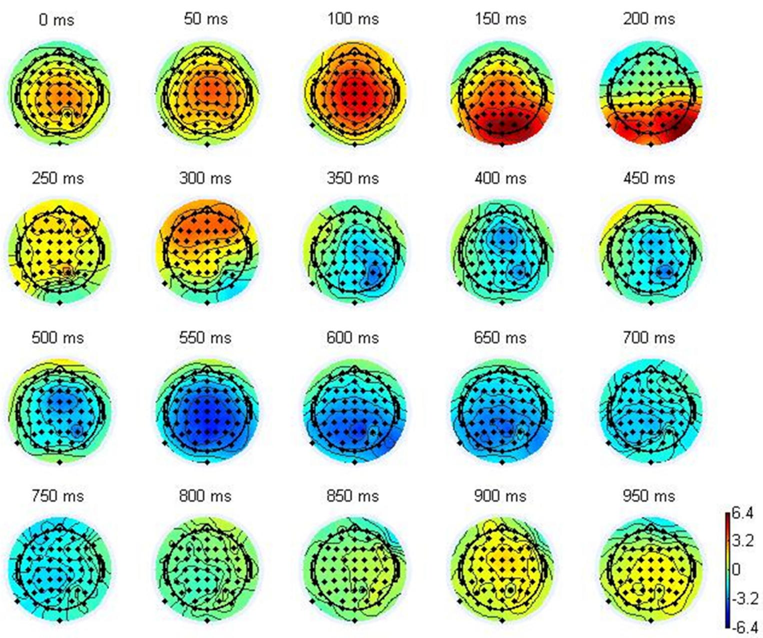

Figure 4.2: *The grand average scalp topographies for all subjects from 0 to 950 ms after error feedback. The channels P2, P8 P10 and O2 are removed due to large noise interference.*

4.1 The response to feedback

The grand average response after feedback of all six subjects can be seen in figure 4.3, 4.4 and 4.5 recorded at Fz, Cz and Pz respectively. The grand averages show a negative peak at 200 ms, positive peak at 300 ms and broad negativity from 400 ms to 700 ms after feedback. The error feedback seem to generate a slightly more negative amplitude between 500 and 600 ms compared to correct feedback. The grand average response after the X-event show negative peak at 200 ms a positive peak at 300 ms and a broader negative peak between 500 and 600 ms. At Fz and Cz the negative peak at 200 ms and the positive at 300 seem to be more clear compared to the response recorded at Pz. The averaged response signals for the subjects individually can be seen in appendix D.

There are clearly some variations between the different signals from subject to subject, but also some consistency in the characteristics. The primary purpose of the X-events showed to the subject was to clear if the response recorded after the error and correct feedback, mainly was a result of the visual stimuli or the actually information about their performance. The three peaks at approximately 200 ms, 300 ms and between 400 and 600 ms respectively are present after error and correct feedback as well as after the event. This implies that none of the elicited peaks are exclusively related to error perception. On the contrary Ferrez & del R. Millán [2007] reports three very similar peaks, with similar latencies as being error related. The error and correct feedback and the event which in this experiment are given by a pop-up window might all be characterized as infrequent events. Therefore the negative peak at 200 ms and the positive at 300 ms, are very likely to be contributed by the N200 and P300 which both are well documented responses after a infrequent visual event.[Patel & Azzam, 2005; Friedmann et al., 2001; Sanei & Chambers, 2007] A negative peak at 400 ms, the N400 is reported to be present after semantic stimuli, such as a word or number within a prior context.[Sanei & Chambers, 2007; Fogelson et al., 2004; Fonseca et al., 2006; Lang & Kotchoubey, 2000] The late negative peak seen between 400 and 600 ms could be related to this semantic process. This peak however has in the response from three subjects (subject 1, 4 and 5) either a more negative amplitude or a longer duration after error feedback than after correct feedback. This implies that the peak also could be contributed by an error potential.

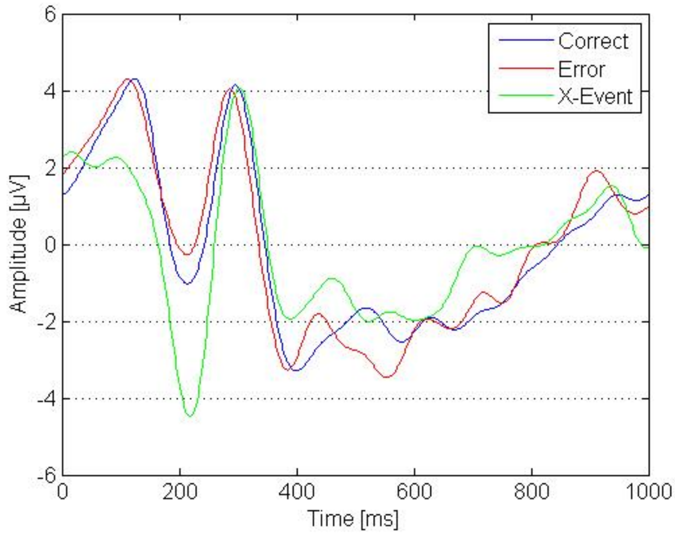

Figure 4.3: *The grand average response signals from correct and error feedback and X-event for all six subjects, recorded at electrode location Fz. Feedback was presented at time 0 seconds. The signals are averages of the recordings from all 3 sessions.*

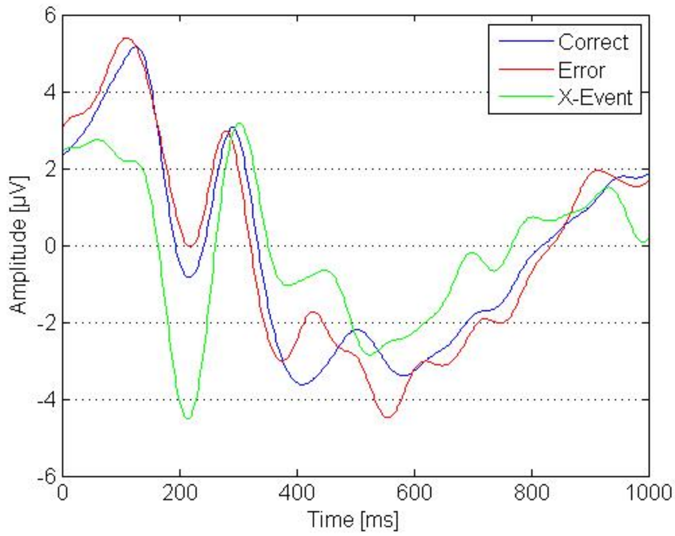

Figure 4.4: *The grand average response signals from correct and error feedback and X-event for all six subjects, recorded at electrode location Cz. Feedback was presented at time 0 seconds. The signals are averages of the recordings from all 3 sessions.*

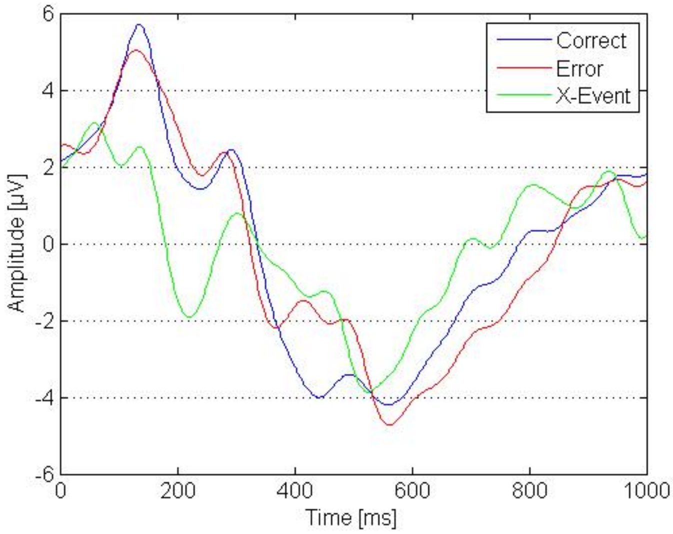

Figure 4.5: *The grand average response signals from correct and error feedback and X-event for all six subjects, recorded at electrode location Pz. Feedback was presented at time 0 seconds. The signals are averages of the recordings from all 3 sessions.*

4.2 Imaginary movements

As the ErrP is suggested to be related to the performance of motor tasks, the motor-related cortical potentials (MRCPs) measured during the subjects imaginary ankle movement tasks will be analyzed. The measured signal was expected to be a slow, but strong negative deflection starting around one second before movement execution. In figure 4.6 the grand average signal from one second before to one second after movement onset is shown. It can be seen that the negative deflection does not start until after movement onset and does not seem to be as slow as reported in the literature.[Brunia & van den Bosch, 1984; do Nascimento et al., 2006] These unexpected findings can be caused by the relative long performance period of six seconds, which may have affected the timing of the task onset to be very subjective. The subjects probably engage to the task after the onset indicator, meaning that the imaginary movement will start sometime after time 0 seconds. The strong similarity of both MRCPs may be an indicator that variations of rate of force development are not something that can be easily imagined. The sharp and large MRCP peaks observed may be a consequence that ballistic movements may be more easily assimilated and generate larger cortical responses.

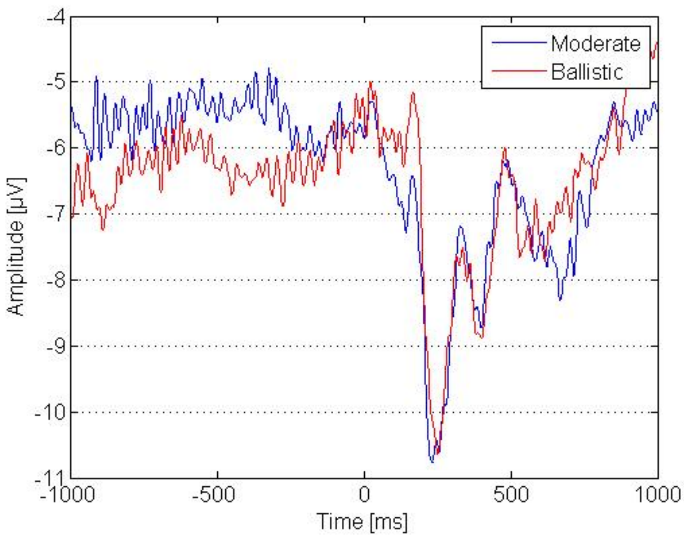

Figure 4.6: *The grand average of the recorded signal for all six subject one second before to one second after onset of imaginary movement. An MRCP can be seen starting after time 0 seconds.*

Chapter 5

Feature extraction

In this chapter feature extraction methods for detection of error related potentials (ErrPs) will be explained. The usefulness of the features will be evaluated in chapter 7.

5.1 Features for brain-computer interface

The ErrPs, are like most event-related potentials from the brain, very difficult to characterize because of large variation from signal to signal. It is probably difficult to establish any morphology features for the ErrP. The amplitude of the signal is sometimes smaller than the background EEG signal which often drowns the ErrP, and make it almost impossible to detect.[Sanei & Chambers, 2007] The difficulties of extracting any useful features made other groups use the recorded signal as a feature vector [Ferrez & del R. Millán, 2005; Parra et al., 2003; Blankertz et al., 2003]. In this study however, it has to be investigated what features are most useful for the classification of ErrP. Various feature extraction methods has been tried by different research groups to classify slow cortical potentials and P300 which characteristics may have some similarity to the ErrP. According to Bashashati et al. [2007]; Mason et al. [2007] various types of time/frequency analysis, correlation with a template and peak and area calculation has been tried and hence these methods were considered in this project.

- Features extracted from a wavelet transform were tried as a time/frequency analysis in this study. This feature extraction approach was tried in two different variants. The first one is based on a method suggested by Bostanov [2004] and called t-CWT.
- Correlation with a template can be characterized as a feature extraction method as well as a classification method and therefore will be described in section 6.2.
- Due the very poor signal to noise ratio in single trials peak and area calculation was not tried because it was almost impossible to find any shapes in the signals. However some statistic features were calculated which could serve as replacement for these features.

In the following the different methods will be explained. It was additionally tried to gather all the features including the signal in one large feature space. To prevent redundancy, principal component analysis (PCA) was calculated and features which did not provide any information to the classification were rejected. The new feature space from the PCA was used as features as well.

5.2 Wavelet feature extraction

The wavelet transform is related to Fourier transform where a signal is described by sine functions. Instead of using sine functions the wavelet transform is using a waveform which changes over time, by changing the scale of the waveform.[Semmlow, 2004] The wavelet transform (WT) is a joint time-frequency analysis. Wavelets have been proven to be appropriate starting points for the classification of the measured signals. They allow extraction of richer problem specific information from sensor signals. Based on this transform, several methods have been developed to capture sensor signal features. [Pittner & Kamarthi, 1999]

The wavelet transform can be implemented as a continuous wavelet transform CWT and a discrete wavelet transform DWT. The two methods are quite similar however the DWT is reducing the number of wavelet coefficients by changing the scale and translation in powers of 2, which will produce a nonredundant transform of a signal. This is not the case with the CWT which is highly redundant by producing a lot of information which is useless if an inverse transformation has to be made.[Semmlow, 2004] However if the wavelet transform is used to find shapes like ERP it is more likely to find a scale of the wavelet which fits the waveform in the signal.[Bostanov, 2004] The definition of the continuous wavelet transform of signal $f(t)$ is:

$$W(a,b) = \frac{1}{\sqrt{a}} \int_{-\infty}^{\infty} f(t)\Psi(\frac{t-b}{a})dt \tag{5.1}$$

Where b denotes the time shift (the position parameter), a denotes the scale parameter (inversely proportional to frequency). The wavelet coefficients, $W(a,b)$, describe the correlation between the waveforms in the signal and the wavelet at various translations and scales: the similarity between the waveform and the wavelet at a given combination of scale and position, a, b. Semmlow [2004]. Ψ is the wavelet function, which has zero mean:

$$\int_{-\infty}^{\infty} \Psi(t)dt = 0 \tag{5.2}$$

The transform is linear and is invariant under translations and dilation:

$$If \quad f(t) \rightarrow W(a,b) \ then \ f(t-\tau) \rightarrow W(a, b-\tau) \tag{5.3}$$

and

$$f(\sigma t) \rightarrow \frac{1}{\sqrt{\sigma}} W(\sigma a, \sigma b) \tag{5.4}$$

The continuous wavelet transform is a kind of template matching, a computation of the cross correlation between the signal and the predefined waveform, the template Ψ, which is shifted forward and backward in time and dilated and constricted in scale. The local extreme values from $W(a,b)$ indicates were the best match between the wavelet template and signal in the time-frequency domain. The choice of which wavelet to use for the continuous wavelet transform depends on how well localized the time or scale has to be. The Mexican Hat wavelet, which is well localized in the time domain, are used for detection of ERP components, whereas wavelets that are well localized in the frequency domain, like the Morlet wavelet, are used for detection of salient oscillations [Bostanov, 2004]. In figure 5.1 the two mother wavelets are shown, where (A) is the Mexican Hat and (B) is the Morlet Hat. In this project a Mexican hat is used which is the second derivative of a Gaussian waveform:

$$\Psi(t) = (1-t^2)e^{-0.5t^2} \tag{5.5}$$

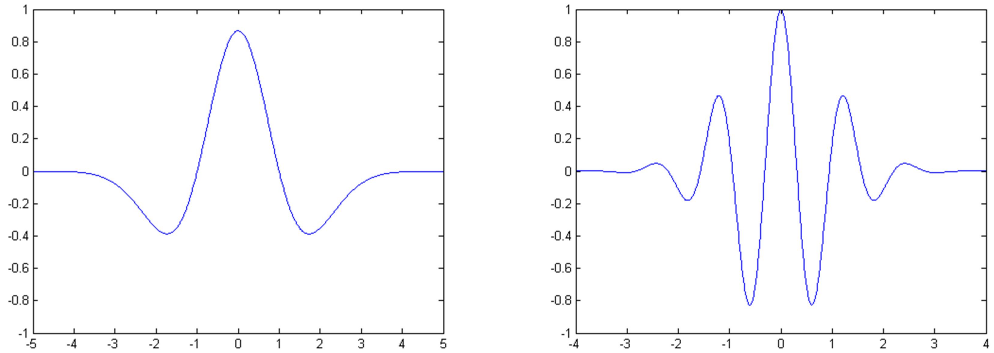

Figure 5.1: *The Mexican Hat wavelet (A) which is good for locate objects in time domain and the Morlet Hat (B) which is used to detect objects in the frequency domain.*

[Sanei & Chambers, 2007]

There have been implemented and tested two different methods to extract features from the continues wavelet function. These methods will be described in the following.

5.2.1 First wavelet feature

In the first method the feature extraction from the wavelet transform is done by a method proposed by Bostanov [2004]. The data is divided in a training set and a test set, same way as classifiers which need both to train and evaluate the classification. In the method the training set is used to find the coordinates which in the end should provide the values where there is most information about the difference between error and correct feedback responses in time and scale. The method proposed is called t-CWT and is performed in five steps.

The first step is to calculate the CWT, $W^n(a,b)$ of the signal $f^n(t)$ which is calculated for every trial n.

The second step is to calculate the mean $\overline{W_g(a,b)}$ and variance $\sigma_g(a,b)$ from each CWT of each trial:

$$\overline{W_g(a,b)} = \frac{1}{N_g}\sum_{n=1}^{N_g} W^n(a,b) \tag{5.6}$$

$$\sigma_g(a,b) = \frac{1}{N_g - 1}\sum_{n=1}^{N_g}(W^n(a,b) - \overline{W_g(a,b)})^2 \tag{5.7}$$

Where N_g is the number of trials in group (g = correct or error)

The third is to calculate the t-statistic of the trials $t(a,b)$:

$$t(a,b) = \frac{\overline{W_{correct}(a,b)} - \overline{W_{error}(a,b)}}{\sqrt{\sigma_{correct-error}(a,b)}} \tag{5.8}$$

Where:

$$\sigma_{correct-error}(a,b) = \frac{(n_{correct}-1)\sigma_{correct} + (n_{error}-1)\sigma_{error}}{n_{correct}+n_{error}-2}\left(\frac{1}{n_{correct}} + \frac{1}{n_{error}}\right) \quad (5.9)$$

[Bostanov, 2004]

In figure 5.2 the $t(a,b)$ is shown from data recorded during one session from test subject 4 with 20 error and 60 correct trials. The t-test is a useful tool to calculate how equal two different populations are. The t-test determines whether two given data sets each characterized by its mean, standard deviation and number of data points are distinct, taking variance into account.[Ross, 2004]

The fourth step is extracting the local extremes of the function $t(a,b)$ referred to as (a^i, b^i)

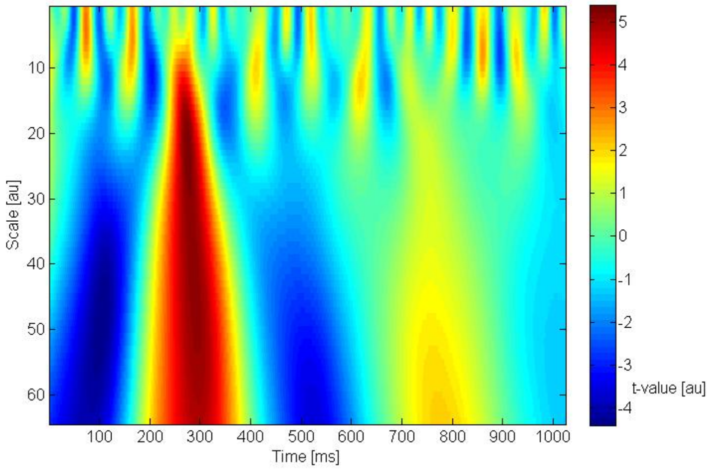

Figure 5.2: *The t-test for each time and scale from the wavelets of correct and error from subject 4.*

which are the point of maximal difference between correct and error feedback responses. The fifth and last step is to compute each point (a^i, b^i) for each single trial n for both the test and the training data.[Bostanov, 2004]

In the figure 5.2 it is possible to see where the largest difference between the two classes after feedback is, which gives a good indication where the error potentials are best located, and thus where the best area for feature extraction is. The area with dark blue and dark red indicate where the largest difference is.
The 15 maximums and 15 minimums with highest values are chosen to use as features for training and test, giving a total number of 30 features for each trial.

5.2.2 Second wavelet feature

The second wavelet feature extraction is similar to the first one but the data is not divided in two sets as in the first one. In the other method the CWT was calculated for all the trials in the training set and used in a t-test to calculate where the large difference was located and detecting the local maximum and minimum values in the data from the t-test. In this method the local maximums values and coordinates are calculated for each trial, which is used as training and

test in the classifier. In this method the 15 maximums and 15 minimums with highest values are chosen and additionally the coordinates are found as well for every extreme value, which brings the total number of features to 90.
As in the other method the first step is to calculate the CWT, $W^n(a,b)$ of the signal $f^n(t)$ for each trial n. The second step is to detect all the local extremes in the wavelet transform. Using this approach information on frequency and time differences between correct and error trials is included in the features.

5.3 Statistical features

As mentioned earlier the SNR of the EEG signals are very low, and it is almost impossible to find any characteristic in single trials. It is still assumed that it should be possible to detect small changes between correct and error trials even in single trials which statistic features maybe could indicate.

Statistical features are useful to describe the probability distribution of the signal from each trial. To describe the probability distribution of the signal mean and variance are calculated, and for describing the shape of the probability distribution skewness and kurtosis are calculated. The mean is calculated by following equation:

$$mean(x) = \frac{1}{n} \cdot \sum_{i=1}^{n} x_i \tag{5.10}$$

And the variance is calculated by following equation:

$$var(x) = \frac{1}{n} \cdot \sum_{i=1}^{n} (x_i - \mu)^2 \tag{5.11}$$

Skewness, the third standardized moment, is a measure of the asymmetry of the probability distribution which is calculated by following equation:

$$skew(x) = \frac{\sqrt{n}\sum_{i=1}^{n}(x_i - \mu)^3}{(\sum_{i=1}^{n}(x_i - \mu)^2)^{3/2}} \tag{5.12}$$

Kurtosis, the fourth standardized moment, is a measure of the "peakedness" of the probability distribution of the signal:

$$kurt(x) = \frac{n\sum_{i=1}^{n}(x_i - \mu)^4}{(\sum_{i=1}^{n}(x_i - \mu)^2)^2} - 3 \tag{5.13}$$

three is subtracted to give a kurtosis of zero which for a standard normal distribution would have been three.[Ross, 2004]

The four statistic features only provide with one value each for one single trials giving a total number of four features which is a bit few with such a complicated signal, however it is very fast to calculate and easy to use in a classifier. If it is giving equally good classification with some of the other methods the statistic features is preferable.

5.4 Principal component analysis

If the signal and the features from wavelet and statistic features are gathered to one feature vector it would end up giving a lot of features where some of them do not add any useful information to the classification. If there are too many features represented with no information of the two classes it will only reduce the chances of making a good classification. Principal Component Analysis (PCA) is used to transform a new feature space and sort out which of the features is most useful, and reduce the feature space by rejection of some of the redundant features.

PCA is an orthogonal linear transformation that transforms the data to a new coordinate system where the greatest variance by any projection of the data is described by the first coordinate, the second greatest variance on the second coordinate, and so forth [Jackson, 1991]. The relation between the input data x and the transformed data y can be expressed as.

$$\mathbf{y} = \mathbf{A}(\mathbf{x} - \mu_x) \tag{5.14}$$

where A contains the eigenvectors e_i as row vectors, hence $\mathbf{A} = [\mathbf{e}_1\mathbf{e}_2 \ldots \mathbf{e}_n]^T$. μ_x is the mean of the data set given by $\mu_x = \frac{1}{n}\Sigma_{i=1}^{n}\mathbf{x}_i$. Since PCA is a linear transformation with orthonormal basis vector it can be expressed as a translation and rotation. In figure 5.3 is the basic principles of PCA illustrated for the two dimensional case. The first two figures illustrate how the data are transformed into another representation where the main part of the variance of the data is represented in the variable y_1. If the second variable is ignored, as illustrated in the last figure, the main variance is kept.

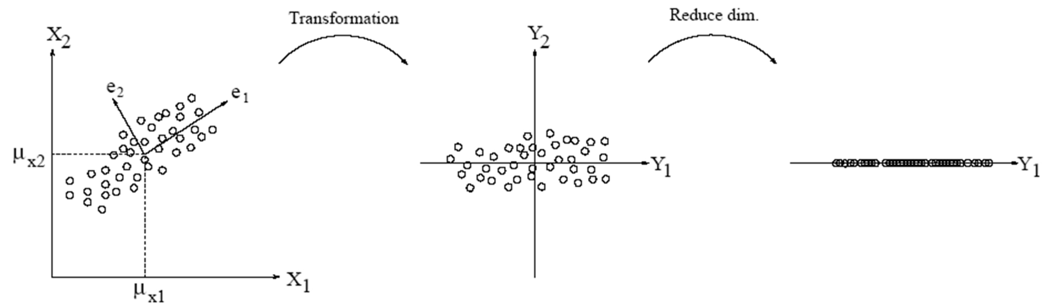

Figure 5.3: *The basic principle of PCA.[Moeslund, 2001]*

The eigenvectors can be found by solving following equation, which is known as the eigenvalue problem:

$$(\mathbf{C}_x - \lambda\mathbf{I}) \cdot \mathbf{e}_i = 0 \tag{5.15}$$

where $\mathbf{C}_x$ is the covariance matrix, λ the eigenvalue and $\mathbf{I}$ the identity matrix.[Moeslund, 2001]

When PCA is calculated from the input signal matrix X which contains all the recorded EEG components, an output matrix y with all the new transformed features will be made. The matrix will have the same size as the input matrix with the same number of features and channels, so nothing is so far gained in terms of data reduction. The problem is now to reduce the required features as much as possible without losing too much information. By sorting all the eigenvectors in such a way where the one with high information is first and the one with low information is last it is a matter of removing some of the last components. It is done by calculating a J-measure which is an expression of which and how good the eigenvectors separates the classes. The J-measure is defined as:

$$J(e_i) = \frac{e_i^T M e_i}{\lambda_i} \tag{5.16}$$

Where $J(e_i)$ denotes the J-measure of the i'th component, e_i denotes the i'th eigenvector. λ_i denotes the I'th eigenvalue and M the scatter matrix of the input data. The scatter matrix is defined as:

$$M = \sum_{i=1}^{K} P(k_i)(\mu_i - \mu)(\mu_i - \mu)^T \tag{5.17}$$

It contains a measure of the variances between the components in each class, where K denotes the number of classes, $P(k_i)$ the probability of the i'th class μ_i the mean of the i'th class in the input data and the μ is the mean of the means. In figure 5.4 the reduction of features is illustrated with the eigenvectors on the first axis and the associated eigenvalues on the second axis. The threshold m separate the eigenvectors in two groups where I_1 represent the features which is kept and I_2 represent the features which is rejected.[Moeslund, 2001]

To make sure the threshold m does not remove too much of the information about the two classes different values were tested. It was tested using from two features to half the numbers of features in the feature vector.

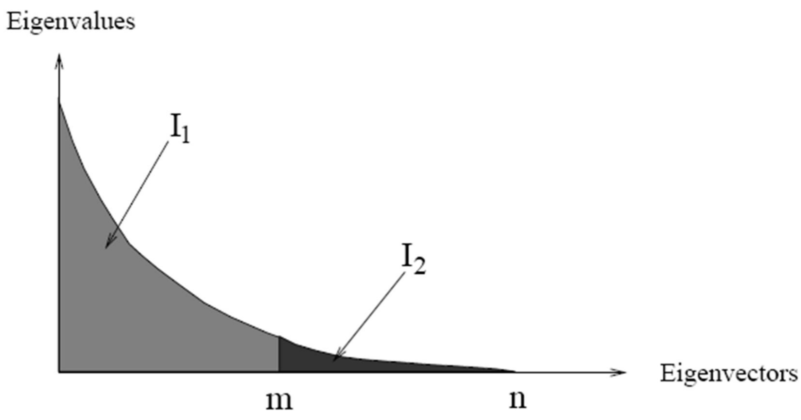

Figure 5.4: *Illustration of which eigenvectors to keep and which to reject, the threshold m seperate the eigenvectors in two groups where I_1 is kept and I_2 rejected.[Moeslund, 2001]*

Chapter 6

Classification

In the following chapter the choice of classification methods for this project will be examined. The choice of classifier is very important for a good result for this reason several classification methods will be tested.

6.1 Choice of classifier

There are several classification methods available for different classification purposes. Among them neural networks (NN), linear discriminant analysis (LDA), k-nearest neighbour (kNN) and support vector machines (SVM), which all have been used in BCI research [Mason et al., 2007]. Which classification method to choose is dependent on the number of classes and the choice of features which needs to be classified. In this project it is a relative complicated signal which makes it very difficult to decide the best classification method which will perform best. Due to this four different classification methods were tested. The four classifiers were tested using data from two subjects, and the classifier giving the best result was chosen for further analysis.

The classifiers were evaluated using 10-fold cross validation. The data samples were divided in 10 equal sized subsamples which were tested separately in the classifier giving nine subsamples for training of the classifier. When all subsamples were tested separately the mean performance for the classification was calculated.

6.2 Template matching

Template matching is a method sometimes used in detecting the P300 component in BCI research.[Bashashati et al., 2007] A template is constructed from previous P300 components and then the cross-correlation is calculated between the P300 template and the signal in which P300 components is wished to be detected. The result of the cross-correlation can be used as a feature or using a simple threshold the method also can be used for classification.

6.2.1 Theory

The error and correct response are divided in a training set and tests set according to the 10-fold cross validation. To make the template of the error response x_e and the correct response x_c the training set is used. The template is calculated by making an average of all the trials N in each of the two subset giving two templates:

$$\bar{x_e} = \frac{1}{N}\sum_{n=1}^{N} x_e(n) \tag{6.1}$$

and

$$\bar{x_c} = \frac{1}{N}\sum_{n=1}^{N} x_c(n) \tag{6.2}$$

The cross-correlation is calculated between the two templates and each of the trials in the testset s_i, where N is the number of samples, i is the number of trials, which is classified:

$$(\bar{x_e} * s)_i(n) = \sum_j \bar{x_e}^*(n) \cdot s_i(n+j) \tag{6.3}$$

and

$$(\bar{x_c} * s)_i(n) = \sum_j \bar{x_c}^*(n) \cdot s_i(n+j) \tag{6.4}$$

[Ross, 2004]

Whether the single trials belong to the correct or the error class is decided by choosing the one giving the best correlation with the single trial:

$$result = MAX[(\bar{x_e} * g)_i \quad (\bar{x_c} * g)_i] \tag{6.5}$$

6.2.2 Implementation considerations of template matching

A data set from a previous study where the identity of each single trial was known was divided and two templates were made, one corresponding to the correct response class and one corresponding to the error response class. Both templates were constructed by making an average of several response signals. For classification the cross-correlation, between the response signal and the two templates, was calculated. The response signal was assigned to the class for which the template gave the highest cross-correlation.

6.3 Linear discriminant analysis

Linear Discriminant Analysis (LDA) is a relatively simple method to discriminate between two classes and is commonly used in classification of EEG patterns. Using this method it is assumed that the two classes is linear separable, which may not be the case in this project and thereby be a disadvantage compared to other non-linear classification methods. However the simplicity of a linear method can also be advantage as the decision boundary will not be overfitted to the training samples. Another consideration is when building non-linear classifiers as multilayer perceptrons or support vector machines, different free parameters have to be carefully selected for the classification to be efficient. They may also need a large number of training samples, which is not available in this project, to outperform a linear classification. Taking these considerations into account using LDA may be more robust and produce better classification results than using non-linear methods.[Bashashati et al., 2007]

6.3.1 Theory

The method used in the LDA is Bayes rule. Bayesian classification is based on probability theory. Instead of making the decision for an observation based on the smallest distance to different classes, the Bayes theory is based on which classes the observation most likely belong to. If the observation has a feature vector x with some attributes that characterize some kind of object. There would be a conditional probability of the object represented by x belonging to class w_i which can be written as: $P(\omega_i|x)$. If the probabilities $P(\omega_1|x)$ and $P(\omega_2|x)$ is determined the decision is like this:

$$if \quad P(\omega_1|x) > P(\omega_2|x) \qquad x \in \omega_1; \tag{6.6}$$

$$if \quad P(\omega_1|x) < P(\omega_2|x) \qquad x \in \omega_2; \tag{6.7}$$

$$if \quad P(\omega_1|x) = P(\omega_2|x) \qquad the\ decision\ is\ arbitrary \tag{6.8}$$

The posterior probabilities $P(\omega_i|x)$ can be computed if the probability density function of the distribution of the feature vector in both classes is known. If so the respective likelihood of x can be calculated: $p(x|\omega_i)$, by Bayes law:

$$P(\omega_i|x) = \frac{p(x|\omega_i)P(\omega_i)}{p(x)} \tag{6.9}$$

$$with \;\; p(x) = \sum_{i=1}^{c} p(x|\omega_i)P(\omega_i), \;\; the\ total\ probability\ of\ x. \tag{6.10}$$

The decision can be made by the following statement:

$$if \quad p(x|\omega_1)P(\omega_1) > p(x|\omega_2)P(\omega_2)\ then\ x \in \omega_1\ else\ x \in \omega_2 \tag{6.11}$$

[Duda et al., 2001]

6.4 Neural networks - multilayer perceptrons

Neural networks has proven to be effective in classification problems where no general priori knowledge of the patterns exists and the classifier has to be build using experience-based learning.[Rangayyan, 2002]

6.4.1 Theory

Artificial neural networks have been motivated from the functionality of the human brain which is a highly complex information processing system. The neural network consists of several information-processing units named neurons after their resemblance to the neurons in the brain. Figure 6.1 shows the model of a single neuron. The neuron has several input signals x_j, each connected by synapses having a weight w_{kj} of their own. A summation of the weighted inputs is input to an activation function φ which gives the range of output signal of the neuron a finite value, normaly a closed unit interval [0,1]. A bias b can be used for increasing or decreasing the input to the activation function.[Haykin, 1999]

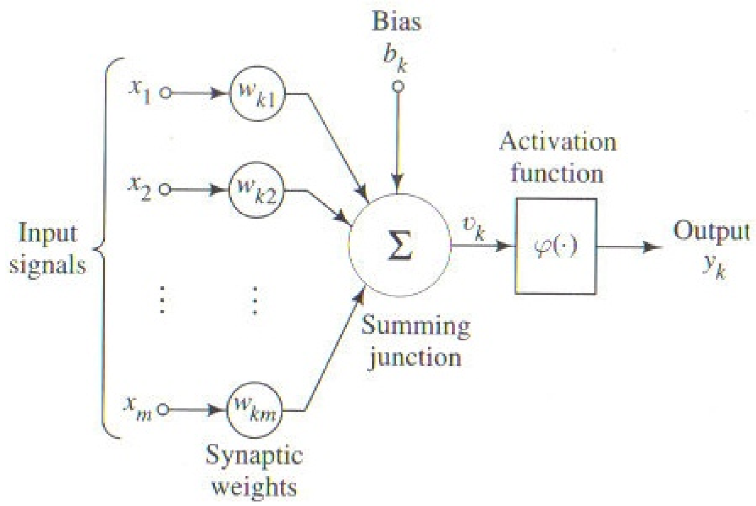

Figure 6.1: *The model of a neuron.[Haykin, 1999]*

A very common used feedforward network is the Multilayer Perceptron (MLP) which consists of a input layer, one or more hidden layers of computation nodes and a output layer of computation nodes. MLP is trained in a supervised manner using the error back-propagation algorithm. Learning by error back-propagation consists of pass forwards and a pass backwards through the network. During the forward pass the input signal is applied to the nodes of the network layer by layer and finally gives an output response. The weights of the network are all fixed during this pass. In the backward pass the output response is compared with the desired response which produces an error signal which is propagated backwards in the network to adjust all the weights in order to make the actual output response approaching the desired response. In figure 6.2 the architecture of the MLP is shown.[Haykin, 1999]

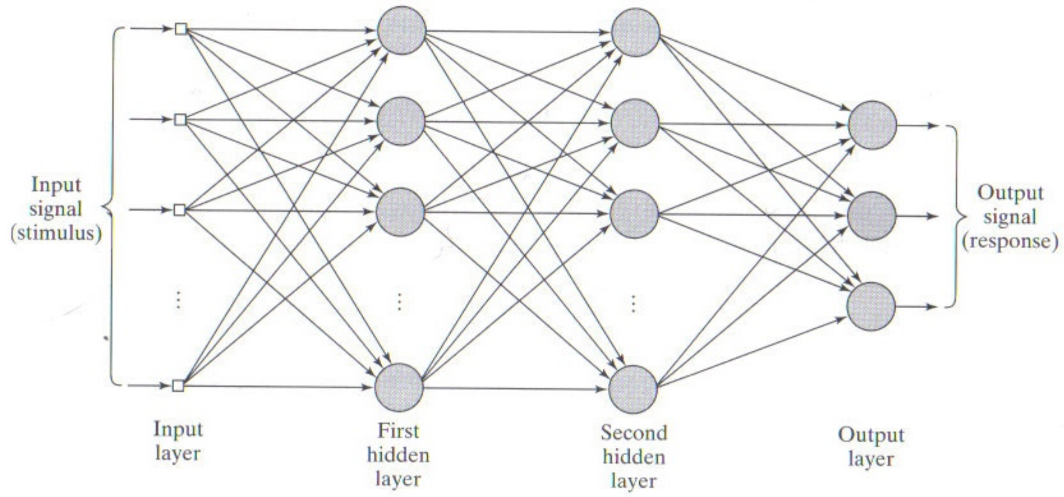

Figure 6.2: *The architecture of a MLP with two hidden layers.[Haykin, 1999]*

Learning processes for a NN

The neural network can be used as self-organization where no training is needed and is called unsupervised classification where no results or classes is known from the data, but in this case where there is knowledge of the classes and data from the environment where the neural network is used it has to be trained before use. By training the neural network is learning from its environment, and improving its performance. Training the neural network is a process where the synaptic weighs and bias level is adjusted. How to adjust the synaptic weighs and bias level on the neural network is achieved by minimizing a cost function or error energy $E(n)$ of the performance. This cost function is designed to make the output signal of a neural network come closer to the desired response. The cost function is defined in terms of an error signal denoted by $e_k(n)$:

$$E(n) = \frac{1}{2}e_k^2(n) \tag{6.12}$$

In figure 6.3 a simple feed-forward neural network is illustrated with only one neuron k in the output layer. The neuron is driven by one signal vector $\bar{x}(n)$, the output signal of the neuron k is denoted by $y_k(n)$. By compared the output with a desired response $d_k(n)$ the error signal is produced:

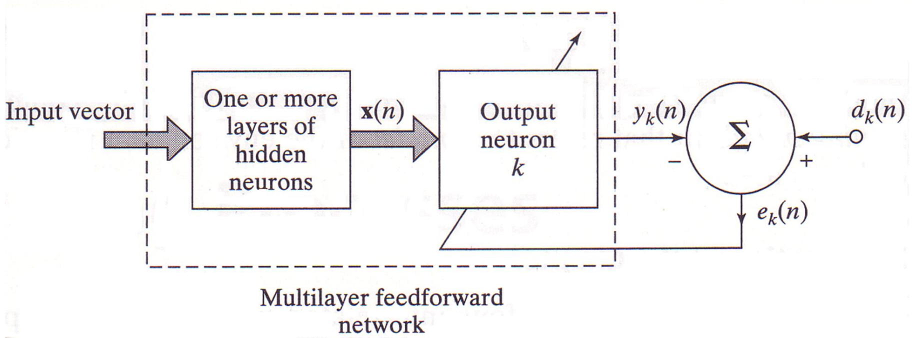

Figure 6.3: *Block diagram of a neural network highlighting the only neuron in the output layer.[Haykin, 1999]*

$$e_k(n) = d_k(n) - y_k(n) \tag{6.13}$$

The training of the neural network is done step by step where the adjustment of the synaptic weights of the neuron k are continued until the system reaches a steady state. The update step of the weight is done according to the delta rule, where the adjustment $\Delta W_{kj}(n)$ is applied to the synaptic weight w_{kj} at time step n:

$$w_{kj}(n+1) = w_{kj}(n) + \Delta w_{kj}(n) \tag{6.14}$$

w_{kj} denotes the value of the synaptic weight of the neuron k activated by element $x_j(n)$ of the signal vector $\bar{x}(n)$. The adjustment $\delta W_{kj}(n)$ is defined by:

$$\Delta w_{kj}(n) = \eta e_k(n) x_j(j) \tag{6.15}$$

Where η is a positive constant that determines the rate of learning.[Haykin, 1999]

6.4.2 Implementation considerations for MLP

The MLP was implemented using the neural networks toolbox in MATLAB. A single hidden layer was used, consisting of 12 neurons. The number of neurons in the hidden layer was chosen by testing which number gave the best classification. As output layer a single neuron was used. The MLP was trained to give a error energy of 0.2 to avoid overfitting to the test samples. If the limit of 0.2 was not met the training will automatically stop after 100 training epochs and use the parameters for the weight and bias from the step which gave the smallest value for the error energy.

6.5 Support vector machine

Support vector machine (SVM) is a non-linear pattern classification method. The central idea of SVM is the adjustment of a discriminating function so that it optimally uses the separability information of the boundary patterns. [de Sá, 2001]

6.5.1 Theory

SVM is a supervised classifier and the concept of this method is easiest approached by considering a binary classification. The function of a linear classifier made from the training samples would be:

$$f(\bar{x}) = sign((\bar{w} \cdot \bar{x}) + b) = +1 \text{ if } \bar{x} \text{ belongs to the first class} \tag{6.16}$$

$$f(\bar{x}) = sign((\bar{w} \cdot \bar{x}) + b) = -1 \text{ if } \bar{x} \text{ belongs to the second class} \tag{6.17}$$

where $\bar{x}$ is the feature vector and $\bar{w}$ determines the orientation of the discriminant plane. There will be an infinite number of planes discriminating the two classes. The optimal classifier finds the plane which seperates the two classes while being furthest from both classes.

Suppose a hyperplane separates the positive and negative class. The data point lying on the plane satisfy

$$\bar{w} \cdot \bar{x} + b = 0 \tag{6.18}$$

where w is the normal to the hyperplane, $|b| / \|\bar{w}\|_2$ is the perpendicular distance from the hyperplane to the origin and $\|\bar{w}\|_2$ is the Euclidean norm of $\bar{w}$.
Let two supporting hyperplanes be defined as

$$\bar{x} \cdot \bar{w} + b \geq +1 \quad \text{for} \quad y = +1 \tag{6.19}$$

$$\bar{x} \cdot \bar{w} + b \leq -1 \quad \text{for} \quad y = -1 \tag{6.20}$$

The SVM algorithm maximizes the margin between these two support hyperplanes. The planes are pushed apart until the meet the closest data points, which will be the support vectors. In figure 6.4 the hyperplane and the support vectors are shown. The margin is defined as

$$\gamma = 2/ \|\bar{w}\|_2 \tag{6.21}$$

and to maximize the margin one have to minimize

$$\bar{w} \cdot \bar{w} \quad \text{subject to constrain} \quad y_i(\bar{x}_i \cdot \bar{w}) - b) \geq 1 \tag{6.22}$$

This is a constrained optimization problem which can reformulated to a Lagrangian problem which can be solved by using quadratic programming algorithms. [Sanei & Chambers, 2007;

Bennett & Campbell, 2000]

When training samples are non-seperable a soft margin classifier most be constructed. This gives following constrained optimization problem. One have to minimize

$$\bar{w} \cdot \bar{w} + C \sum xi_i \text{ subject to constrain } y_i((\bar{x}_i \cdot \bar{w} + b) \geq 1 - \xi_i \tag{6.23}$$

C is parameter representing the tradeoff between minimizing the training set error and maximizing the margin.

In many non-separable cases a nonlinear classification function can help separating the classes. SVM uses kernel mapping where the data are nonlinearly projected into a higher-dimensional space which then makes the data separable by a linear hyperplane. Two of the most used kernel functions K(u,v) are the polynomial:

$$K(u,v) = ((u \cdot v) + c)^2 \tag{6.24}$$

and gaussian radial basis function:

$$K(u,v) = exp(-\frac{\|u-v\|_2^2}{2\sigma^2}) \tag{6.25}$$

[Sanei & Chambers, 2007]

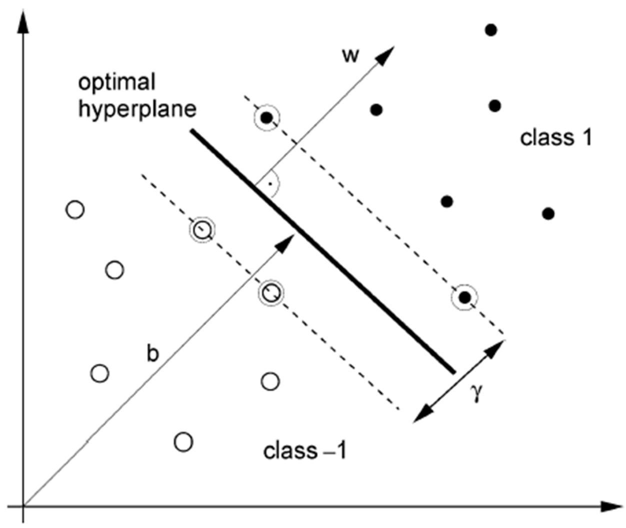

Figure 6.4: *SVMs find the optimal hyperplane (solid line) to separate two classes by maximizing the margin. It can be described by the vector w and the bias term b. Only support vectors (bordered circles) are necessary to calculate w and b.[Kaper et al., 2004]*

An exclusive-OR (XOR) is a simple example which cannot be solved using a linear classification method on the features itself. In figure 6.5 on the next page (A) the problem is illustrated, where the points $k = 1,3$ at $x = (1,1)^t$ and $(-1,-1)^t$ are in category ω_1(marked with red) and $k = 2,4$ at $x = (1,-1)^t$ and $(-1,1)^t$ are in category ω_2(marked with black). By preprocessing the features to map them in a higher dimension space the XOR problem can be solved linear. By using a second order function the four features $\mathbf{x}$ are mapped to a six-dimensional space by

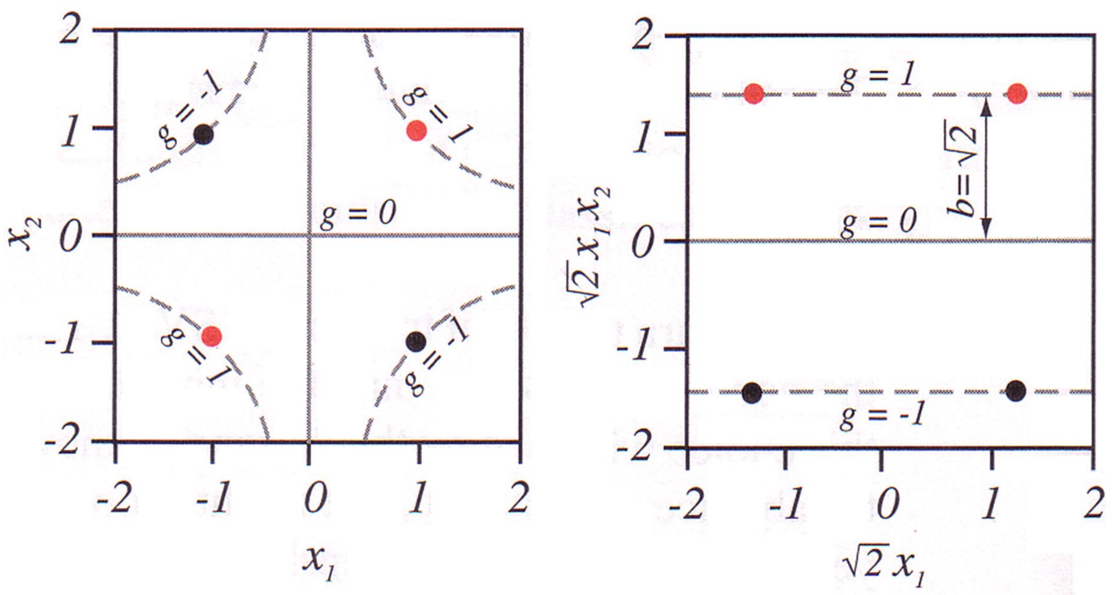

(A) *(B)*

Figure 6.5: *In (A) the original x_1x_2-space is shown, the two red patterns are in category ω_1 and the black ones in ω_1. The four training patterns $\boldsymbol{x}$ are mapped in a new feature space shown in (B) which makes the four features linear separable.[Haykin, 1999]*

1, $\sqrt{2}x_1$, $\sqrt{2}x_2$, $\sqrt{2}x_1x_2$, x_1^2, x_2^2. As seen in figure 6.5 (B) two of the new features can be separated linear with a optimal hyperplane $g(x_1, x_2) = x_1x_2 = 0$ and the margin $b = \sqrt{2}$.[Haykin, 1999]

6.5.2 Implementation considerations for SVM

In this project the SVM used is implemented by Chang & Lin [2001]. This is a C implementation of the method, which also include a MATLAB interface.

To get good results Hsu et al. [2007] suggest the radial basis function (RBF) kernel as first choice for many classification problems. The polynomial kernel has more parameters which gives a higher complexity in finding the best classification. The RBF kernel also has less numerical difficulties. However the RBF kernel may not produce better results in case of a very high feature number where the less complex linear kernel will give a similar performance.[Hsu et al., 2007]

When using the linear kernel for classification only the parameter C has to be chosen initially. When using the RBF kernel in addition another parameter σ has to be chosen. The goal is to find the parameters C and σ to obtain the best classification. One will not necessarily get the best results by just optimizing the parameters to improve the training accuracy which may produce the over fitting problem. To get better results Hsu et al. [2007] recommend to do a grid search using cross validation to find the best values for C and σ.

In this project a 10-fold cross validation was used, initially on a rough grid with $C = [2^{-5}, 2^{-3}, .., 2^{15}]$ and $\sigma = [2^{-15}, 2^{-13}, .., 2^{3}]$. When the initial values of C and σ were found another finer grid search was used to find the best values. Afterwards the parameters were used together with the entire training set to train the classifier.

6.6 Evaluation of classification methods

In the following tables the classification results are listed for the template matching, LDA, MLP and SVM respectively. Only results for subject 1 and 2 have been calculated. As input for the classifiers the first wavelet features, statistical features and the signal downsampled were used separately.

The results have been calculated using 10-fold cross-validation. Each day have 20 error samples and 60 correct samples. To get the most reliable results the error samples were mixed randomly and 20 of the 60 correct samples were taken out in random order and used for the cross-validation. This step was repeated 30 times. The mean and standard deviation of the 30 10-fold cross-validation results are shown in the tables. Se the three different tables from each of the classifiers; table 6.1 contains the template results, table 6.2 the LDA result and finally table 6.4 for the SVM.

It can be seen from the results that this is indeed a difficult classification problem. Using template matching most error responses is assigned to the error class, but so are the correct responses. LDA and MLP have similar performance, with LDA having higher total classification accuracy for subject 1. The SVM does not outperform the other classifiers. However for subject 1 day where the clearest deviation between error and correct response was shown the SVM is giving slightly better classification results. For that reason the SVM method has been chosen for classification of ErrP's in this project and because it unlike many other classifiers perform well in the following situations:

- the number of features is high;
- there is a limited time for performing the classification;
- there is a nonuniform weighting among the features;
- there is a nonlinear map between inputs and outputs;
- the distribution of the data is unknown;

[Sanei & Chambers, 2007]
In addition a study by Schlögl et al. [2005] investigated the performance of the classifiers LDA, KNN and SVM, to solve a EEG signal classification test, and found the latter to be significantly better, whereas Garrett et al. [2003] found SVM to be only slightly better than LDA and NN.

	Subject 1	Subject 2	**Average**
	10-fold cross validation day 1		
E	99.0±3.0	96.3±6.0	
C	4.0±6.5	16.3±12.7	
	10-fold cross validation day 2		
E	91.0±8.1	98.7±3.2	
C	13.2±11.2	4.8±6.2	
	10-fold cross validation day 3		
E	100.0±0.0	54.6±28.4	
C	10.7±6.7	44.8±27.9	
E			**89.8±8.1**
C			**15.7±11.9**

Table 6.1: The classification accuracy (mean and standard deviation) for error trials (E) and correct trials (C) for subject 1 and 2 using template matching.

	Signal		Wavelet		Statistical		
	Subject 1	Subject 2	Subject 1	Subject 2	Subject 1	Subject 2	**Average**
			10-fold cross validation day 1				
E	63.8±7.5	63.5±8.1	62.2±9.3	58.7±9.5	49.5±32.1	55.2±31.9	
C	53.8±9.7	54.3±10.0	48.5±9.0	57.2±9.3	57.0±21.7	41.3±25.9	
			10-fold cross validation day 2				
E	68.0±6.5	52.5±10.6	61.3±9.1	60.5±7.6	73.3±19.7	70.3±17.9	
C	55.5±7.1	38.2±10.0	49.8±10.2	53.6±8.8	27.3±20.0	32.3±14.2	
			10-fold cross validation day 3				
E	64.3±5.0	55.5±7.8	70.5±6.3	61.3±8.9	89.8±0.9	32.2±18.5	
C	68.2±6.9	57.3±9.1	52.7±10.6	63.3±9.3	55.6±7.8	63.2±25.0	
E							**61.8±12.1**
C							**51.6±12.5**

Table 6.2: The classification accuracy (mean and standard deviation) for error trials (E) and correct trials (C) for subject 1 and 2 using the proposed features in LDA.

	Signal		Wavelet		Statistical		
	Subject 1	Subject 2	Subject 1	Subject 2	Subject 1	Subject 2	**Average**
			10-fold cross validation day 1				
E	57.8±10.3	62.2±8.0	59.0±8.6	63.3±9.2	59.2±8.3	55.0±8.6	
C	53.3±9.4	54.8±8.1	47.5±11.7	57.8±11.6	54.3±11.4	54.3±9.0	
			10-fold cross validation day 2				
E	57.3±12.2	56.7±11.2	57.5±8.3	50.7±10.6	51.7±11.3	51.6±12.3	
C	55.8±10.8	52.0±10.0	53.3±9.4	49.8±10.2	49.5±8.9	54.0±11.3	
			10-fold cross validation day 3				
E	63.5±10.4	57.2±8.8	62.5±9.1	57.5±10.9	70.8±8.5	53.2±11.1	
C	55.2±9.0	56.2±10.3	57.9±9.4	54.8±10.2	75.0±10.3	50.8±11.3	
E							**58.2±9.9**
C							**54.8±10.1**

Table 6.3: The classification accuracy (mean and standard deviation) for error trials (E) and correct trials (C) for subject 1 and 2 using the proposed features in MLP.

	Signal		Wavelet		Statistical		
	Subject 1	Subject 2	Subject 1	Subject 2	Subject 1	Subject 2	**Average**
			10-fold cross validation day 1				
E	55.8±10.1	62.7±13.9	57.5±8.0	61.5±9.5	51.2±8.1	46.0±10.5	
C	71.2±14.4	70.5±14.2	72.8±9.2	61.5±8.5	65.2±14.1	59.7±12.2	
			10-fold cross validation day 2				
E	58.8±15.8	68.6±16.7	47.8±9.8	49.2±10.3	42.7±14.9	47.5±10.3	
C	63.7±11.5	53.8±17.7	56.3±11.0	51.7±10.3	52.7±19.8	52.6±10.2	
			10-fold cross validation day 3				
E	78.8±8.7	56.2±19.7	68.5±10.2	54.0±11.4	66.8±7.0	45.7±14.3	
C	81.0±8.7	66.8±15.0	61.0±11.1	52.2±11.0	81.0±7.6	55.2±10.2	
E							**56.6±11.6**
C							**62.2±12.0**

Table 6.4: The classification accuracy (mean and standard deviation) for error trials (E) and correct trials (C) for subject 1 and 2 using the proposed features in SVM.

Chapter 7

Classification results

In this chapter all the results from the classification will presented in separate tables. The best performing classification method found in chapter 6 is used on all features from the six subjects.

In the following tables classification results are listed for all six subjects using a support vector machine (SVM). Some of the features proposed in chapter 5 have given very poor classification results and are therefore not listed. It concerns the second wavelet based features and the PCA transformed features. The second wavelet based features gave an accuracy rate of approximately 50% or less and PCA did not improve anything. Figure 7.1 illustrates the process for evaluation of the features and classifiers. The calculation of the classification accuracy of the other proposed features is done by 10-fold cross validation using the same procedure as described in section 6.6.

In table 7 the classification results from subject 1 to 6 are shown. The feature vector used

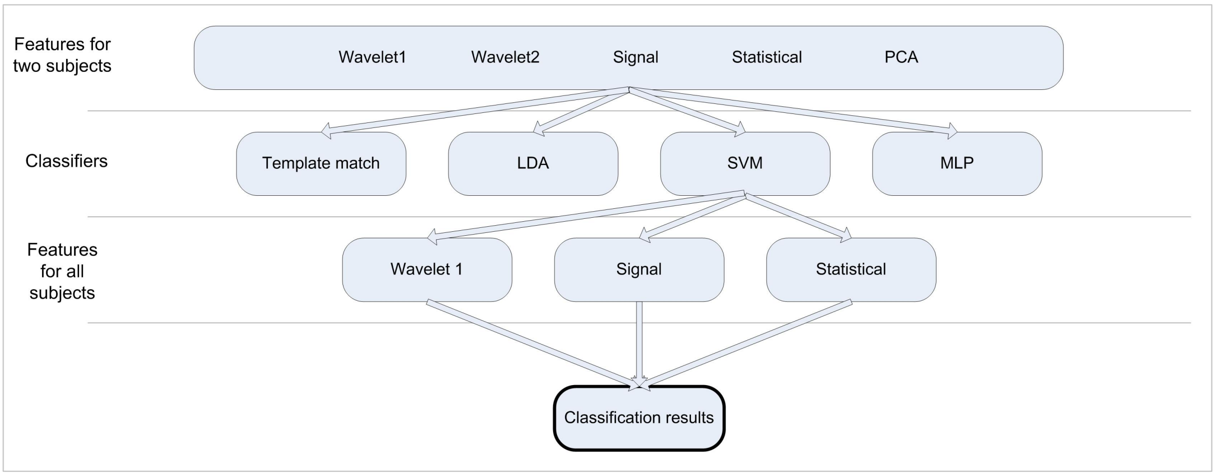

Figure 7.1: *Illustration of evaluation process for features and classifiers.*

to obtain these results was samples of the 700 ms long signal recorded after feedback. To reduce the size of the feature vector the signal was downsampled with 8 giving 45 features.
It can be seen from the tables that the average classification rate is 64.6%. Only subject 1 and subject 4 on day 3 show significantly better classification rates around 80%. These results are in accordance with the averaged response signals showed earlier in section 4.1 which also showed

	Subject 1	Subject 2	Subject 3	Subject 4	Subject 5	Subject 6	**Average**
			10-fold cross validation day 1				
E	55.8±10.1	62.7±13.9	58.8±14.5	43.3±32.2	56.2±19.5	62.0±6.2	**56.5±16.1**
C	71.2±14.4	70.5±14.2	56.7±12.3	64.3±28.0	59.2±16.0	67.3±9.7	**64.9±15.8**
			10-fold cross validation day 2				
E	58.8±15.8	68.6±16.7	62.7±20.2	74.3±9.3	56.8±14.4	60.0±7.9	**63.5±14.1**
C	63.7±11.5	53.8±17.7	61.7±18.1	70.7±7.7	65.8±13.7	75.8±12.4	**65.3±13.5**
			10-fold cross validation day 3				
E	78.8±8.7	56.2±19.7	58.5±15.0	83.3±7.2	68.5±12.7	62.0±10.3	**67.9±12.3**
C	81.0±8.7	66.8±15.0	66.7±12.3	76.7±6.9	62.0±19.0	65.3±11.1	**69.8±12.2**
E							**62.6±14.2**
C							**66.7±13.8**

Table 7.1: The classification accuracy (mean and standard deviation) for error trials (E) and correct trials (C) for all six subjects in the test group using the response signal as feature vector.

that the deviation between correct and error trials were most clear in these two subjects.

In table 7 the classification results using wavelet features are shown. The feature vector used was based on wavelet transformation giving 30 features with supposedly the most deviation between the two classes. In the tables it can be seen that using these features did not improve the overall classification rate which was 58.3% for all subjects.

In table 7 the classification results when using statistical features are shown. The feature vector included the four statistical features mean, variance, kurtosis and skewness. These features give the lowest overall classification rate at 56% and the rate for subject 4 is now significantly lower compared to the classification rate when using the signal as feature vector.

As indicated by the classification results, it seems that it is extremely difficult to extract information which can successfully separate correct trials from error trials. Even with a strong classifier as the SVM it still not possible to obtain satisfying results. However the classification for subject 1 and subject 4 on day 3 show reasonable results, compared to rates presented in the literature [Ferrez & del R. Millán, 2005, 2007].

	Subject 1	Subject 2	Subject 3	Subject 4	Subject 5	Subject 6	**Average**
			10-fold cross validation day 1				
E	57.5±8.0	61.5±9.5	57.0±11.6	50.2±11.8	46.0±12.0	57.7±5.4	**55.0±9.7**
C	72.8±9.2	61.5±8.5	55.7±10.1	57.5±10.7	48.8±13.7	66.8±9.0	**60.5±10.2**
			10-fold cross validation day 2				
E	47.8±9.8	49.2±10.3	50.5±11.2	64.0±8.9	50.5±10.4	57.5±7.2	**53.3±9.6**
C	56.3±11.0	51.7±10.3	51.3±7.1	67.8±10.1	59.0±10.0	72.0±9.8	**59.7±9.7**
			10-fold cross validation day 3				
E	68.5±10.2	54.0±11.4	55.2±9.4	82.7±6.4	44.5±10.3	52.8±11.0	**59.6±9.8**
C	61.0±11.1	52.2±11.0	58.5±9.7	74.7±6.5	62.0±10.4	60.0±11.0	**61.4±10.0**
E							**56.0±9.7**
C							**60.5±10.0**

Table 7.2: The classification accuracy (mean and standard deviation) for error trials (E) and correct trials (C) for all six subjects in the test group using the wavelet coefficients as feature vector.

	Subject 1	Subject 2	Subject 3	Subject 4	Subject 5	Subject 6	**Average**
			10-fold cross validation day 1				
E	51.2±8.1	46.0±10.5	72.0±12.1	53.2±14.3	49.3±10.8	42.3±11.5	**52.3±11.2**
C	65.2±14.1	59.7±12.2	58.7±9.0	45.7±16.5	59.7±10.1	55.0±12.5	**57.3±12.4**
			10-fold cross validation day 2				
E	42.7±14.9	47.5±10.3	44.3±9.8	64.7±10.2	53.0±11.3	49.5±11.5	**50.3±11.3**
C	52.7±19.8	52.6±10.1	72.0±12.4	68.8±10.1	61.2±11.3	51.8±14.6	**59.9±13.1**
			10-fold cross validation day 3				
E	66.8±7.0	45.7±14.3	49.3±8.6	55.7±12.9	46.3±11.8	61.2±9.3	**54.2±10.7**
C	81.0±7.6	55.2±10.2	57.5±13.7	59.0±12.4	58.5±14.8	63.8±14.4	**62.5±12.2**
E							**52.3±11.1**
C							**59.9±12.6**

Table 7.3: The classification accuracy (mean and standard deviation) for error trials (E) and correct trials (C) for all six subjects in the test group using statistical features.

Part III

Discussion and conlusion

Chapter 8

Discussion

Research in the area of Brain-Computer Interfaces (BCIs) has been in progress for several years to develop methods to assist patients with severe neuromuscular impairments such as patients suffering from amyotrophic lateral sclerosis (ALS), brainstem stroke or cerebral palsy. The purpose of BCI research is to give these patients an opportunity to communicate and control external devices only by measuring the patients intent from the brain activity, which may improve their quality of life significantly.

A BCI system normally consist of different parts including signal acquisition, preprocessing, feature extraction, classification, and a application interface. Different approaches are being used to obtain information from different cortical areas and to discriminate between the signals measured, which would give BCI users a high level of control opportunities. Especially event related potentials (ERPs) are used for BCI for example the P300 component and motor-related cortical potentials (MRCPs). A problem with using ERPs is their relative low amplitude compared to the surrounding EEG. In addition different artifacts such as eye movement and muscle activity are present which all are contributing to a low signal to noise ratio (SNR). Although advanced signal processing- and feature extraction methods are implemented in the BCI, classification errors may still occur. This is not only due to the low SNR but also due to high intra- and inter-user variations in the electroencephalography (EEG). These challenges have to be met when developing a reliable BCI system. One way to minimize the rate of classification errors is to make the classifier adapt to the signal variations throughout its use.

To achieve a more reliable and robust BCI system the classifier needs a feedback on its performance. It have been suggested to use error related potentials (ErrPs) as feedback of the classifiers performance. If ErrPs can be detected during the BCI systems, it might be possible to improve the performance by making a adaptive classifier based on these ErrPs. Furthermore it could prevent incorrect execution of commands

ErrPs have been investigated in numerous studies including a few studies in the context of BCI research. In these studies it has been shown that ErrP can be triggered by recognition of an incorrect response by the subject itself or by feedback.[Falkenstein et al., 2000; Holroyd & Coles, 2002; Ferrez & del R. Millán, 2007; Buttfield et al., 2006] The ErrP have similar characteristics but also differs depending on the experimental protocol used. ErrP triggered by an incorrect feedback to the subjects correct response has recently been investigated, that is ErrPs induced by the interface[Ferrez & del R. Millán, 2005, 2007]. Most of these studies have in common that the subject had to make a response by performing some motor task, for example by pressing buttons.

The aim of our study was ato investigate ErrPs, but it was emphasized to simulate a realistic BCI situation where only imaginary movements and no real movements were involved. The hypothesis was

'ErrPs induced by incorrectly classification of imaginary movements can be detected and classified successfully.'

When no real movement is made it is obviously more unclear for the subject what has caused the error. It could be due to an incorrect imaginary task from the subject, a lack of the subjects concentration when performing the task or it could be entirely an error made by the interface. This unclearness may also effect the measured response after error feedback and thus it might not be completely comparable to other studies.

Six subjects were included in this study. In every trial of the experiment they were asked to imagine moderate or a ballistic ankle flexion and were afterwards given feedback on their performance by a pop-up window with the text "Correct" for correct feedback and "Wrong" for error feedback. Correct and error feedback was given in random order with a rate of 75% and 25% of the trials respectively. In 10% of trials an event was included in terms of a pop-up window with the letter X. The X-event was included for comparison with the response to the feedback. The measured EEG was band-pass filtered and electrooculography (EOG) was removed using independent component analysis (ICA).

The analysis of the EEG recordings show that correct and error feedback and the event all generate a similar response from the subjects. In the grand average of all six subjects a negative and a positive peak is present at 200 ms and 300 ms after feedback onset respectively and a second broader negative peak is present around 500 ms after feedback. From these results none of the peaks can exclusively be explained by an ErrP although all three peaks in other studies have been suggested to be error related [Ferrez & del R. Millán, 2005; Buttfield et al., 2006; Ferrez & del R. Millán, 2007]. The first two peaks could very likely be the N200 and P300 caused by a deviant visual stimuli. The second negative peak does not have the same easily explainable cause although it have same characteristics as the N400 seen in subjects during semantic processing. However it seems like the error feedback generates a larger negative deflection from 400 ms to 600 ms compared to a correct feedback in three out of six subjects, which implies that the ErrP could contribute to this negative peak.

The MRCPs was investigated to verify existence of the ErrP and it was shown that a negative deflection was present after imaginary movement onset similar to the findings described by do Nascimento et al. [2006]. It was however difficult to visually discriminate the two MRCPs corresponding to the ballistic and moderate movements. It seems to have been difficult for the subjects to imagine two different force rate developments.

The fact that the characteristics of the response to error and correct feedback are very similar makes a single trial classification of the responses difficult. In this project different methods for feature extraction were investigated to extract relevant information and thereby enhance the following classification. Features based on wavelet transformation and simple statistical features were tried. A downsampled version of the measured response were also tried as a feature vector. To extract most relevant information of the proposed features, principal component analysis (PCA) was tested as well.

To discriminate between the response to error feedback and the response to correct feedback four different classifiers were investigated. The first was based on a simple correlation between a template made of the error response and the trials. The second simple method was based on linear discriminant analysis (LDA) and the last two were nonlinear methods in form of neural networks and support vector machine (SVM). As the number of error trials per subject were relatively low (20 trials per day) the feature set obviously also were relatively small. Therefore the classifiers were evaluated using 10-fold cross validation. The best classification was obtained using the SVM with a downsampled version of the recorded response as feature vector. This gave an overall classification accuracy rate of 62.6% and 66.7% for error and correct trials, when including the average accuracy for all six subject all three days. The accuracy achieved is not impressive, but two subjects showed on day three an accuracy rates of approximately 80% for both error and correct trials, which are comparable to other reported results. As it seems very difficult to see any clear deviations between correct and error trials from the averaged signals in the three out of six subjects these classification results are not surprising. The relatively low number of samples available when training the SVM classifier may also have affected the classification rate negatively.

Methodological considerations

In this study it seems difficult to discriminate between components from some error processing system and components related to visual or cognitive processing. In the experimental design it was chosen to give a strong visual feedback of the subjects performance in form of a pop-up window with the message "correct" or "wrong". This type of feedback may be problematic as the large visual components may interfere with the ErrP. In addition there may be components related to some kind of semantic processing also interfering with the components of interest. The pop-up window may also provoke the subject to blink more often than if another type of feedback was used. The eye movements are in this study corrected using independent component analysis, but it can be argued that some remains of EOG components still are corrupting the signal. Especially it seems that most subjects blink after feedback which indeed can corrupt the interpretation of the average signals as well as reduce the classification accuracy if their components are not completely removed. For further investigation of the ErrP a new experimental protocol should be designed to reduce all other interfering factors. In relation to improvements of classification rate of ErrPs a new study should also include more trials to achieve a larger number of training samples for the classifier. It has proven to be very important to keep the subject engaged and motivated in the task to see the MRCPs which has to be more in focus in a new experiment. In this experiment subjects only practiced real movement in the beginning. To keep the subjects primed to the difference of the two imaginary movement, practice of real movements throughout the experiment may be necessary.

8.1 Conclusion

In conclusion we have investigated the presence of error related potentials following error feedback to imaginary movements. The result implys that a negative component is present approximately 500 ms after error feedback in some of the subjects. There are however some large variations in the measured responses between the subjects and it is also not clear if the ErrP is related to execution of an imaginary motor task. The findings in this study in addition with findings reported in the literature suggest that it could be possible to detect ErrPs after incorrect feedback to an imaginary motor task. A new study with an improved experimental protocol might give more clear indications whether this detection of ErrPs could be reliable enough to improve the performance of BCI systems.

Bibliography

Ackerman, S. (1991). *Discovering the Brain*. National Academies Press. ISBN 9780309045292.

Bashashati, A., Fatourechi, M., Ward, R. K. & Birch, G. E. (2007). A survey of signal processing algorithms in brain-computer interfaces based on electrical brain signals. *Journal of Neural Engineering*, 4:R32–R57.

Bear, M. F., Connors, B. W. & Paradiso, M. A. (2001). *Neuroscience - Explore the Brain*. Williams & Wilkins, 2nd. ed. Edition ISBN 0-683-30596-4.

Beauregard, M. (2003). *Consciousness, Emotional Self-Regulation and the Brain*. John Benjamins Publishing Company. ISBN 9781588114587.

Bell, A. J. & Sejnowski, T. J. (1995). An information-maximization approach to blind separation and blind deconvolution. *Neural Computation*, 7:1129–1159.

Bennett, K. P. & Campbell, C. (2000). Support vector machines: Hype or hallelujah? *SIGKDD Explorations*, 2(2):1–13.

BioSemi (2008). URL `http://www.biosemi.com/headcap.htm`.

Blankertz, B., Dornhege, G., Schäfer, C., Krepki, R., Kohlmorgen, J., Müller, K.-R., Kunzmann, V., Losch, F. & Curio, G. (2003). Boosting bit rates and error detection for the classification of fast-paced motor commands based on single-trial eeg analysis. *IEEE Transactions on Neural Systems and Rehabilitation Engineering*, 11(2):127–131.

Bostanov, V. (2004). Bci competition 2003-data sets ib and iib: Feature extraction from event-related brain potentials with the continuous wavelet transform and the t-value scalogram. *IEEE Transactions on Biomedical Engineering*, 51(6).

Brunia, C. & van den Bosch, W. (1984). Movement-related slow potentials. i. a contrast between finger and foot movements in right-handed subjects. *Electroencephalography and clinical Neurophysiology,*, 57:515–527.

Buttfield, A., Ferrez, P. W. & del R. Millán, J. (2006). Towards a robust bci: Error potentials and online learning. *IEEE Transactions on Neural Systems and Rehabilitation Engineering*, 14(2):164–168.

Chang, C.-C. & Lin, C.-J. (2001). Libsvm : a library for support vector machines, 2001. URL `http://www.csie.ntu.edu.tw/~cjlin/libsvm`.

CNL/The Salk Institute (2008). URL `http://sccn.ucsd.edu/eeglab/allfunctions/runica.html`.

de Sá, J. P. M. (2001). *Pattern Recognition - Concepts, Methods and Applications*. Springer. ISBN 3-540-42297-8.

Delorme, A. & Makeig, S. (2004). EEGLAB: an open source toolbox for analysis of single-trial EEG dynamics. *Journal of Neuroscience Methods*, 134:9–21.

do Nascimento, O. F., Nielsen, K. D. & Voigt, M. (2006). Movement-related parameters modulate cortical activity during imaginary isometric plantar-flexions. *Experimental Brain Research*, 171:78–90.

Dobkin, B. H. (2007). Brain-computer interface technology as a tool to augment plasticity and outcomes for neurological rehabilitation. *Journal of Physiology*, 579.3:637–642.

Duda, R. O., Hart, P. E. & Stork, D. G. (2001). *Pattern Classification*. Nr. 2. John Wiley & Sons, Inc. ISBN 0-471-05669-3.

Falkenstein, M., Hoormann, J., Christ, S. & Hohnbein, J. (2000). Erp components on reaction errors and their functional significance: a tutorial. *Biological Psychology*, 51:87–107.

Farina, D., do Nascimento, O. F., Lucas, M.-F. & Doncarli, C. (2007). Optimization of wavelet for classification of movement-related cortical potentials generated by variation of force-related parameters. *Journal of Neuroscience Methods*, 162:357–363.

Fatorechi, M., Bashashati, A., Ward, R. K. & Birch, G. E. (2007). Emg and eog artifacts in brain computer interface systems: A survey. *Clinical Neurophysiology*, 118:480–494.

Ferrez, P. W. & del R. Millán, J. (2005). You are wrong!-automatic detection of interaction errors from brainwaves. *Proc. 19th Int. Joint Conf. Artificial Intell.*

Ferrez, P. W. & del R. Millán, J. (2007). Error-related eeg potentials generated during simulated brain-computer interaction. *IEEE Transactions on Biomedical Engineering*, PP.

Fogelson, N., Loukas, C., Brown, J. & Brown, P. (2004). A common n400 eeg component reflecting contextual integration irrespective of symbolic form. *Clinical Neurophysiology*, 115:1349–1358.

Fonseca, L. C., Tedrus, G. M. & Gilbert, M. A. P. (2006). Event related potentials during the visual discrimination of words and pseudowords by children. *Arq Neuropsiquiatr*, 64:553–558.

Friedmann, D., Cycowisc, Y. M. & Gaeta, H. (2001). The novelty p3: an event-related brain potential (erp) sign of the brain's evaluation of novelty. *Neuroscience and biobehavioral reviews*, 25:355–373.

Garrett, D., Peterson, D. A., Anderson, C. W. & Thaut, M. H. (2003). Comparison of linear, nonlinear, and feature selection methods for eeg signal classification. *IEEE Transactions on Neural Systems and Rehabilitation Engineering*, 11(2):141–144.

Graimann, B., Allison, B. & Gräser, A. (2007). New applications for non-invasive brain-computer interfaces and the need for engaging training environments. *Brain-Computer Interfaces and Games Workshop at ACE (Advances in Computer Entertainment) 2007*, side 25–28.

Haykin, S. (1999). *Neural Networks - A Comprehensive Foundation*. Prentice-Hall, 2nd. ed. Edition ISBN 0-13-908385-5.

Holroyd, C. B. & Coles, M. G. H. (2002). The neural basis of human error processing: Reinforcement learning, dopamine, and the error-related negativity. *Psychological Review*, 109(4):679–709.

Hsu, C.-W., Chang, C.-C. & Lin, C.-J. (2007). A practical guide to support vector classification. URL `http://www.csie.ntu.edu.tw/~cjlin`.

Jackson, J. E. (1991). *A usert's guide to principal components.* JAC. ISBN 0471622672.

Jung, T.-P., Makeig, S., Humphries, C., Lee, T.-W., Mckeown, M. J., Iragui, V. & Sejnowski, T. J. (2000). Removing electroencephalographic artifacts by blind source separation. *Psychophysiology*, 37:163–178.

Kaper, M., Member, S., Meinicke, P., Grossekathoefer, U., Lingner, T. & Ritter, H. (2004). Bci competition 2003-data set iib: Support vector machines for the p300 speller paradigm. *IEEE Transactions on Biomedical Engineering*, 51(6):1073–1076.

Kübler, A., Kotchoubey, B., Kaiser, J., Wolpaw, J. R. & Birbaumer, N. (2001). Brain-computer communication: Unlocking the locked in. *Psychological Bulletin*, 127(3):358–375.

Kübler, A., Mushahwar, V. K., Hochberg, L. R. & Donoghue, J. P. (2006). Bci meeting 2005-workshop on clinical issues and applications. *IEEE Transactions on Neural Systems and Rehabilitation Engineering*, 14(2):131–134.

Krigolson, O. E. & Holroyd, C. B. (2006). Evidence for hierarchical error processing in the human brain. *Neuroscience*, 137:13–17.

Krigolson, O. E. & Holroyd, C. B. (2007). Hierarchical error processing: Different errors, different systems. *Brain Research*, 1155:70–80.

Krishnaveni, V., Jayaraman, S., Aravind, S., Hariharasudhan, V. & Ramadoss, K. (2006). Automatic identification and removal of ocular artifacts from eeg using wavelet transform. *Measurement Science Review*, 6(4).

Lang, S. & Kotchoubey, B. (2000). Learning effects on event-related brain potentials. *NeuroReport*, 11:3327–3331.

Li, Y., Ma, Z., Lu, W. & Li, Y. (2006). Automatic removal of the eye blink artifact from eeg using an ica-based template matching approach. *Physiological Measurement*, 27:425–436.

Malmivuo, J. & Plonsey, R. (1995). *Bioelectromagnetism - Principles and Applications of Bioelectric and Biomagnetic Fields.* Oxford University Press, New York. ISBN 978-0195058239.

Mason, S. G., Bashashati, A., Fatourechi, M., Navarro, K. F. & Birch, G. E. (2007). A comprehensive survey of brain interface technology designs. *Annals of Biomedical Engineering*, 35(2):137–169.

Moeslund, T. B. (2001). *Principal Component Analysis - An Introduction.* Laboratory of Computer Vision and Media Technology, Aalborg University.

Parra, L. C., Spence, C. D., Gerson, A. D. & Sajda, P. (2003). Response error correction-a demonstration of improved human-machine performance using real-time eeg monitoring. *IEEE Transactions on Neural Systems and Rehabilitation Engineering*, 11(2):173–177.

Patel, S. H. & Azzam, P. N. (2005). Characterization of n200 and p300: Selected studies of the event-related potential. *International Journal of Medical Sciences*, 2:147–154.

Pfurtscheller, G., Neuper, C. & Birbaumer, N. (2005). *Motor Cortex in Voluntary Movements.* CRC Press LLC. ISBN 0-8493-1287-6.

Pittner, S. & Kamarthi, S. V. (1999). Feature extraction from wavelet coefficients for pattern recognition tasks. *IEEE Transactions on Pattern Analysis and Machine Intelligence*, 21(1).

Rangayyan, R. M. (2002). *Biomedical Signal Analysis - A Case-Study Approach.* John Wiley & Sons, Inc. ISBN 0-471-20811-6.

Ross, S. M. (2004). *Introduction to Probability and Statistics for Engineers and Scientists.* Academic Press, 3. Edition. ISBN 0-12-590857-4.

Sanei, S. & Chambers, J. A. (2007). *EEG Signal Processing.* John Wiley & Sons, Ltd. ISBN 978-0-470-02581-9.

Schalk, G., Wolpaw, J. R., McFarland, D. J. & Pfurtscheller, G. (2000). Eeg-based communication: presence of an error potential. *Clinical Neurophysiology*, 111:2138–2144.

Schlögl, A., Lee, F., Bischof, H. & Pfurtscheller, G. (2005). Characterization of four-class motor imagery eeg data for the bci-competition 2005. *Journal of neural engineering*, 2:L14–L22.

Semmlow, J. L. (2004). *Biosignal and Biomedical Image Processing: MATLAB-based applications.* Marcel Dekker, 1. Edition. ISBN 0824750683.

Werkhoven, P. J. & van Erp, J. B. F. (2007). Serious gaming requires serious interfaces. *Brain-Computer Interfaces and Games Workshop at ACE (Advances in Computer Entertainment) 2007*, side 49–52.

Wolpaw, J. R., Birbaumer, N., McFarland, D. J., Pfurtscheller, G. & Vaughan, T. M. (2002). Brain-computer interfaces for communication and control. *Clinical Neurophysiology*, 113:767–791.

Wolpaw, J. R., Loeb, G. E., Allison, B. Z., Donchin, E., do Nascimento, O. F., Heetderks, W. J., Nijboer, F., Shain, W. G. & Turner, J. N. (2006). Bci meeting 2005-workshop on signals and recording methods. *IEEE Transactions on Neural Systems and Rehabilitation Engineering*, 14(2):138–141.

Part IV

Appendix

Appendix A

Brain anatomy

To understand the location of the electrodes, it is an advantage to know some of the interesting parts of the brain for BCI. In figure A.1 the major parts of the brain is showed, the brain is lateral showed. The brain is divided into a left and a right hemisphere by a deep groove that runs from the front of the head to the back. The cerebral cortex is divided into four main divisions, or lobes, separated by noticeable folds in the surface. The frontal lobes house the motor cortex as well which is located in the back of the frontal lobes. Broca's area, which handles the production of speech, is also a part of the frontal lobes. Planning and mental representation of the outside world are also attributed to the frontal lobes. The parietal lobes process the signals that come from sensation. The temporal lobes are concerned with memory, hearing, and, in Wernicke's area, with the ability to understand language. The occipital lobes are specialized to manage the intricate processing of vision.[Ackerman, 1991]
Another important part of the brain for this study is the anterior cingulate cortex which is a part of the limbic network which deals with evaluative, cognitive and emotional components, among other things. The anterior cingulate cortex is a part of the cingulate gyrus which lies deep in the center of the brain illustrated in figure A.2. The interest in this part of the brain is because an error-related potentials, is seen regularly when actions are discrepant from an intended goal representation. [Beauregard, 2003]

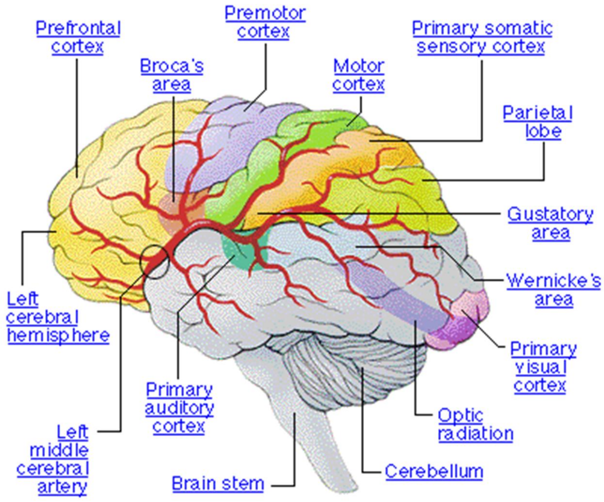

Figure A.1: *The brain illustrated in a lateral view.*

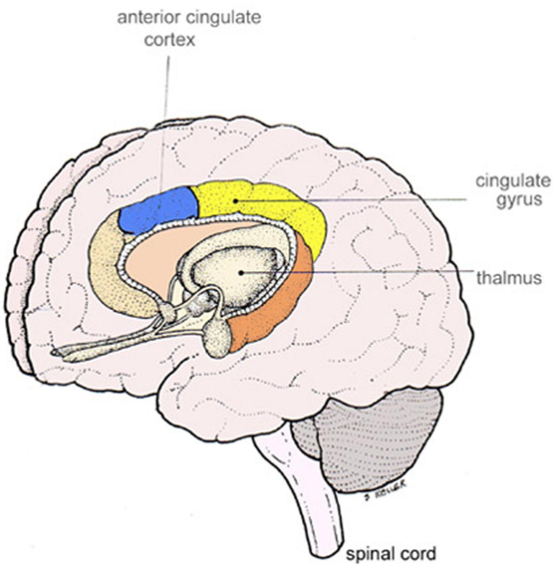

Figure A.2: *The location of the anterior cingulate cortex.*

Appendix B

Measurement techniques

Brain signals used in BCI can be divided into invasive and non-invasive signals. The invasive signals comprises the electrocorticography (ECoG) recorded using electrodes placed beneath the skull either subdural or epidural as well as intracortical signals. The non-invasive signals include the electroencephalography (EEG) which is recorded using surface electrodes placed on the skull. The EEG recordings reflects the common activity of several millions of neurons extending over some square centimeters of the cortical tissue. In contrast to the EEG, the ECoG represents integrated bioelectrical activity over a much smaller cortical area, but still constitutes the common activity of many thousands of neurons. The multichannel intracortical recordings reflect extracellular activity generated by small neuronal populations in the order of about 100 cells or fewer. The invasive methods obviously gives better signal resolution but are also associated with the risks of brain surgery, and will not be discussed any further.[Sanei & Chambers, 2007]

Using EEG both the spatial and temporal resolution of the brain signal becomes limited due to the overlapping electrical activity generated by different cortical areas. Furthermore, during the passive conductance of these signals through brain tissue, bone and skin, resolution is also lost owing to the low-pass filtering of the EEG signals. Artifacts from EMG and EOG will also affect the EEG signals. Despite these disadvantages EEG is being used all over in the field of BCI research and many systems using EEG has been developed.[Sanei & Chambers, 2007]

Conventional Electrode Positioning

The mostly used measurement technique for EEG is electrode caps. The electrodes are fixed on the cap after a conventional electrode setting for 21 electrodes recommended from the International Federation of Societies for Electroencephalography and Clinical Neurophysiology called 10-20, as shown in figure B.1[Sanei & Chambers, 2007]

The most common reference electrodes are the earlobe electrodes, connected respectively to the left and right earlobe. The placement of the electrodes considers some constant distance by using specific anatomic landmarks from which the measurement would be made and then uses 10 to 20% of that specified distance as the electrode interval. The numbering of the electrodes is done by giving the left electrodes odd numbers and the right even numbers. When using a larger number of electrodes mentioned in 10-20 the rest of the electrodes are placed in between the above electrodes with equidistance between them. Extra electrodes are sometime used for eliminating different kinds of artifacts. The main artifacts can be divided into patient-related and system artifacts. For BCI it is normally electrodes on the top of the scalp which has the most interest.[Sanei & Chambers, 2007]

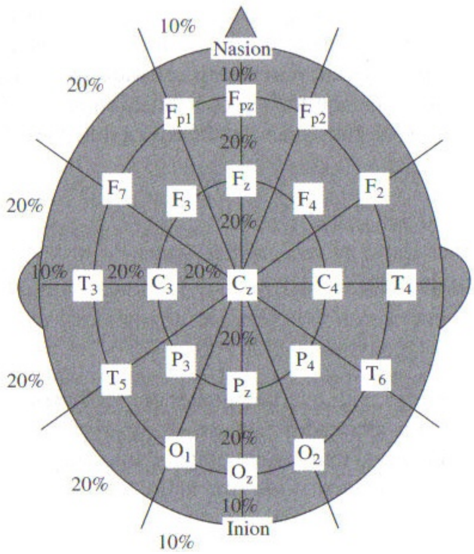

Figure B.1: *The electrode positions on the cap using the 10-20 system.[Sanei & Chambers, 2007]*

Appendix C

EEG generation

The current flowing during synaptic excitations of the dendrites of many pyramidal neurons in the cerebral cortex are called electroencephalography (EEG). The synaptic currents are produced within the dendrites when the brain cells are activated. The current is generated by pumping the positive ions of the sodium, Na^+, potassium, K^+ calcium, Ca^{++} and the negative ion of chlorine, Cl^-, through the neuron membranes.[Sanei & Chambers, 2007]

The amplitude of the EEG is about 100 μV when measured on the scalp, and about 1-2 mV when measured on the surface of the brain. A neurons resting potentials is around -70 mV, and the peak of the action potential is positive. The amplitude of the nerve impulse is about 100 mV and lasts about 1 ms.[Malmivuo & Plonsey, 1995]. Only large populations of active neurons can generate enough potential to be recordable using the scalp electrodes, the reason for this is the attenuation from the different layers the head consists of. The signal has to penetrate several layers of non-neural tissue including the meninges, fluid, bones of the skull, and the skin, to reach the electrodes. Therefore it takes many thousands synchronous neurons to generate a large enough EEG signal which can be detected by the electrodes. When a large group for neurons is excited simultaneously, the tiny signals sums to on signal large enough to reach the surface for the skull.[Bear et al., 2001] The attenuation of the signal in the brain can be illustrated by a volume conductor models showed in figure C.1. The radius of the skull in the illustration is set to 8 and 8.5 cm, and the radius of the head is 9.2 cm. The brain and the scalp has approximated a resistivity on 2.22 Ωm whereas for the skull the resistivity is approximated 177 Ωm.[Malmivuo & Plonsey, 1995]

The noise interfering with the signal is generated either within the brain or over the scalp. The EEG signal is generated from approximately 10^{11} neurons from a newly born baby, this makes an average of 10^4 neurons per cubic mm. The numbers of synapses per neuron increases with age, adults have approximately $5 \cdot 10^{14}$.

When EEG is measured different rhythms will appear in the signal if synchronous excitation of a large group of cells is repeated again and again. The EEG rhythms can be divided into five main groups: delta(δ), theta(θ) alpha (α), beta(β) and gamma (γ) mentioned from the lowest to highest frequencies.[Sanei & Chambers, 2007; Bear et al., 2001]

- Delta waves lie within the range of 0.5-4 Hz. These low frequencies are primarily associated with deep sleep and may appear during waking state.
- Theta waves lie within the range of 4-7.5 Hz. Theta waves appear as consciousness slips towards drowsiness.

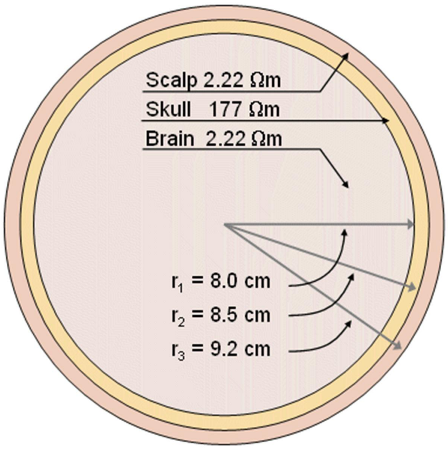

Figure C.1: *A model of the conductivity of the three main lairs in the head [Malmivuo & Plonsey, 1995].*

- Alpha waves lie within the range of 8-13 Hz. Alfa waves have been thought to indicate a relaxed awareness without any attention or concentration. The alpha waves appear in the posterior half of the head and are often found in the optical region of the brain.
- Beta waves lie within the range of 14-26 Hz. The beta rhythms are present during active thinking, like solving concrete problems.
- The frequency above 30 Hz is the gamma waves. Gamma waves have proved to be a good indication of event-related synchronization of the brain.

Delta(δ), theta(θ) alpha (α), beta(β) waves can be seen in figure C.2. In BCI the most important waves is beta and mu rhythms. The mu rhythms frequency lies within the regions as alpha rhythms. Mu rhythms is strongly related to the motor cortex.[Sanei & Chambers, 2007]

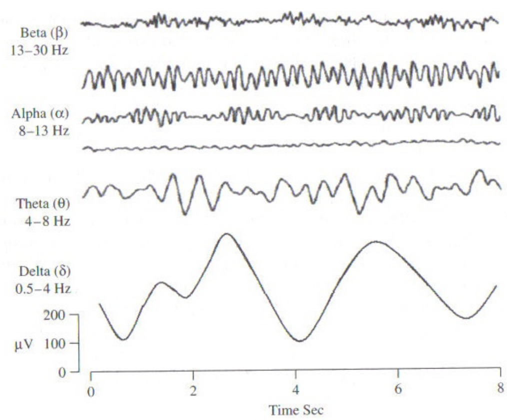

Figure C.2: *The most common brain rhythms.*

Appendix D

Individual EEG recordings

For each subject included in the experiment there are three figures. They all contains an average of the response signal from error and correct feedback and the X-event for Fz, Cz and Pz respectively. The signals are filtered and EOG is removed using ICA as explained in the preprocessing chapter. The average for error and correct feedback are made from 60 and 180 trials respectively which are all trials for one subject from all three days.Subject 1, see figure D.1, show a negative peak and a positive peak at respectively 230 ms and 300 ms after feedback. A broader deflection peaking around 600 ms after feedback is also present. The two negative peaks deviate between correct and error feedback. The first negative peak is less negative for error feedback whereas the second negative peak more negative for error feedbacks. The response to the X-event has very similar characteristics as to the correct and error feedback. The same peaks are present with similar amplitudes and latencies, which is a negative peak at 220 ms, a positive at 320 ms and another negative peak at 500 ms after the event. The response recorded at Fz, Cz and Pz has very similar characteristics except from the negative peak at 230 ms which is not so clear from Pz.

Subject 2, see figure D.2, show only a large negative peak around 400 ms after feedback. There is no clear negative around 200 ms and no clear positive at 300 ms after feedback. There seems to be a slightly shorter latency for this peak after error feedback. The response to the X-event show a very clear negative peak at 200 ms, a positive at 280 ms and another negative at 400 ms after the event. The response recorded at Pz differs from Fz and Cz in having a more clear positive peak at 180 ms.

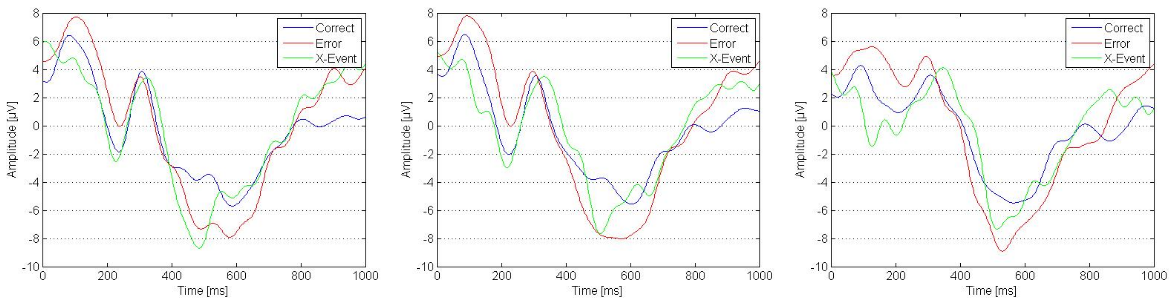

Figure D.1: *The response signals from correct and error feedback and the X-event for subject 1, recorded at electrode location Fz, Cz and Pz respectively. Feedback was presented at time 0 seconds. The signals are averages of the recordings from all 3 sessions.*

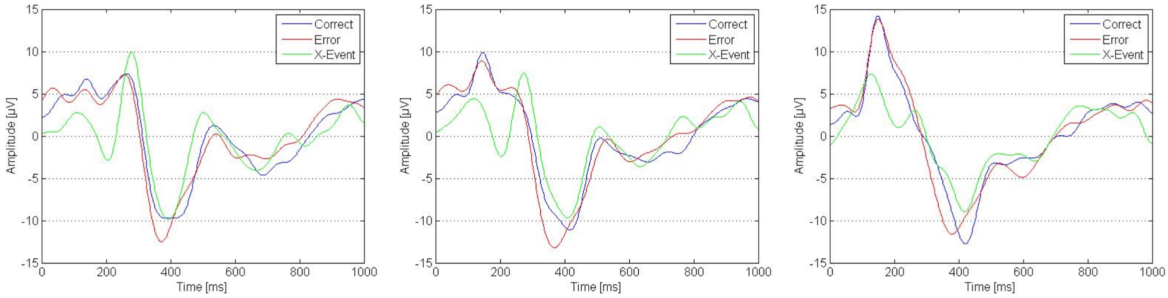

Figure D.2: *The response signals from correct and error feedback and the X-event for subject 2, recorded at electrode location Fz, Cz and Pz respectively. Feedback was presented at time 0 seconds. The signals are averages of the recordings from all 3 sessions.*

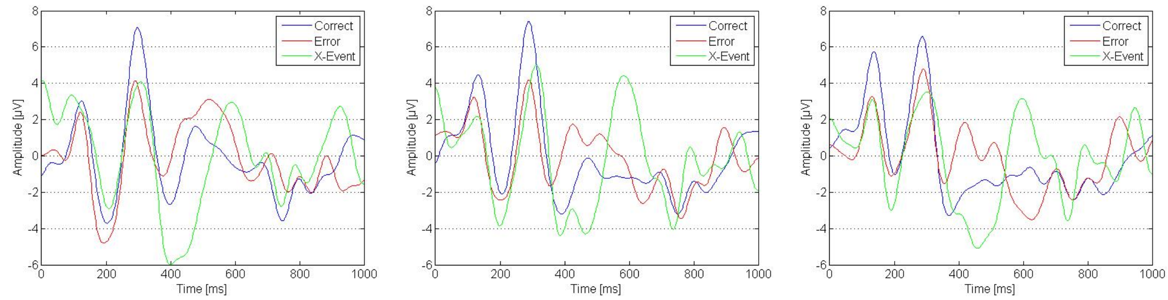

Figure D.3: *The response signals from correct and error feedback and the X-event for subject 3, recorded at electrode location Fz, Cz and Pz respectively. Feedback was presented at time 0 seconds. The signals are averages of the recordings from all 3 sessions.*

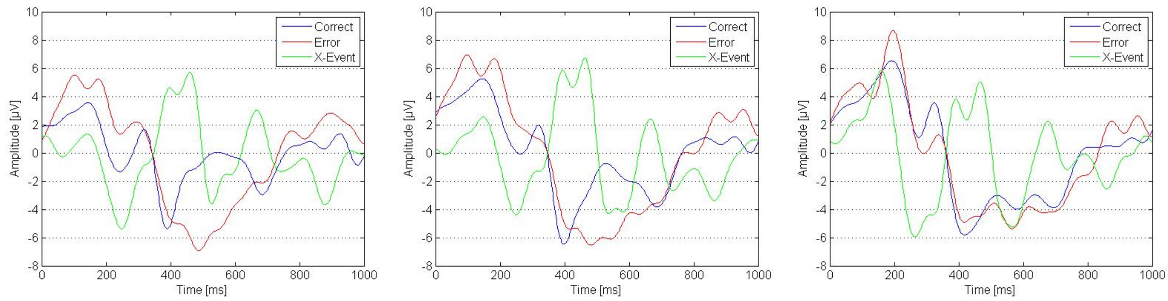

Figure D.4: *The response signals from correct and error feedback and the X-event for subject 4, recorded at electrode location Fz, Cz and Pz respectively. Feedback was presented at time 0 seconds. The signals are averages of the recordings from all 3 sessions.*

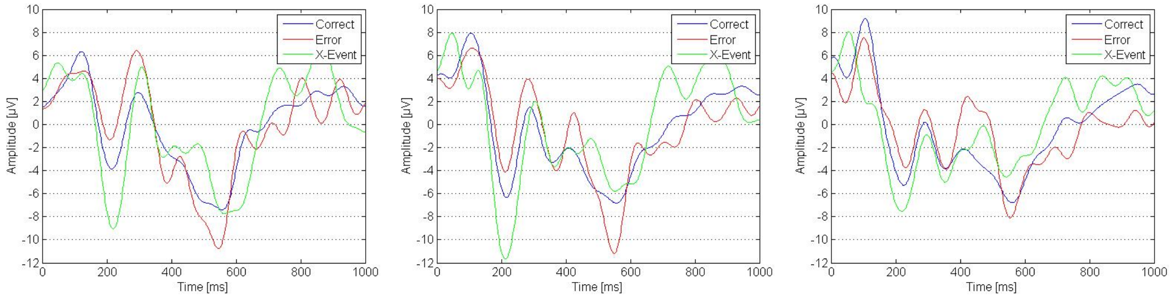

Figure D.5: *The response signals from correct and error feedback and the X-event for subject 5, recorded at electrode location Fz, Cz and Pz respectively. Feedback was presented at time 0 seconds. The signals are averages of the recordings from all 3 sessions.*

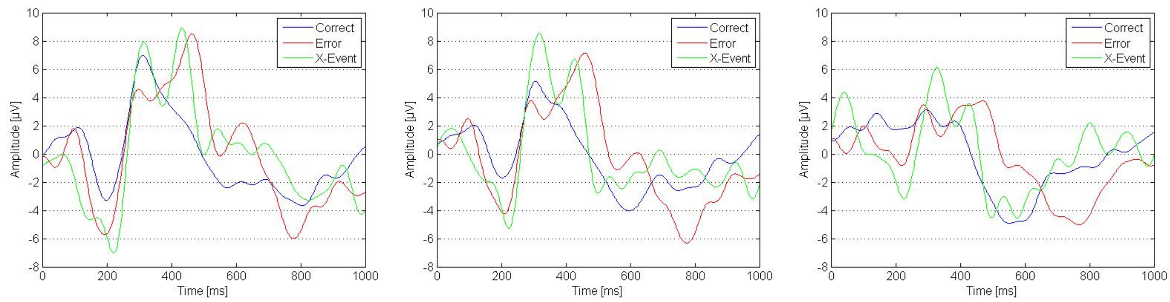

Figure D.6: *The response signals from correct and error feedback and the X-event for subject 6, recorded at electrode location Fz, Cz and Pz respectively. Feedback was presented at time 0 seconds. The signals are averages of the recordings from all 3 sessions.*

Subject 3, see figure D.3, show a clear negative peak at 200 ms a positive at 300 and another negative again between 350 and 400 ms after feedback. The error feedback show smaller amplitudes at the last two peaks and a shorter latency for the last negative peak. The response to the X-event show also a clear negative peak at 200 ms, a positive peak at 300 ms and a negative between 400 and 500 ms after the event.

Subject 4, see figure D.4, show a small negative peak at 270, a small positive peak at 320 ms and a large negative peak at 400 ms after correct feedback. After error feedback only the large negative peak around 400 ms is present. This peak is however much broader than during correct feedback. The response to the X-event show a negative peak at 250 ms, a positive around 400 ms and another negative peak between 500 and 600 ms after the event. The response recorded at Pz show a equally broad negative peak around 400 ms for both error and correct feedback whereas Fz and Cz show a much broader peak during error feedback.

Subject 5, see figure D.5, show a negative peak at 200 ms, a positive at 300 ms and a negative beween 500 and 600 ms after feedback. The error feedback show a less amplitude for the first peak and a larger amplitude for the last two peaks compared to the correct feedback. The response to the X-event shows a large negative peak at 200 ms, a positive a 300 ms and a negative peak between 500 and 600 ms after the event.

Subject 6, see figure D.6, show a negative peak at 200 ms, a positive at 300 ms and a negative a 600 ms after correct feedback. After error feedback the same peaks are present but with larger amplitudes and approximately 200 ms longer latency for the last two peaks. The response for the X-event show a negative peak at 220 ms and a postive peak between 300 and 400 ms after the response. No clear second negativity is present.

Detection of error-related potentials to improve brain-computer interfaces

Esben Wermuth Ingstrup and Christian Kannegård Nikolajsen

***Abstract*— The brain-computer interface (BCI) permit the use of brain signals to control external devices. The signal to noise ratio is however low and the intra-individual variations of the signals are high, which complicate the recognition of the users intent. To improve the performance of BCI systems, the detection of error related potentials (ErrPs) have been suggested as they may indicate that the system have made an erroneous action. In this paper the detection of single trial ErrPs following erroneous feedback to imaginary tasks is described. An experiment including a test group of ten subjects and a control group of three subjects was conducted. The results reveal a significant difference between error and correct trials which cannot be explained by the presence of an oddball. By using a support vector machine (SVM) we achieved an averaged classification accuracy of 73.6% and 72.3% for single error trials and single correct trials respectively. The results reported in this paper support the idea that ErrPs possibly will improve the accuracy of future BCI systems.**

***Index Terms*— Error-related potentials, movement-related cortical potentials, P300, brain-computer interfaces, independent component analysis, continues wavelet transformation, support vector machine.**

I. Introduction

The brain-computer interface (BCI) utilizes neurological signals from the human brain and converts them into command signals which can control computers and external devices. The goal of BCI research is to develop technologies that will benefit severely disabled people by improving their independence and ability to perform daily activities and potentially restore lost function. [1]

For a reliable BCI system a suitable control signal from the electroencephalogram (EEG) has to be determined. Due to the nature of the EEG it can be difficult to find a control signal which can be precisely characterized, readily modulated and be detected and tracked consistently and reliably. One problem in BCI is separating the control signals from the background EEG. Another problem with the use of EEG is the variety of artifacts which can interfer with the control signal. The signal has to be restored from artifacts like eye-blinking, muscle activity, cardiac activity, and any other internal or external disturbing effects. [2]

A third issue concerning the stability of a BCI system is the intra- and inter-user variations in the EEG signals. Signal features are likely to differ greatly between different users and there will possibly be even more variation in users with disabilities. Potential users of BCI are patients with locked-in syndrome due to late- or end-stage amyotrophic lateral sclerosis (ALS). [3] These patients are fed by tubes, require ventilation support and are bound to a bed or a wheelchair. This may lead to intermittent lung and bladder infections, autonomic dysfunction with fluxes in blood pressure, diabetes mellitus, hypertension, and other toxic and metabolic complications which are commonly seen in immobile people. All these factors may also affect the cortical activity and thus the reliability of the EEG as a command signal. [4] The EEG will in addition naturally change over time, both between different sessions and within a single session. Studies have shown pronounced intra-individual variations in the BCI performance occurring within minutes. These changes can be due to individual factors like level of alertness, reaction speed, working memory capacity and the ability to perform parallel tasks. [5]–[7].

The signal variations obviously generate great challenges for the development of BCI systems. To deal with these variations the classifier of the BCI system needs to adapt throughout its use and keep it tuned to drift in the signals it is receiving. [6], [7] To achieve a more reliable and robust BCI system the classifier needs a feedback on its performance. First of all it could be useful to detect if the classifier makes a wrong decision based on the recorded EEG and stop the BCI from executing incorrect commands. During ongoing use it might be possible to improve the performance of the classifier as well, by constantly adjusting it. One option could be to use error related potentials (ErrP) as feedback of the classifiers performance. [7]

An ErrP is an event related response from the brain as a response to an error. ErrPs provide important evaluative information, since they indicate that a behavior was inadequate given the current context and that, in future, a different response needs to be selected [8]. ErrPs can be elicited by negative feedback and by error commission itself and the generation of the ErrP is equally sensitive to errors committed by different motor modalities. Investigations suggest that the ErrP is generated in anterior cingulate cortex (ACC) and it is elicited by a high-level error processing system. The ACC has a great diversity of inputs from cortical and subcortical areas and is believed to be a neural center where motor intentions are mapped into action. It is believed to provide a critical pathway for emotional and motivational factors influencing motor activity and that anterior cingulate motor areas are involved in learning the mapping from intention to action by reward-related information carried to the ACC by the mesencephalic dopamine system. [8]

ErrPs have been investigated by different psychophysiology research groups [8]–[13] and in recent years also in the context of BCI research [6], [7], [14]–[18].

Three different types of ErrPs have been reported. A negative deflection peaking 100 ms after error commission in a speeded response task have been reported by [10] and is sometimes referred to as response ErrP. A second negative deflection peaking 250 ms after feedback has been reported by [8], [9], [11] and is sometimes referred to as feedback ErrP. Both the response and the feedback ErrP are present after errors made by the subject himself. A third ErrP referred to as interaction ErrP has been reported by [18]. This ErrP is triggered by an erroneous feedback caused by the interface and it consists of four peaks. First a positive peak at 200 ms after feedback. Then a negative peak and a positive peak at 250 ms and 320 ms after feedback, respectively. Finally a broader negative peak is present at 450 ms after feedback.

In a realistic BCI situation however erroneous feedback can be caused by non-optimal performance of the interface as well as by the users own mistakes. Another important aspect is that the reported ErrPs always followed a motor task, for example pressing a button. In a realistic BCI situation no tasks are performed by the subject overtly, only mentally (e. g. by performing imaginary movements). As a consequence it will never be clear to the user what exactly caused the erroneous feedback. It is therefore interesting to clarify if an erroneous feedback in this type of situation also elicits an ErrP that is large and consistent enough for single trial detection to improve the accuracy of BCI systems.

The objective of this study is to investigate the presence of ErrPs in a BCI situation as just described. The detection of ErrPs should be used to improve the accuracy of a BCI system described in [19]. The system classifies movement-related cortical potentials (MRCPs) generated by variation in force-related parameters during imaginary foot movement. The ErrPs should therefore follow an incorrectly classification of imaginary foot movements. To our knowledge ErrPs in relation to MRCPs during imaginary motor tasks have not previously been investigated. This study is based on a fake online BCI setup, as controlling the rate of error trials is important in the investigation of ErrPs.

II. Methods

A. Subjects

The experiment included a test group and a control group. Ten subjects, six males and four females, with age ranging from 20 to 25 (mean 22.2 ± 1.5), constituted the test group. Three subjects, two males and one female with age ranging from 25 to 27 (mean 26.3 ± 1.2), constituted the control group. All subjects had no known history of any motor or neurological pathology. The experiment was approved by local ethical committee (N-20070001) and written and verbal information were given to the subjects prior to the experiment. All subjects gave a written informed consent for their participation.

B. Experimental Activity

1) Test Group: The subjects were told that they were in an experiment in which a BCI system was being tested and that imaginary movements of the foot were measured and classified online.

The subjects were seated in a comfortable chair with the right foot placed on a pedal instrumented with a force gauges which measured the exerted force. The force exerted to the pedal was shown to the subjects through an oscilloscope. Before the actual experiment there was a preparation period where the subjects practiced real foot movements to become familiar with the tasks. The tasks during practice consisted of real isometric plantar flexions of the right foot using two different force rates, either high rate (ballistic) or low rate (moderate). During both ballistic and moderate movement the aim was a force level at 70% of maximum voluntary contraction (MVC). Ballistic movement consisted of reaching the force level as fast as possible and the moderate movement was reaching the force level by a steady increase of force with 40% of MVC per second.

During the actual experiment the subjects were told only to imagine the isometric plantar flexion and to follow the same parameters for the imaginary movement as during practice. From a computer screen the subject were instructed to perform either an imaginary moderate plantar flexion or imaginary ballistic plantar flexion. The number of the two tasks were equally sized and shown in random order. The graphical user interface was made in LabView, as shown in figure 1.

On the screen a clock with one hand was shown. One clock cycle had a duration of ten seconds which determined the duration of one trial. A trial started when the clock hand was at the 3 o'clock marker. The subject was instructed to stop the clock hand at the 12 o'clock marker for each trial by performing the correct imaginary movement. Hence the correct feedback was a stopping hand at the 12 o'clock marker for two seconds and the error feedback was a continuing hand. As there was no online detection of the imaginary movements, the feedback was chosen in random order with a probability of 75% for correct trials and 25% for error trials.

The execution of an imaginary movement should start exactly when the clock hand passed into the red colored area of the clock (three seconds before feedback). To minimize the EOG interference the subject was told to blink only within the white colored area of the clock if possible.

Each subject participated in the experiment in two sessions during two different days. One session consisted of eight blocks of 20 trials, giving a total of 160 trials per session. In between every block of 20 trials, the subjects practiced real ankle flexions as during the preparation period to keep them primed on the task that should be imagined. To keep the subjects further motivated they could follow a progress bar on the screen, which filled up progressively each time a correct feedback was given. It was obviously not possible to completely fill up the bar, although this was told to be the aim for the subjects. Half way through the session the subjects had a five to ten minutes break.

2) Control Group: Investigations of P300 normally follow the oddball paradigm, where the subject is given a frequent and an infrequent stimuli. The infrequent and deviant stimuli elicite the P300 component. As the procedure in this experiment can be characterized as an oddball paradigm, a control group was included to investigate the interaction of the P300 and the ErrP. The experimental activity for the subjects in the control group was exactly the same as for the test group. The only difference was the information given to the subjects.

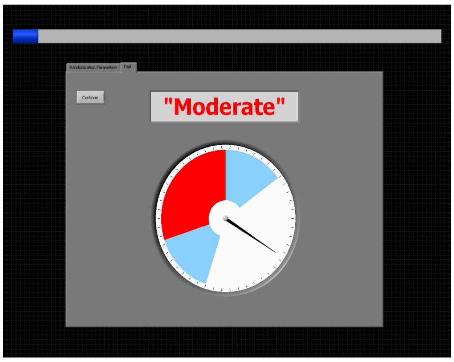

Fig. 1. The graphical user interface shown to the subjects during the experiment.

The subjects were not told that they were in an experiment in which a BCI system was being tested and were not convinced that imaginary movements of the foot were measured and classified online. Instead they were instructed only to keep focused on the clock hand which would stop at the 12 o'clock marker or continue in random order with no relation to their task performance. In addition they were instructed not to pay attention to the progress bar.

C. Data Acquisition

The EEG recordings were performed with a 40 channel digital DC EEG amplifier (Neuro Scan, model NuAmps), and data were recorded with the Acquire module of the Scan 4.3 software (Neuro Scan). For EEG recordings 28 electrodes placed on a cap according to 10-20 system were used, i.e.: FP_1, FP_2, F_7, F_3, F_Z, F_4, F_8, FC_5, FC_1, FC_2, FC_6, T_3, C_3, C_Z, C_4, T_4, CP_3, CP_Z, CP_4, T_5, P_3, P_Z, P_4, T_6, PO_Z, O_1, O_2, and FP_Z was used as ground. Each monopolar EEG electrode (tin) was referenced to common reference electrodes (tin) placed on the earlobes (A1, A2). Four standard tin electrodes was used for EOG recording, with two positioned above and beneath the right eye and two electrodes positioned on the outer and inner canthi on the right eye. The EEG and EOG signals was amplified by a gain of 19, band-pass filtered from DC to 100 Hz and digitized at 500 Hz using a 16-bit A/D converter.

D. Preprocessing

The processing of the collected data was performed using MATLAB version 7.4.0 (The MathWorks, Inc.). The signal was band-pass filtered using a 1st order high-pass and a 10th order low-pass Butterworth filter with cutoff frequencies at 0.1 Hz and 45 Hz respectively. For removal of EOG from the EEG an automatic method based on independent components analysis (ICA) is proposed. The ICA algorithm used in this study was the one included in the EEGLAB toolbox [20] which is based on the infomax algorithm developed by [21]. The problem about making an automatic method based on ICA is that the independent components (ICs) reflecting the EOG have to be identified before removal [22]. This was solved by calculating the angle between the eye recorded EOG channels and the ICs which gives a similarity between the recorded EOG and the decomposed ICs. The angle was calculated by following equation:

$$\alpha_{j,i} = cos^{-1}\left[\frac{ICeeg_j \cdot EOG_i}{\|ICeeg_j\| \, \|EOG_i\|}\right] \tag{1}$$

The angle was calculated between each of the four EOG channels and the scalp recorded independent components, $ICeeg_j$, $j = 1, ..., N$, where N is the number of independent components and $i = 1, .., K$ where K is the number of recorded EOG channels. If α_j was less or higher than two predefined thresholds the j'th IC was assumed to be an EOG component and removed. The high and low thresholds were set to 1.8 and 1.4 radians, where 1.6 corresponds to completely independence between the IC and EOG. After the EOG components were removed, the EEG was restored by inverse ICA.

After EOG removal the signal epochs of interest were extracted for further analysis. To investigate the presence of MRCPs, signal from 1.5 second before to 1.5 seconds after movement onset were extracted. For investigation of ErrPs the response signal from 0 to 1 second after feedback were extracted. The response signals were furthermore band-pass filtered with a 4th order high-pass and a 5th order low-pass Butterworth filter with cutoff frequencies at 1 Hz and 10 Hz respectively, as the ErrP is reported to be in this range [7].

E. Statistical analysis

To validate the presence of ErrPs an ANOVA was conducted to calculate if there was significant difference between the recorded response signals. In the test group, correct and error feedback were compared by performing ANOVA on the maximum amplitude from the averaged response signals from each subject in the interval 200 ms to 600 ms after feedback. The same procedure was done for comparing the trials with stopping hand (corresponding to correct feedback) and trials with a continuing hand (corresponding to error feedback) in the control group. In between the two groups the ANOVA was performed to compare correct feedback and the hand stopping as well as to compare error feedback with the hand continuing.

F. Feature Extraction

According to [23], [24] time/frequency analysis and the signal itself are often used as features in the contexts of ERP classification. In this study the two approaches were compared. The response signal was a window from 200 to 600 ms after feedback downsampled by 5. The time/frequency analysis was implemented using the continuous wavelet transform (CWT). The CWT is highly redundant and time consuming to compute compared to the discrete wavelet transform (DWT). However the DWT is reducing the wavelet coefficients by changing the scale and translation in powers of 2, which will produce a nonredundant transform of a signal. [25] If the wavelet transform is used to find shapes like ERP it is more likely to find a scale of the wavelet which fits the waveform in the signal by using the CWT. [26] The definition of the CWT of a signal $f(t)$ is:

$$W(a,b) = \frac{1}{\sqrt{a}} \int_{-\infty}^{\infty} f(t)\Psi(\frac{t-b}{a})dt \quad (2)$$

Where b denotes the time shift (the position parameter), a denotes the scale parameter (inversely proportional to frequency), and Ψ is the wavelet function. The CWT is a computation of the cross correlation between the signal and the predefined waveform, the template Ψ, which is shifted forward and backward in time and dilated and constricted in scale. The Mexican Hat was chosen as the wavelet function for the CWT. The method used for feature extraction from the CWT is proposed by [26]. The method suggests using a t-test to calculate where the largest difference between the CWT of the error and correct trials. The method is performed in five steps: The first step is to calculate the CWT, $W^n(a,b)$ of the signal $f^n(t)$ which is calculated for each trial n. The second step is to calculate the mean $\overline{W_g(a,b)}$ and variance $\sigma_g(a,b)$ from each CWT of each trial:

$$\overline{W_g(a,b)} = \frac{1}{N_g} \sum_{n=1}^{N_g} W^n(a,b) \quad (3)$$

$$\sigma_g(a,b) = \frac{1}{N_g - 1} \sum_{n=1}^{N_g} (W^n(a,b) - \overline{W_g(a,b)})^2 \quad (4)$$

Where N_g is the number of trials in group (g = correct or error)
The third step is to calculate the t-statistic for error and correct trials $t(a,b)$:

$$t(a,b) = \frac{\overline{W_{correct}(a,b)} - \overline{W_{error}(a,b)}}{\sqrt{\sigma_{correct-error}(a,b)}} \quad (5)$$

Where $\sigma_{correct-error}(a,b)$ is defined according to equation 6.

The fourth step is extracting the local extremes of the function $t(a,b)$ refered to as (a^i, b^i) which are the points of maximal difference between correct and error feedback responses. The 15 maximums and 15 minimums were chosen to use as features for training and test, giving a total number of 30 features for each trials.
The fifth and last step is to compute each point (a^i, b^i) for each single trial n for both the test and the training data. [26]

G. Classification

The classification was performed by support vector machines (SVM) as implemented by [27]. The SVM is a nonlinear pattern classification method. The central idea of SVM is the adjustment of a discriminating function so that it optimally uses the separability information of the boundary patterns. [28] A training set of i examples is defined with the data vector x_i and a class label y_i:

$$(x_1, y_1), \ldots, (x_i, y_i) \in R^N \times -1, 1 \quad (7)$$

To separate the training set, a classification method needs to find a hyperplane which satisfy some optimality criterion. The class label of a new data vector x can be predicted by projecting x on the weight vector w:

$$f(x) = w \cdot x + b \quad (8)$$

The sign of this equation would reveal the predicted class label. To describe the hyperplane, only the vectors on the margin, the so-called support vectors, are necessary. The margin γ described by the support vectors is maximized by minimizing $(1/2)\|w\|^2$ subject to constraint $y_i(w \cdot x_i + b) \geq 1$. A so called slack-variable ξ_i is introduced to allow violation which gives the SVM optimization problem:

$$min\ \frac{1}{2}\|w\|^2 + C\sum_i \xi_i \quad (9)$$

$$s.t.\ \ y_i(wx_i + b) \geq 1 - \xi_i, \ \ \xi_i < 0 \forall i \quad (10)$$

Where C is parameter representing the tradeoff between minimizing the training set error and maximizing the margin.

By using a Kernel function $K(x, x_i)$ the given data space can be transformed into a higher dimensional feature space which then makes the data separable by a linear hyperplane. [29] In this study a Gaussian radial basis function kernel was used which is defined by:

$$K(x, x_i) = exp\left(-\frac{\|x - x_i\|^2}{2\sigma^2}\right) \quad (11)$$

The SVM classifier is controlled by the regularization parameter C and the bandwidth σ of the Gaussian kernel. To get better results [30] recommend to do a grid search using cross validation to find the best values for C and σ. In this study best values of C and σ were found by cross validation with $C = [2^{-5}, 2^{-3}, .., 2^{15}]$ and $\sigma = [2^{-15}, 2^{-13}, .., 2^{3}]$.

III. Results

A. Signal analysis

In figure 2(a) the grand averages of the response signals measured after feedback are shown. It is evident that there is a difference in amplitude between error and correct feedback. The conducted ANOVA revealed a significant difference in amplitude $F(1,18)=8.41$, $p<0.01$. The grand average response signal from the control subjects, figure 2(b), does not show a clear amplitude difference between the two types of feedback and the difference did not reach significance $F(1,4)=0.03$, $p=0.87$. There is however a significant difference in amplitude between the correct feedback and the stopping hand, $F(1,11)=8.15$, $p<0.05$. A significant amplitude difference is also the case between the error feedback and the continuing hand, $F(1,11)=8.6$, $p<0.01$. There were no statistical significant difference in latencies between the two types of feedback nor between the feedback in the two groups.

The averaged difference signal (error minus correct) can be seen in figure 3(a) where a clear negative peak and a positive peak are present at 380 ms and 560 ms after feedback respectively. The scalp topographies of the response difference signal (error minus correct) in figure 3 show a widely distributed negativity centred in the parietal area and a positivity more centred at Cz.

$$\sigma_{correct-error}(a,b) = \frac{(n_{correct}-1)\sigma_{correct} + (n_{error}-1)\sigma_{error}}{n_{correct}+n_{error}-2}(\frac{1}{n_{correct}} + \frac{1}{n_{error}}) \tag{6}$$

One of the main factors in keeping the experimental activity for the two groups exactly the same was the performance of an imagninary plantar flexion prior to the feedback. In figure 4(a) and 4(b) the grand averaged MRCPs for respectively the test group and the control group is shown. Both the test and control group show a slow negative deflection from 1500 ms before the movement to 1500 ms after the movement is executed.

B. Single trial classification

In table I and II the single trial classification rates are listed for all ten subjects in the test group. The results are shown from a 10-fold cross validation using the recordings of day one, 10-fold cross validation using the recordings of day two and by training the classifier with recordings of day one and testing with the recordings of day two, respectively. In table I the results were obtained by using a downsampled version of the response signal as feature vector to the SVM. Using this approach averaged accuracy of 73.6% and 72.3% for error and correct trials were obtained training with recordings from day one and testing with recordings from day 2. In table II the results are obtained using wavelet coefficients as feature vector to the SVM. Using this approach averaged accuracies of 75.5% and 70.0% for error and correct trials were optained training with recordings from day one and testing with recordings from day 2.

IV. Discussion

A. Error related potentials

The aim of this study was to investigate the presence of ErrPs following feedback indicating incorrectly interpretation of imaginary movements. In a realistic BCI setting the error could be due to an incorrect imaginary task from the subject, a lack of the subjects concentration when performing the task or it could be entirely an error made by the interface. All three situations could possibly give an error in the recognition of the users intent while it is not clear to the user which of the three situations that have caused it. If ErrPs should be useful to improve performance of BCI systems they should be elicited in this type of BCI setting and more importantly, single trial classification of errors should be feasible. It was hypothesized that the ErrP elicited in the conducted experiment would be similar to the feedback ErrP, which has been reported as a negative deflection peaking approximately 250 ms after erroneous feedback [8], [9], [11]. The ErrP can however easily interact with the P300 component which is elicited by a rare or significant stimuli and which amplitude is strongly related to the unpredictability of the stimulus as would be the case of the feedback given in this experiment. The P300 is normally appearing between 300 ms and 400 ms after stimuli, but latencies can range from 250 ms to 900 ms [31]. If the ErrP and the P300 is present in the same time interval the resulting outcome could be a response similar to the P300 in shape and latency, but with a decreased amplitude. The control subjects in the experiment was included to confirm that the difference between error and correct trials could not entirely be explained by the changes in P300 amplitude due to the difference in probability of the two types of feedback, often referred to as an oddball paradigm. The feedback to the control group was exactly the same as for the test group. The only difference was in terms of the information given to the subjects in the two groups, which resulted in a positive outcome (correct feedback) and a negative outcome (error feedback) for the test group, whereas both types of feedback would be perceived as neutral for the control group.

The results from this study reveal that there indeed is a significant difference between error and correct trials. The grand average of the correct trials show a clear P300 peaking at 380 ms after feedback, whereas error trials show a reduced P300 peaking around 430 ms after feedback. This reduced amplitude could very likely be caused by the presence of the negative component of the ErrP. In the control group the stopping hand also elicit a P300 response with approximately the same latency at 380 ms after feedback. The averaged amplitude is however decreased significantly with maximum of 2.7 μV compared to a maximum amplitude of 11 μV in the test group. The continuing hand did not show a significantly decreased P300 compared to the hand stopping, as it was the case in the test group.

The scalp topographies of the grand averaged difference signal (error minus correct) implies that the medio-parietal area contributes most to the difference, although the difference is widely distributed over the cortical areas. This finding is in conflict with the general assumption that ErrP generation is localized in the medio-frontal area [8], [11], [18]. The explanation to this contradiction could very likely be that the difference between error and correct trials is strongly contributed by the P300 component which is generated in the parietal area [31].

The difference between error and correct trials is presumably caused by two factors: 1) there is negative component very similar to the feedback ErrP after error feedback. The negative component is very likely an ErrP although it has a latency of approximately 380 ms after feedback. 2) The P300 component has increased amplitude when the subjects are given a correct feedback. This finding is in agreement with the fact that P300 is larger after positive outcomes in reward-based learning tasks reported by [32]. The findings are also similar to the ones reported by [16] where they discovered that a correct classification elicits a P300 whereas an erroneous classification did not in a P300-based BCI system.

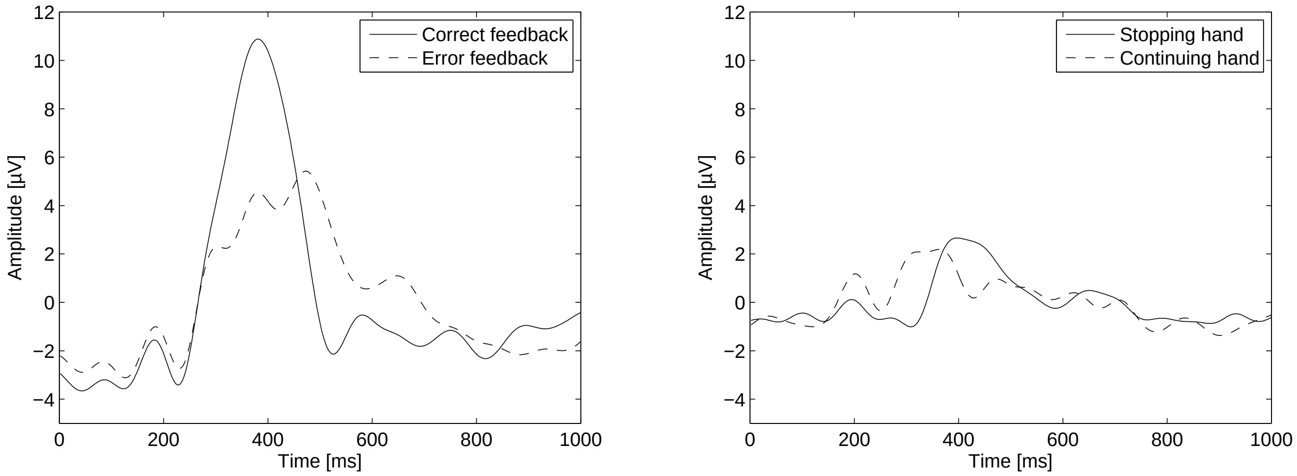

(a) (b)

Fig. 2. a) The grand average of the response signal after error and correct feedback for all ten subjects in the test group recorded at Cz. b) The grand average of the response signal after a stopping and a continueing hand for all three subjects in the control group recorded at Cz.

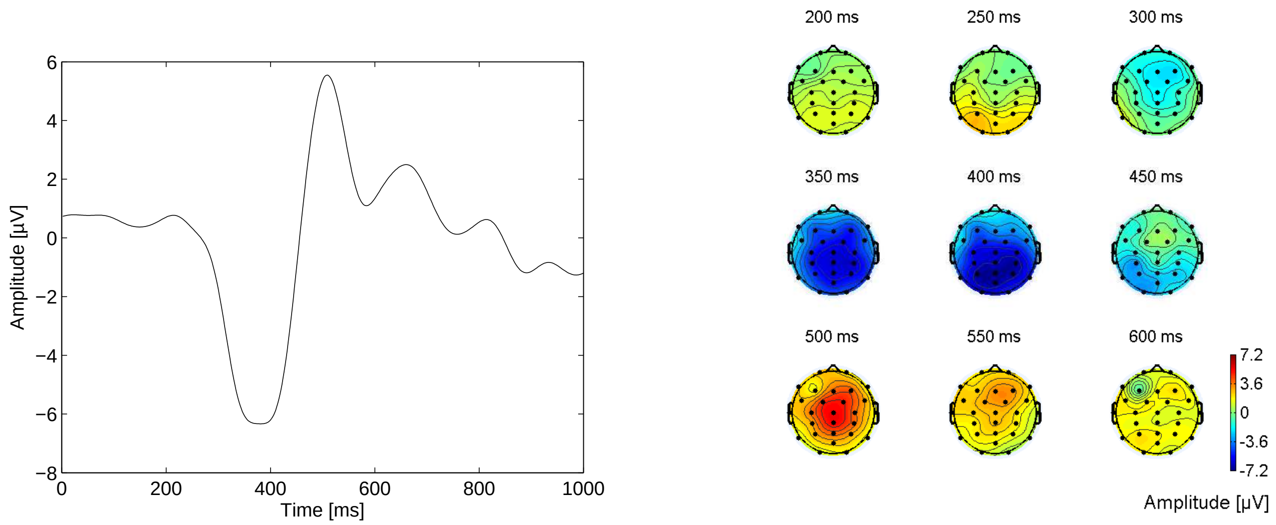

(a) (b)

Fig. 3. a) The grand average difference signal (error minus correct) for all ten subjects in the test group recorded at Cz. b) Grand average scalp topographies for all teen subjects in the test group.

	Subject 1	Subject 2	Subject 3	Subject 4	Subject 5	Subject 6	Subject 7	Subject 8	Subject 9	Subject 10	**Average**
						10-fold cross validation day 1					
E	82.5±5.2	73.2±8.3	72.8±5.9	67.6±5.9	70.1±7.1	59.8±9.6	80.3±8.8	87.7±5.0	85.1±4.9	94.6±3.4	**77.4±6.4**
C	63.8±7.6	71.4±6.0	62.6±7.6	55.0±8.5	70.3±6.5	56.3±9.0	50.3±8.1	83.7±5.0	75.8±5.3	86.5±4.3	**67.6±6.8**
						10-fold cross validation day 2					
E	86.8±3.8	63.5±6.6	87.1±3.1	54.7±9.3	58.5±5.7	74.7±4.7	79.9±5.5	90.8±2.6	88.9±5.2	86.0±3.1	**77.1±5.0**
C	81.3±5.1	62.6±7.1	69.8±5.3	58.5±7.9	78.5±7.6	68.3±7.9	69.3±5.6	85.9±5.7	78.0±7.1	81.8±5.8	**73.4±6.5**
						Day 2 classified with day 1					
E	79.9±8.8	56.6±6.2	78.8±9.5	77.5±8.4	60.4±7.7	71.0±13.4	69.6±13.5	87.5±6.4	93.0±3.1	62.1±6.7	**73.6±8.4**
C	81.2±6.8	74.2±7.6	68.9±8.3	34.9±7.0	80.1±8.7	63.3±13.9	69.7±7.3	85.6±5.0	72.6±6.4	92.8±4.3	**72.3±7.5**

TABLE I

The classification accuracy (mean and standard deviation) for error trials (E) and correct trials (C) for all ten subjects in the test group using the response signal as feature vector.

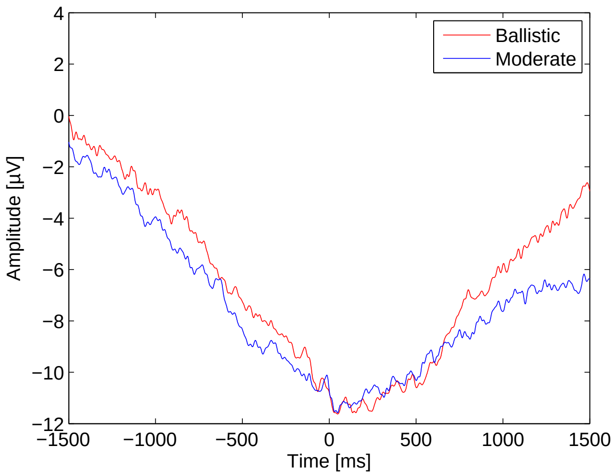

(a)

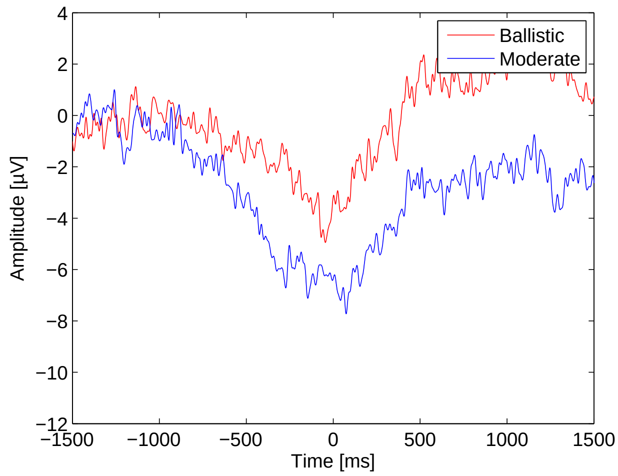

(b)

Fig. 4. a) The grand average MRCP for all ten subjects in the test group recorded at Cz. Time 0 corresponds to the onset of the movement. b) The grand average MRCP for all three subjects in the control group recorded at Cz. Time 0 corresponds to the onset of the movement.

	Subject 1	Subject 2	Subject 3	Subject 4	Subject 5	Subject 6	Subject 7	Subject 8	Subject 9	Subject 10	**Average**
						10-fold cross validation day 1					
E	79.4±7.8	78.5±5.6	70.2±8.1	64.8±7.4	74.0±8.1	59.0±9.5	79.3±6.6	86.9±5.5	86.5±5.9	94.2±3.0	**77.3±6.8**
C	68.1±6.1	69.1±7.8	62.2±7.4	55.8±7.9	71.5±5.0	54.8±10.0	54.6±7.4	84.4±5.2	74.9±6.9	88.6±5.0	**68.4±6.9**
						10-fold cross validation day 2					
E	89.7±5.6	72.5±4.2	85.3±4.4	58.1±10.1	59.0±4.6	77.1±6.2	78.7±7.0	90.8±2.9	88.7±5.0	87.6±6.3	**78.8±5.6**
C	82.2±5.6	63.2±6.6	71.4±6.1	64.3±6.5	78.9±6.4	69.8±6.6	68.8±6.0	88.0±5.8	75.0±6.6	78.3±4.7	**74.0±6.1**
						Day 2 classified with day 1					
E	81.0±7.1	56.2±7.4	81.7±10.4	73.6±11.1	58.4±5.3	65.7±20.0	69.4±13.0	87.1±6.7	90.2±4.7	91.6±4.5	**75.5±9.0**
C	81.5±5.6	78.0±5.3	69.0±6.1	40.7±13.6	85.8±7.7	56.4±16.5	69.2±8.8	84.0±7.0	74.6±6.1	60.5±4.0	**70.0±8.1**

TABLE II

The classification accuracy (mean and standard deviation) for error trials (E) and correct trials (C) for all ten subjects in the test group using the wavelet coefficients as feature vector.

B. MRCPs

There was a clear negative deflection in the grand average of the MRCPs for the test and control group which verifies that imaginary movements were performed and that no deviation in this matter could be causing the difference in the measured response signal. The difference between the ballistic and the moderate movements is however not significant as reported by [33]. In the control group the difference is most likely due to large MRCP amplitude variations between the subjects. [33] suggested that the difference between ballistic and the moderate is a matter of rate of force development, i.e. the duration of the task, and not force level. The strong similarity of both MRCPs may be an indicator that variations of rate of force development is not something that can be easily imagined.

C. Classification

The classification accuracies revealed in the result section show that it is feasible to perform single trial detection of ErrPs. The SVM seem to be a strong tool for discriminating error trials from correct trials. By using a downsampled version of the response signal recorded 200 ms to 600 ms after feedback as feature vector we obtained an averaged classification accuracy above 70%. This was done by training the classifier with data recorded at day one of the experiment and testing with data recorded at day two. The CWT- and t-test based feature extraction method did not show improvements of the classification. The classification accuracies obtained in this study should evidently be explained by the presence of the large P300 in the correct trials. Therefore classification of ErrP with an accuracy rate as reported in this paper is dependent on a P300 eliciting feedback. This is however presumably the case in BCI where the systems execution of a command often would be characterized as a deviant and infrequent stimulus to the user.

In conclusion this study have shown that incorrectly classification of imaginary movements elicit an ErrP and that correct classification increases the P300 which in total gives a difference in the two types of outcome that can be detected with the suggested approach. The reported findings support the idea that the ErrP very likely can be used to improve the overall performance of future BCI systems.

REFERENCES

[1] A. Kübler, V. K. Mushahwar, L. R. Hochberg, and J. P. Donoghue, "BCI Meeting 2005-Workshop on Clinical Issues and Applications," *IEEE Transactions on Neural Systems and Rehabilitation Engineering*, vol. 14, no. 2, pp. 131–134, 2006.

[2] S. Sanei and J. A. Chambers, *EEG Signal Processing*. John Wiley & Sons, Ltd, 2007.

[3] J. R. Wolpaw, G. E. Loeb, B. Z. Allison, E. Donchin, O. F. do Nascimento, W. J. Heetderks, F. Nijboer, W. G. Shain, and J. N. Turner, "BCI Meeting 2005-Workshop on Signals and Recording Methods," *IEEE Transactions on Neural Systems and Rehabilitation Engineering*, vol. 14, no. 2, pp. 138–141, 2006.

[4] B. H. Dobkin, "Brain-computer interface technology as a tool to augment plasticity and outcomes for neurological rehabilitation," *Journal of Physiology*, vol. 579.3, pp. 637–642, 2007.

[5] J. R. Wolpaw, N. Birbaumer, D. J. McFarland, G. Pfurtscheller, and T. M. Vaughan, "Brain-computer interfaces for communication and control," *Clinical Neurophysiology*, vol. 113, pp. 767–791, 2002.

[6] L. C. Parra, C. D. Spence, A. D. Gerson, and P. Sajda, "Response Error Correction-A Demonstration of Improved Human-Machine Performance Using Real-Time EEG Monitoring," *IEEE Transactions on Neural Systems and Rehabilitation Engineering*, vol. 11, no. 2, pp. 173–177, 2003.

[7] A. Buttfield, P. W. Ferrez, and J. del R. Millán, "Towards a Robust BCI: Error Potentials and Online Learning," *IEEE Transactions on Neural Systems and Rehabilitation Engineering*, vol. 14, no. 2, pp. 164–168, 2006.

[8] C. B. Holroyd and M. G. H. Coles, "The Neural Basis of Human Error Processing: Reinforcement Learning, Dopamine, and the Error-Related Negativity," *Psychological Review*, vol. 109, no. 4, pp. 679–709, 2002.

[9] W. H. R. Miltner, C. H. Braun, and M. G. H. Coles, "Event-Related Brain Potentials Following Incorrect Feedback in a Time-Estimation Task: Evidence for a Generic Neural System for Error Detection," *Journal of Cognitive Neuroscience*, vol. 9, no. 6, pp. 788–798, 1997.

[10] M. Falkenstein, J. Hoormann, S. Christ, and J. Hohnbein, "ERP components on reaction errors and their functional significance: a tutorial," *Biological Psychology*, vol. 51, pp. 87–107, 2000.

[11] G. Hajcak, C. B. Holroyd, J. S. Moser, and R. F. Simons, "Brain potentials associated with expected and unexpected good and bad outcomes," *Psychophysiology*, vol. 42, pp. 161–170, 2005.

[12] O. E. Krigolson and C. B. Holroyd, "Evidence for hierarchical error processing in the human brain," *Neuroscience*, vol. 137, pp. 13–17, 2006.

[13] O. E. Krigolson and C. B. Holroyd "Hierarchical error processing: Different errors, different systems," *Brain Research*, vol. 1155, pp. 70–80, 2007.

[14] G. Schalk, J. R. Wolpaw, D. J. McFarland, and G. Pfurtscheller, "EEG-based communication: presence of an error potential," *Clinical Neurophysiology*, vol. 111, pp. 2138–2144, 2000.

[15] B. Blankertz, G. Dornhege, C. Schäfer, R. Krepki, J. Kohlmorgen, K.-R. Müller, V. Kunzmann, F. Losch, and G. Curio, "Boosting Bit Rates and Error Detection for the Classification of Fast-Paced Motor Commands Based on Single-trial EEG Analysis," *IEEE Transactions on Neural Systems and Rehabilitation Engineering*, vol. 11, no. 2, pp. 127–131, 2003.

[16] J. D. Bayliss, S. A. Inverso, and A. Tentler, "Changing the P300 Brain Computer Interface," *CyberPhysiology & Behavior*, vol. 7, no. 6, pp. 694–704, 2004.

[17] P. W. Ferrez and J. del R. Millán, "You Are Wrong! -Automatic Detection of Interaction Errors from Brain Waves," *Proc. 19th Int. Joint Conf. Artificial Intell*, 2005.

[18] P. W. Ferrez and J. del R. Millán "Error-Related EEG Potentials Generated During Simulated Brain-Computer Interaction," *IEEE Transactions on Biomedical Engineering*, vol. PP, 2007.

[19] D. Farina, O. F. do Nascimento, M.-F. Lucas, and C. Doncarli, "Optimization of wavelet for classification of movement-related cortical potentials generated by variation of force-related parameters," *Journal of Neuroscience Methods*, vol. 162, pp. 357–363, 2007.

[20] A. Delorme and S. Makeig, "EEGLAB: an open source toolbox for analysis of single-trial EEG dynamics," *Journal of Neuroscience Methods*, vol. 134, pp. 9–21, 2004.

[21] A. J. Bell and T. J. Sejnowski, "An Information-Maximization Approach to Blind Separation and Blind Deconvolution," *Neural Computation*, vol. 7, pp. 1129–1159, 1995.

[22] M. Fatorechi, A. Bashashati, R. K. Ward, and G. E. Birch, "EMG and EOG artifacts in brain computer interface systems: A survey," *Clinical Neurophysiology*, vol. 118, pp. 480–494, 2007.

[23] A. Bashashati, M. Fatourechi, R. K. Ward, and G. E. Birch, "A survey of signal processing algorithms in brain-computer interfaces based on electrical brain signals," *Journal of Neural Engineering*, vol. 4, pp. R32–R57, 2007.

[24] S. G. Mason, A. Bashashati, M. Fatourechi, K. F. Navarro, and G. E. Birch, "A Comprehensive Survey of Brain Interface Technology Designs," *Annals of Biomedical Engineering*, vol. 35, no. 2, pp. 137–169, 2007.

[25] J. L. Semmlow, *Biosignal and Biomedical Image Processing: MATLAB-based applications*, 1st ed. Marcel Dekker, 2004.

[26] V. Bostanov, "BCI Competition 2003-Data Sets Ib and IIb: Feature Extraction From Event-Related Brain Potentials With the Continuous Wavelet Transform and the t-Value Scalogram," *IEEE Transactions on Biomedical Engineering*, vol. 51, no. 6, 2004.

[27] C.-C. Chang and C.-J. Lin, "LIBSVM : a library for support vector machines, 2001." 2001. [Online]. Available: http://www.csie.ntu.edu.tw/ cjlin/libsvm

[28] J. P. M. de Sá, *Pattern Recognition - Concepts, Methods and Applications*. Springer, 2001.

[29] M. Kaper, S. Member, P. Meinicke, U. Grossekathoefer, T. Lingner, and H. Ritter, "BCI Competition 2003-Data Set IIb: Support Vector Machines for the P300 Speller Paradigm," *IEEE Transactions on Biomedical Engineering*, vol. 51, no. 6, pp. 1073–1076, 2004.

[30] C.-W. Hsu, C.-C. Chang, and C.-J. Lin, "A Practical Guide to Support Vector Classification," 2007. [Online]. Available: http://www.csie.ntu.edu.tw/ cjlin

[31] S. H. Patel and P. N. Azzam, "Characterization of N200 and P300: Selected Studies of the Event-Related Potential," *International Journal of Medical Sciences*, vol. 2, pp. 147–154, 2005.

[32] C. Bellebaum and I. Daum, "Learning-related changes in reward expectancy are reflected in the feedback-related negativity," *European Journal of Neuroscience*, vol. 27, pp. 1823–1835, 2008.

[33] O. F. do Nascimento, K. D. Nielsen, and M. Voigt, "Movement-related parameters modulate cortical activity during imaginary isometric plantarflexions," *Experimental Brain Research*, vol. 171, pp. 78–90, 2006.

Detection of error-related potentials to improve brain-computer interfaces

Supplementary worksheets

31st May 2008

Chapter 1

Individual EEG recordings

1.1 Error-related potentials

In the following figures, from 1.1 to 1.5, the response signals recorded after feedback are showed. It can be seen that the signals from all subjects have similar characteristics. The correct feedback elicit a small negative peak at approximately 220 ms after feedback and a large positive peak between 380 ms and 400 ms after feedback. These findings were expected as an infrequent and deviant stimuli has been reported to elicite the N200 and P300 in numerous studies [Sanei & Chambers, 2007; Patel & Azzam, 2005; Friedmann et al., 2001]. The response to error feedback have some of the same charateristics. For some of the subject the error feedback also elicit a N200. The positive peak around 400 ms after feedback seems however to be broader, have a smaller amplitude and a longer latency. Especially the smaller amplitude has also been reported by Hajcak et al. [2005]; Bayliss et al. [2004]. The difference in amplitude could be due the presence of an error-related potential in the response signals after error feedback.

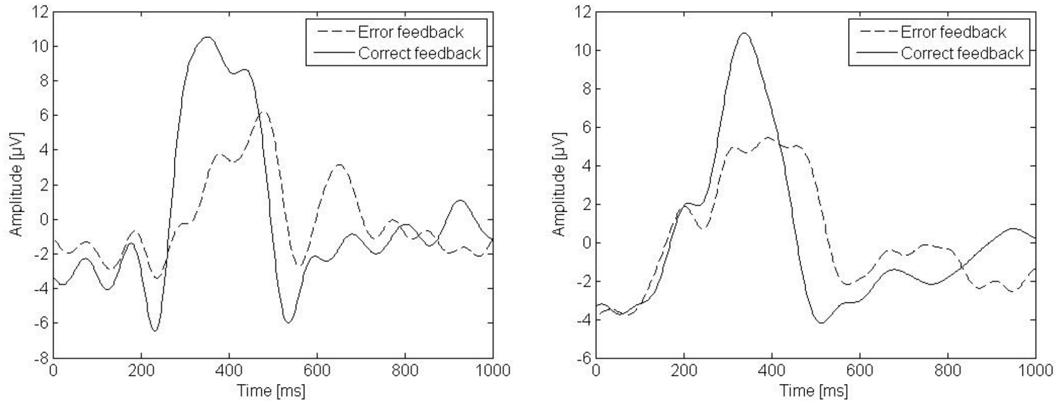

(A) ***(B)***

Figure 1.1: *The averages of the response signals recorded after feedback at Cz. In (A) from subject 1 and (B) from subject 2.*

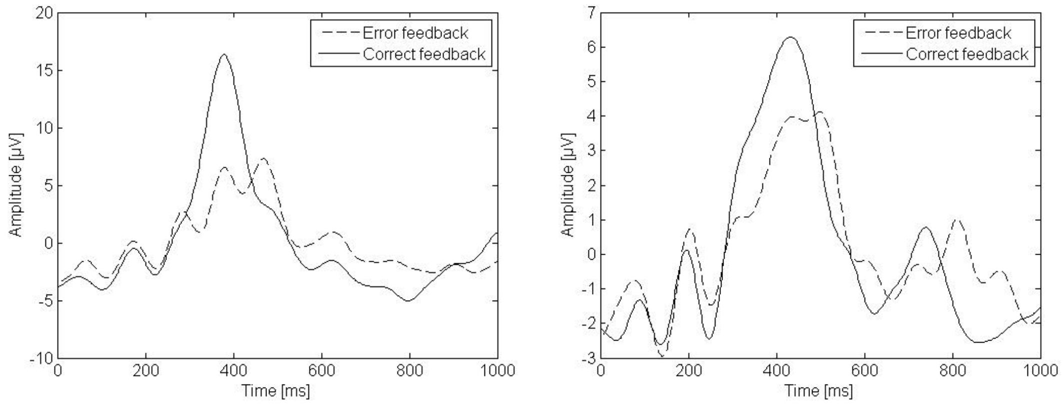

(A) ***(B)***

Figure 1.2: *The averages of the response signals recorded after feedback at Cz. In (A) from subject 3 and (B) from subject 4.*

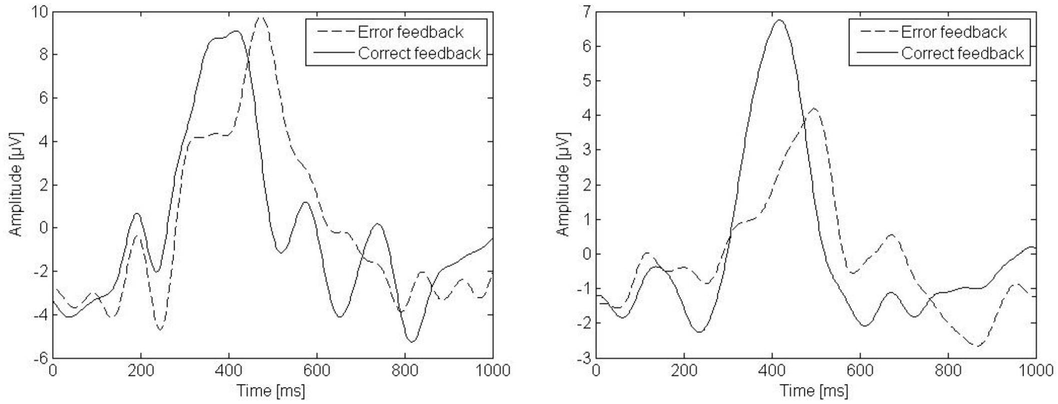

(A) ***(B)***

Figure 1.3: *The averages of the response signals recorded after feedback at Cz. In (A) from subject 5 and (B) from subject 6.*

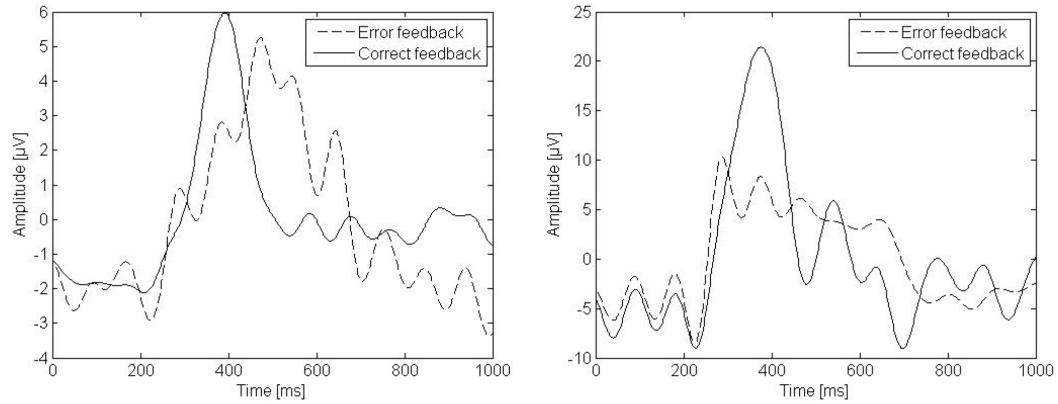

(A) ***(B)***

Figure 1.4: *The averages of the response signals recorded after feedback at Cz. In (A) from subject 7 and (B) from subject 8.*

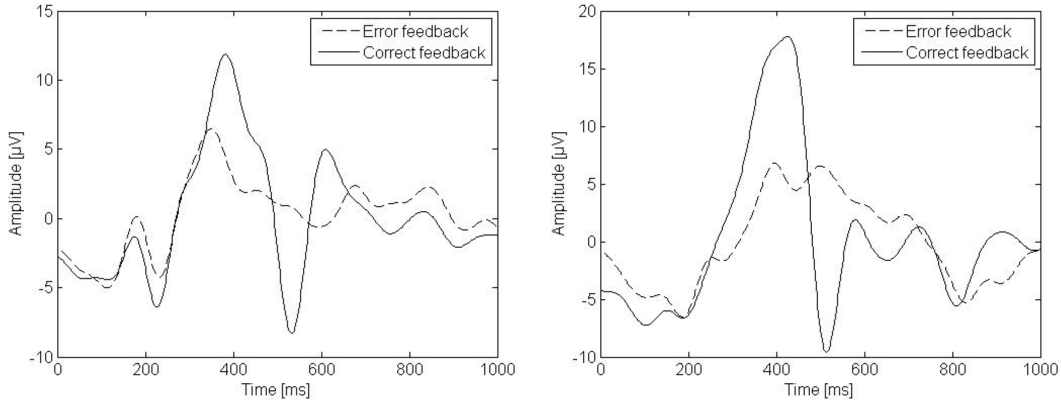

(A) *(B)*

Figure 1.5: *The averages of the response signals recorded after feedback at Cz. In (A) from subject 9 and (B) from subject 10.*

1.2 Classification of MRCPs

The detection of error-related potentials (ErrPs) should be used to improve the accuracy of a BCI system described in Farina et al. [2007]. The system classifies movement-related cortical potentials (MRCPs) generated by variation in force-related parameters during imaginary foot movement. The experiment was implemented with an imaginary movement followed by a feedback of the subject performances. One of the ideas of the experiment was to see if the ErrPs could improve the classification ratio of the MRCPs, according to the classification ratio found in Farina et al. [2007]. In this study a clear negative deflection was found in the grand average of the MRCPs which verifies that imaginary movements were performed. However the difference between the ballistic and the moderate movements was not significant as reported by do Nascimento et al. [2006] and by using the method proposed in Farina et al. [2007] a classification accuracy of approximately 50% was achieved. In figure 1.6 to 1.10 the averaged MRCPs for each subject in the test group is showed. do Nascimento et al. [2006] suggested that the difference between ballistic and the moderate is a matter of rate of force development, i.e. the duration of the task, and not force level. The strong similarity of both MRCPs may be an indicator that variations of rate of force development is not something that can be easily imagined. It was furthermore reported that the difference between the MRCPs was smaller for imaginary movement compared to real movement. In Farina et al. [2007] the execution of the two movements was different from the one in this experiment both in force level as well as rate of force development for the moderate movement. These two factors could explain why the classification rate of MRCPs in this study is not comparable to the findings in Farina et al. [2007] where a classification accurracy of 85% was obtained.

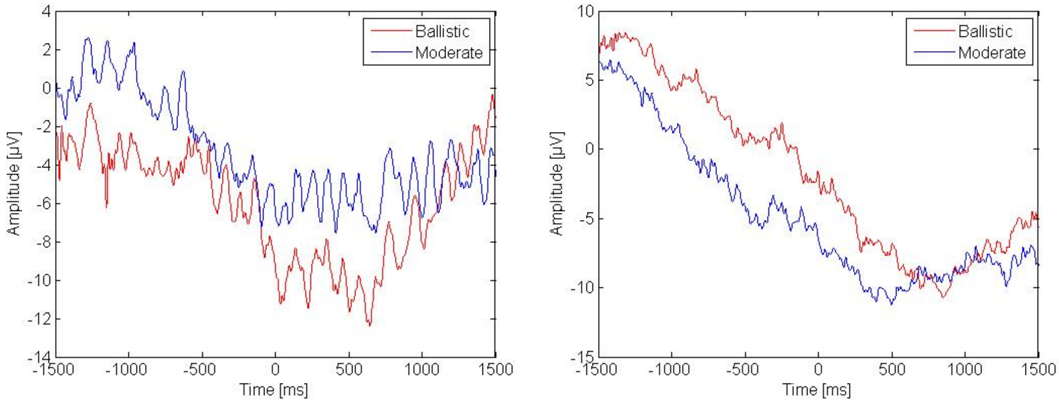

(A) ***(B)***

Figure 1.6: *The averages of the MRCPs recorded at Cz. In (A) from subject 1 and in (B) from subject 2.*

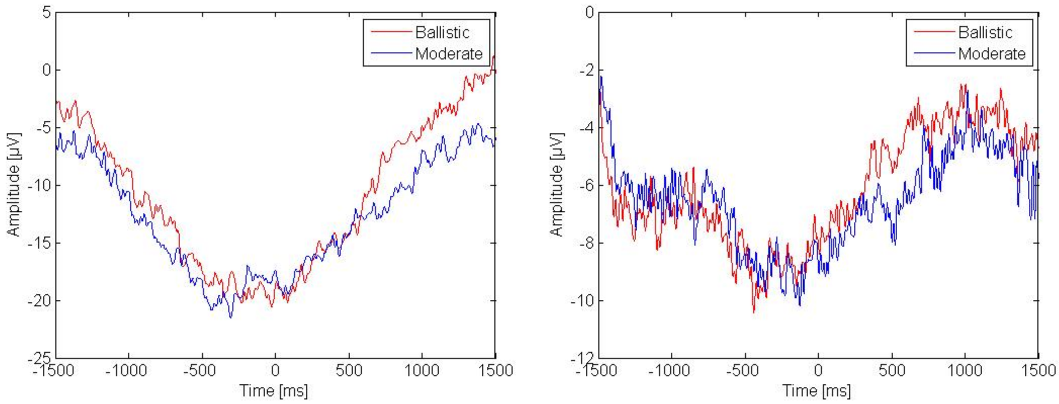

(A) ***(B)***

Figure 1.7: *The averages of the MRCPs recorded at Cz. In (A) from subject 3 and in (B) from subject 4.*

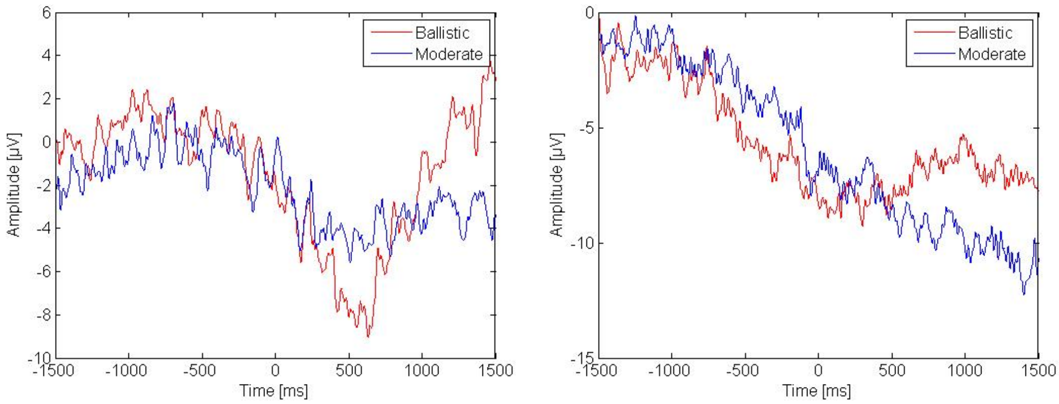

(A) ***(B)***

Figure 1.8: *The averages of the MRCPs recorded at Cz. In (A) from subject 5 and in (B) from subject 6.*

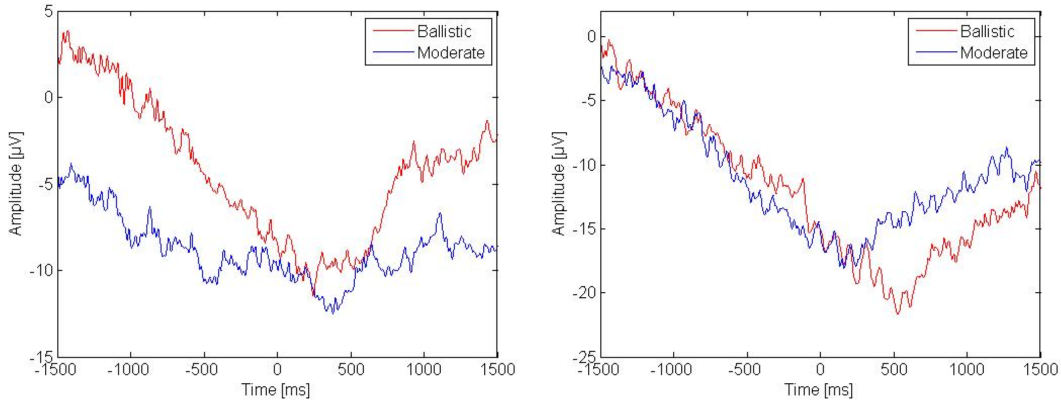

(A) ***(B)***

Figure 1.9: *The averages of the MRCPs recorded at Cz. In (A) from subject 7 and in (B) from subject 8.*

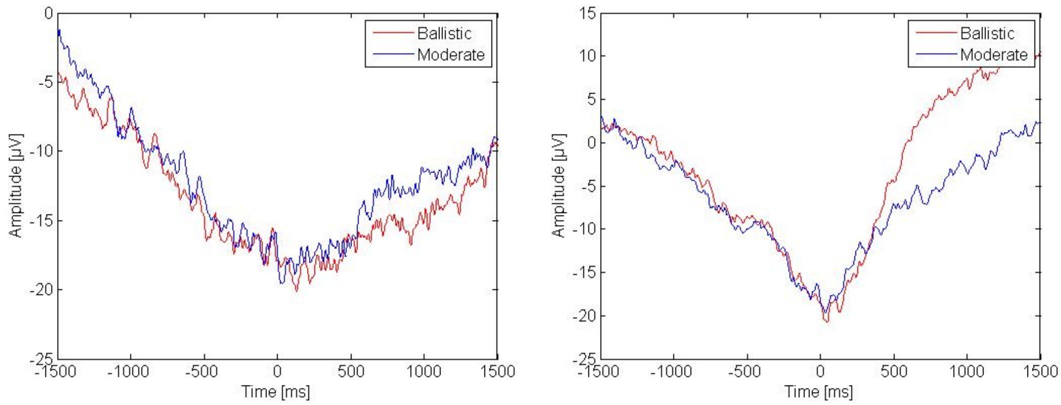

(A) ***(B)***

Figure 1.10: *The averages of the MRCPs recorded at Cz. In (A) from subject 9 and in (B) from subject 10.*

1.3 Improvement of the BCI using ErrPs

[Schalk et al., 2000; Blankertz et al., 2003; Ferrez & del R. Millán, 2005; Buttfield et al., 2006] have showed that detecting ErrPs will improve the performance of BCI in terms of increasing the bit rate. The bit rate is the amount of information communicated per unit time and depends on speed and accuracy p of the system. It is a standard measure in communication systems, originally derived from [Shannon & Weaver, 1964], and it is also used to as a measure of the performance of BCI systems [Schalk et al., 2000; Blankertz et al., 2003; Bayliss et al., 2004; Ferrez & del R. Millán, 2005]. The bit rate can be calculated in bits/sec or bits/trial (BpT).

$$p = \frac{Correct\ MRCP}{All\ trials} \tag{1.1}$$

$$BpT = 1 + p \cdot log_2(p) + (1-p) \cdot log_2(1-p) \tag{1.2}$$

This equation holds when the number of possible selections in the BCI system is 2. [Schalk et al., 2000; Wolpaw et al., 2000]

If the ErrP is introduced with a classification accuracy of erroneous trials, e, and a classification accuracy of correct trials, c, the detection of ErrPs could be used to simply stop and not sent the outcome of the classification of the MRCPs. The new accuracy p' of the BCI becomes:

$$p' = \frac{All\ Hits - Rejected\ Hits}{All\ Trials - Rejected\ Trails} \tag{1.3}$$

This can be rewritten in probabilities:

$$p' = \frac{p - p \cdot (1-c)}{1 - (p \cdot (1-c) + (1-p) \cdot e)} \tag{1.4}$$

With this new accuracy the information transfer rate in bits/trial is:

$$BpT = 1 + p' \cdot log_2(p') + (1-p') \cdot log_2(1-p') \cdot [1 - (p \cdot (1-c) + (1-p) \cdot e)] \tag{1.5}$$

However if this bit rate calculation should give a reasonable result a decent classification of the MRCPs is required which was not the case in this study.

1.3.1 Example

If the classification rate on 85% which was found in Farina et al. [2007] for MRCPs can be obtained, the bit rate only for MRCPs would have been:

$$1 + 0.85 \cdot log_2(0.85) + (1-0.85) \cdot log_2(1-0.85) = 0.39[bit/trails] \tag{1.6}$$

By introducing the ErrP classification with accuracies found in this study the MRCP classification could have been improved to:

$$\frac{0.85 - 0.85 \cdot (1-0.72)}{1 - (0.85 \cdot (1-0.72) + (1-0.85) \cdot 0.74)} = 0.94 \tag{1.7}$$

Which would give a new bit rate at:

$$(1+0.94 \cdot log_2(0.94)+(1-0.94) \cdot log_2(1-0.94)) \cdot [1-(0.85 \cdot (1-0.72)+(1-0.85) \cdot 0.74)] = 0.44[bit/trails] \tag{1.8}$$

Which would give a bit rate improvement of:

$$\frac{0.44 - 0.39}{0.39} = 0.12 \tag{1.9}$$

Bibliography

Bayliss, J. D., Inverso, S. A. & Tentler, A. (2004). Changing the P300 Brain Computer Interface. *CyberPhysiology & Behavior*, 7(6):694–704.

Blankertz, B., Dornhege, G., Schäfer, C., Krepki, R., Kohlmorgen, J., Müller, K.-R., Kunzmann, V., Losch, F. & Curio, G. (2003). Boosting bit rates and error detection for the classification of fast-paced motor commands based on single-trial eeg analysis. *IEEE Transactions on Neural Systems and Rehabilitation Engineering*, 11(2):127–131.

Buttfield, A., Ferrez, P. W. & del R. Millán, J. (2006). Towards a robust bci: Error potentials and online learning. *IEEE Transactions on Neural Systems and Rehabilitation Engineering*, 14(2):164–168.

do Nascimento, O. F., Nielsen, K. D. & Voigt, M. (2006). Movement-related parameters modulate cortical activity during imaginary isometric plantar-flexions. *Experimental Brain Research*, 171:78–90.

Farina, D., do Nascimento, O. F., Lucas, M.-F. & Doncarli, C. (2007). Optimization of wavelet for classification of movement-related cortical potentials generated by variation of force-related parameters. *Journal of Neuroscience Methods*, 162:357–363.

Ferrez, P. W. & del R. Millán, J. (2005). You are wrong!-automatic detection of interaction errors from brainwaves. *Proc. 19th Int. Joint Conf. Artificial Intell.*

Friedmann, D., Cycowisc, Y. M. & Gaeta, H. (2001). The novelty p3: an event-related brain potential (erp) sign of the brain's evaluation of novelty. *Neuroscience and biobehavioral reviews*, 25:355–373.

Hajcak, G., Holroyd, C. B., Moser, J. S. & Simons, R. F. (2005). Brain potentials associated with expected and unexpected good and bad outcomes. *Psychophysiology*, 42:161–170.

Patel, S. H. & Azzam, P. N. (2005). Characterization of n200 and p300: Selected studies of the event-related potential. *International Journal of Medical Sciences*, 2:147–154.

Sanei, S. & Chambers, J. A. (2007). *EEG Signal Processing.* John Wiley & Sons, Ltd. ISBN 978-0-470-02581-9.

Schalk, G., Wolpaw, J. R., McFarland, D. J. & Pfurtscheller, G. (2000). Eeg-based communication: presence of an error potential. *Clinical Neurophysiology*, 111:2138–2144.

Shannon, C. E. & Weaver, W. (1964). A Mathematical Theory of Communication. *Urbana, IL: Univ. Illinois Press.*

Wolpaw, J. R., Birbaumer, N., Heetderks, W. J., McFarland, D. J., Peckham, P. H., Schalk, G., Donchin, E., Quatrano, L. A., Robinson, C. J. & Vaughan, T. M. (2000). Brain-computer interface technology: A review of the first international meeting. *IEEE Transactions on Neural Systems and Rehabilitation Engineering*, 8(2):164–173.